Investigating the importance of PAK1 kinase activity during breast cancer cell spreading and migration

Gale, Madeline Emma

Awarding institution:
King's College London

Investigating the importance of PAK1 kinase activity during breast cancer cell spreading and migration

Madeline Emma Gale

2018

A thesis submitted to fulfil the requirements for the degree of Doctor of Philosophy

Division of Cancer Studies

King's College London

Declaration of Authorship

I declare that the work presented in this thesis is the work of the author. Contributions from others have been properly acknowledged and cited where included.

Madeline Gale

Acknowledgements

When selecting a PhD project, I was advised to consider my choice of supervisor carefully as this was as important if not more important than the topic itself. Dr Claire Wells has been motivational, encouraging and exceptionally supportive during my time in her lab, and for that I would like to express my deepest gratitude to her. There hasn't been a day when I doubted my choice in supervisor. I would like to thank my second supervisor Dr Simon Ameer-Beg for not only his patience when teaching me techniques that unfortunately didn't make it into this thesis, but also for his guidance in other aspects of my project. I would like to extend my thanks to the three additional members of my thesis committee- Prof. Tony Ng, Dr James Arnold and Dr Fiona Wardle. I really appreciate your time, interest and valuable suggestions.

To Dr Klaus Hahn and his team, namely Dr Onur Dagliyan, Dr Dan Marston and Orrin Stone- thank you for the cells, advice and making my trip to North Carolina one to remember. This thesis would be very different if it wasn't for your collaboration.

Some special thanks go to the many Wells' lab members past and present. Your teachings, suggestions and reassurance in the lab were always comforting, and the nights out, coffee readings, inappropriate jokes, lunches inside, lunches outside, Christmas parties, snack times and so much more have made the last four years a lot of fun. I couldn't imagine my time in the lab without the originals- Dr Katerina Pipili (the best lab Mumma going), Dr Mario De Piano (the avid sandwich shaker and vitamin taker), Dr Hoyin Lam (the very important business man who is often with a cold) and Dr Kiruthikah Thillai (the only other person in the world who likes to snack as much as me and my lab/real life best friend…right?). To later members Dr/Mr Christian Benzing, Beth Russell, Noor Jalal, Dr Sevil Oskay and Dr Michaela Lesjak thank you for being equally as wonderful and filling in the holes the originals left. To the current members Valeria Manuelli and Lujain Kuwair I am sorry for 'leaving' you but am hugely thankful for your kindness during the most stressful months of my PhD. Valeria, I am so very sorry I won't be around to see your project unfold, teach you to inject fish and watch you settle into your new lab life. Lujain, I will do my best to still remind you of all upcoming bank holidays. I am also very grateful to various PhD students and post docs on the second floor for their help and friendly faces over the past years, especially Dr Peter Gordon for all the work time hugs.

A massive shout out to all my home friends for your inappropriate, insulting yet uplifting humour and friendships. Seven years on with a Brackley bond that is stronger than ever before, we are certainly the exception to the 'you don't stay in touch with your friends from school' theory. My extended love goes to Leela Fair and Dani Skerrett for building a home from home with me here in London, from the wondrous birthday celebrations to deliverooing crêpes/churros/cheesecake on a mundane middle of the week evening and everything in between, the last few years would have been a lot less fun without you both. I would also like to thank Ichha Johar for her many words of wisdom and general life advice, and Helen Fielden for being an all-round great gal who constantly amuses me for all the right reasons. You are both wonderful and dependable friends that I am lucky to have. And lastly while on the topic of friends, I could write another 200 pages on my love and appreciation for my favourite person, Mai Ta. Thank you for your 21 (and counting) years of friendship, always being the voice on the end of the phone that can make anything seem a million times easier and without a doubt being the best friend anyone could even hope to have.

To my Mum, Dad, brother and sister, thank you for being a constant bundle of unconditional love and support even when I'm mega annoying. I am endlessly grateful to my Mum for her nonchalant 'it'll be fine but just get on with it' attitude and my Dad for his charming comments like 'you know 40,000 words is only 40 words a day over four years'. You are wonderful parents who forever manage to strike the perfect balance between comfort, mockery and tough love to get me where I need to be. Sophie and Felix thanks for being stand up siblings, a joy to be around and generally just two of the best people I know. I am very pleased I accidentally completed our family all those years ago and am stuck with you all. To my extended family- I promise you can now stop asking me what I do, what job I will get afterwards, if I've saved the world yet and whether I still give cancer to baby fish. Thanks for your ever-encouraging questions.

And finally, last but definitely not least, I am incredibly grateful to my Grandad, who sadly passed away during my second year. As a professional advocate of further education, he was always very encouraging of my studies. I wish I could show you this, but I will take comfort in the fact I would now undoubtedly be your favourite grandchild (sorry Adam) and hope it makes you proud.

Abstract

Breast cancer is a primary cause of cancer lethality in women due to its ability to metastasise to other organs. Currently there are no therapeutic interventions specifically targeting breast cancer metastasis. p-21 activated kinases (PAK 1-6) are recognised regulators of cell morphology and thus promotion of migration. Therefore, these proteins have been implicated in driving metastasis and many pharmaceutical companies have developed PAK programmes.

In particular PAK1 is associated with breast cancer. The PAK1 gene is located in a genomic region which is frequently amplified in many breast cancers. Indeed, PAK1 is reported to be overexpressed and/or hyperactivated in over 50% of human breast cancers. However, the importance of PAK1 kinase activity over PAK1 protein interactions is not well established. This is crucial given many drug discovery programmes are focused on kinase inhibition. Furthermore, the downstream targets of PAK1 specifically in breast cancer are not fully described; especially those proteins most important for cell spreading. This project focuses on the role PAK1 plays in breast cancer cell spreading and migration, with an emphasis on unravelling the kinase dependent pathways.

PAK1 depletion via shRNA and CRISPR-Cas9 technology in a triple negative breast cancer cell line caused a decrease in both cell spread area and cell migration. These findings were replicated using a pharmacological inhibitor of PAK1 kinase activity. The importance of PAK1 kinase activity in breast cancer cell migration was confirmed where pharmacological inhibition or depletion of PAK1 lead to a decrease in *in vitro* cell invasion and *in vivo* cell migration. Using an inducible system to stimulate PAK1 kinase activity a specific role in cell spreading was observed. Induction of cell spreading via PAK1 activation was associated with the serine 910 phosphorylation of FAK and serine 189 phosphorylation of ERK3. These are novel pathways in breast cancer. Taken together these results place PAK1 at the centre of cell spreading and migration and suggest that kinase activity is essential for these cellular responses. Thus, findings in this thesis support pharmaceutical inhibition of kinase activity as a valid therapeutic approach.

Table of Contents

Declaration of Authorship 2

Acknowledgements 3

Abstract 5

List of Figures 9

List of Tables 11

Abbreviations 12

Chapter 1 Introduction 17

1.1 Breast cancer 17
1.1.1 Triple negative breast cancer 18
1.1.2 Tumour metastasis 18

1.2 The importance of cell migration 22
1.2.1 Modes of Cell migration 22
1.2.2 The role of cell spreading in cell migration 25
1.2.3 Actin dynamics in cell migration 26
1.2.4 Focal adhesions in cell migration 26
1.2.5 Focal adhesion kinase 27

1.3 The Rho GTPase family 29
1.3.1 Rho GTPases in cell migration 31

1.4 The p-21 activated kinase family 35
1.4.1 PAK domain structure and regulation 37
1.4.2 PAK1 in cancer 42
1.4.3 PAK1 in cell motility and cancer cell migration 44

1.5 Project aims 47

Chapter 2 Materials and methods 49

2.1 Materials 49
2.1.1 General materials 49
2.1.2 Buffers and solutions 51
2.1.3 Primary antibodies 52
2.1.4 Secondary antibodies 53
2.1.5 shRNA sequences 53
2.1.6 CRIPSPR constructs 53

2.2 Methods 56
2.2.1 Transformation of competent *E.coli* cells 56

2.2.2 DNA plasmid purification 56
2.2.3 Cell culture 56
2.2.4 Cell storage and recovery 58
2.2.5 Transfection of HEK293 with calcium phosphate 58
2.2.6 Transfection of MDA-MB-231 with viafect 59
2.2.7 Generation of stable fluorescent LifeAct cells 59
2.2.8 Single cell cloning 60
2.2.9 Fluorescence-activated cell sorting 60
2.2.10 Cell lysis 60
2.2.11 Gel electrophoresis and immunoblotting 61
2.2.12 Stripping nitrocellulose membranes 61
2.2.13 Densitometry 61
2.2.14 Coverslip preparation 62
2.2.15 Collagen coating of coverslips 62
2.2.16 Fibronectin coating of coverslips 62
2.2.17 Immunofluorescent staining and imaging 62
2.2.18 Image processing and cell morphology analysis 63
2.2.19 2D migration random migration assay and analysis 63
2.2.20 Spheroid assay and analysis 64
2.2.21 Zebrafish embryo maintenance 64
2.2.22 Zebrafish yolk invasion assay and imaging 65
2.2.23 Rapamycin experiments 66
2.2.24 Cytoskeleton phospho antibody array 66
2.2.25 Statistical analysis 67

Chapter 3 The effect of PAK1 perturbation on cell morphology and migration 69

3.1 Introduction 69

3.2 Results 72
3.2.1 PAK1 is expressed in breast, pancreatic and prostate cancer cell lines 72
3.2.2 Knockdown of PAK1 impacts cell morphology and migration 74
3.2.3 CRISPR of PAK1 impacts cell morphology and behaviour 80
3.2.4 Pharmacological inhibition of PAK1 impacts cell morphology and migration . 91

3.3 Discussion 95

3.4 Future work 102

Chapter 4 Assess the requirement of PAK1 activity in *in vitro* invasion and *in vivo* cell migration 104

4.1 Introduction 104

4.2 Results 106
4.2.1 PAK1 kinase activity plays a role in 3D cell invasion 106
4.2.2 Zebrafish xenograft assay to study cancer cell migration 110

4.2.3 Development of fluorescent MDA-MB-231 cells for zebrafish xenograft assay 112
4.2.4 Optimisation of the zebrafish xenograft assay for MDA-MB-231 cells 114
4.2.5 PAK1 kinase activity plays a role in *in vivo* cell migration 117
4.3 Discussion 120
4.4 Future work 126
Chapter 5 Utilise an inducible PAK1 model system to monitor PAK1 specific cellular responses 128
5.1 Introduction 128
5.2 Results 131
5.2.1 UniRapR-PAK1 is stably expressed in MDA-MB-231 cells 131
5.2.2 Significant differences in cell morphology identified between MDA-MB-231 wild-type populations 133
5.2.3 Phosphorylation levels of PAK1-rap increase on rapamycin stimulation 135
5.2.4 Specific activation of PAK1 induces MDA-MB-231 cell spreading 139
5.2.5 Cytoskeletal phospho-array reveals changes in protein phosphorylation levels on PAK1 activation 144
5.2.6 Phosphorylation levels of LIMK1 threonine 508 and LIMK2 threonine 505 increase on PAK1 activation 147
5.2.7 Phosphorylation levels of CRKII tyrosine 221 decrease on PAK1 activation 150
5.2.8 Phosphorylation levels of FAK serine 910 increase on PAK1 activation 153
5.2.9 Phosphorylation levels of ERK1 threonine 202 and ERK2 tyrosine 204 remain constant on PAK1 activation 156
5.2.10 Phosphorylation levels of ERK3 serine 189 increase on PAK1 activation 158
5.3 Discussion 161
5.4 Future work 169
5.4.1 Further exploration of FAK and ERK3 169
5.4.2 Further exploration into the reduction in cell spreading and downstream signalling 170
Chapter 6 Concluding remarks 172
References 178

List of Figures

Figure 1.1 Schematic diagram of the metastatic cascade. 21
Figure 1.2 A schematic diagram of the modes of cancer cell migration. 24
Figure 1.3 Regulation of the Rho GTPases. 30
Figure 1.4 Rho GTPase effector pathways that regulate cytoskeletal dynamics. 34
Figure 1.5 p21-activated kinase family structures. 36
Figure 1.6 Regulation of group I and group II PAKs. 39
Figure 2.1 Schematic diagram of CRISPR constructs. 54
Figure 2.2 Schematic diagram of PAK1 CRISPR target sites on the PAK1 gene. 55
Figure 3.1 PAK1 expression in cancer cell lines. 73
Figure 3.2 shRNA knockdown of PAK1 in MDA-MB-231 cells. 75
Figure 3.3 Morphology of shRNA PAK1 knockdown MDA-MB-231 cells 77
Figure 3.4 2D migration of shRNA PAK1 knockdown MDA-MD-231 cells 79
Figure 3.5 Validation of PAK1 CRISPR constructs in HEK293 cells. 81
Figure 3.6 Flow diagram of CRISPR protocol. 83
Figure 3.7 CRISPR screening using western blotting. 84
Figure 3.8 PAK1 expression in CRISPR PAK1 knockdown cells. 86
Figure 3.9 Morphology of CRISPR PAK1 knockdown MDA-MB-231 cells. 88
Figure 3.10 2D migration of CRISPR PAK1 knockdown MDA-MD-231 cells. 90
Figure 3.11 The effect of IPA-3 on MDA-MB-231 cell morphology. 92
Figure 3.12 The effect of IPA-3 on MDA-MB-231 cells in 2D migration 94
Figure 4.1 shRNA PAK1 knockdown leads to a decrease in cell invasion. 107
Figure 4.2 CRISPR PAK1 knockdown leads to a decrease in cell invasion. 108
Figure 4.3 IPA-3 treatment leads to a decrease in cell invasion. 109
Figure 4.4 AsPC-1 cells dissemination in a zebrafish xenograft assay. 111
Figure 4.5 Successful generation of wildtype, control and PAK1 knockdown cells labelled with LifeAct-RFP. 113
Figure 4.6 PAK1 knockdown leads to a decrease in in vivo cell migration. 118
Figure 4.7 IPA-3 pharmacological inhibition of PAK1 leads to a decrease in *in vivo* cell migration 119
Figure 5.1 A schematic diagram of rapamycin induces PAK1-rap stability and activity. 129
Figure 5.2 Expression of PAK1-rap in S44 cells. 132
Figure 5.3 Morphology of K-WT and UNC-WT cells. 134
Figure 5.4 Phosphorylation levels of PAK1-rap at threonine 423 increase on stimulation of rapamycin in S44 cells. 136
Figure 5.5 No change in endogenous PAK1 threonine 423 phosphorylation levels on stimulation of rapamycin in S44 cells. 137

Figure 5.6 No change in endogenous PAK1 threonine 423 phosphorylation levels on stimulation of rapamycin in WT-UNC cells. 138
Figure 5.7 Rapamycin activation of PAK1-rap induces S44 cell spreading**.** 140
Figure 5.8 Statistical analysis of S44 cell spreading on rapamycin induced PAK1-rap activation. 141
Figure 5.9 No change in UNC-WT cell area or perimeter on rapamycin stimulation in UNC-WT cells. 142
Figure 5.10 Rapamycin stimulation of UNC-WT induced no significant changes to cell area or perimeter 143
Figure 5.11 Cytoskeletal phospho-array slide images. 145
Figure 5.12 Phosphorylation levels of LIMK1 threonine 508 and LIMK2 threonine 505 increase on PAK1 activation in S44 cells. 148
Figure 5.13 No change in the phosphorylation levels of LIMK1 threonine 508 and LIMK2 threonine 505 on PAK1 activation in UNC-WT cells. 149
Figure 5.14 Phosphorylation levels of CRKII tyrosine 221 decrease on PAK1 activation in S44 cells. 151
Figure 5.15 No change in the phosphorylation levels of CRKII tyrosine 221 on PAK1 activation in UNC-WT cells. 152
Figure 5.16 Phosphorylation levels of FAK serine 910 increase on PAK1 activation in S44 cells. 154
Figure 5.17 No change in the phosphorylation levels of FAK serine 910 on PAK1 activation in UNC-WT cells. 155
Figure 5.18 No change in the phosphorylation levels of ERK1 threonine 202 and ERK2 tyrosine 204 on PAK1 activation in S44 cells. 157
Figure 5.19 Phosphorylation levels of ERK3 serine 189 increase on PAK1 activation in S44 cells. 159
Figure 5.20 No change in the phosphorylation levels of ERK3 serine 189 on PAK1 activation in UNC-WT cells**.** 160
Figure 6.1 A schematic diagram of PAK1 downstream signalling to promote cell spreading and migration. 177

List of Tables

Table 1.1 PAK1 regulators and effectors 41
Table 1.2 PAK1 alterations in human cancers. 43
Table 2.1 General materials 51
Table 2.2 Buffers and solutions 52
Table 2.3 Primary antibodies used 53
Table 2.4 Secondary antibodies used 53
Table 2.5 shRNA constructs used 53
Table 2.6 CRISPR constructs used 53
Table 2.7 Calcium phosphate kit transfection mix 58
Table 2.8 Viafect transfection mix 59
Table 3.1 Area values for shRNA, CRISPR and IPA- 3 morphology**.** 101
Table 3.2 Mean cell speed values for shRNA, CRISPR and IPA- 3 morphology. 101
Table 4.1 Zebrafish xenograft assay needle size optimisation. 116
Table 4.2 Zebrafish xenograft assay cell density optimisation. 116
Table 4.3 Zebrafish xenograft assay pulse duration of injection optimisation. 116
Table 5.1 Proteins with altered phosphorylation levels on PAK1 activation 146

Abbreviations

2D	2-dimensional
3D	3-dimensional
Arp2/3	Actin-related proteins 2/3
ADP	Adenosine diphosphoate
ATP	Adenosine triphosphate
AID	Autoinhibitory domain
APS	Ammonium persulfate
BSA	Bovine serum albumin
$CaCl_2$	Calcium chloride
Cas9	CRISPR associated protein 9
Cdc42	Cell division control protein 42
CRIPak	Cysteine rich inhibitor of PAK1
CRISPR	Clustered regularly interspaced short palindromic repeats
DAPI	4',6-diamidino-2-phenylindole
DMEM	Dulbecco's Modified Eagle's Medium
DMSO	Dimethyl sulfoxide
DNA	Deoxyribose nucleic acid
dpf	Days post fertilisation
dpi	Days post injection
DTT	Dithiothreitol
E.coli	*Escherichia coli*
ECL	Enhance chemiluminescence
ECM	Extracellular matrix
EDTA	Ethylenediaminetetraacetic acid
EGF	Epidermal growth factor
EGFR	Epidermal growth factor receptor
EMT	Epithelial to mesenchymal transition

ER	Oestrogen receptor
ERK	Extracellular-signals regulated kinase
F-actin	Filamentous actin
FACS	Fluorescence-activated cell sorting
FAK	Focal adhesion kinase
FBS	Foetal bovine serum
G-actin	Globular actin
GAA	Glacial acetic acid
Gab1	GRB2-associated-binding protein 1
GAPs	GTPase-activating proteins
GAPDH	Glyceraldehyde 3-phosphate dehydrogenase
GBD	p21-GTPase-binding domain
GDIs	Rho guanine-nucleotide-dissociation inhibitors
GEFs	Guanine nucleotide exchange factors
GFP	Green fluorescent protein
Grb2	Growth factor receptor-bound protein 2
H_2O	Water
HCl	Hydrochloric acid
HDR	Homologous directed repair
HEPES	4-(2-hydroxyethyl)-1-piperazineethanesulfonic acid
HER2	Human epidermal growth factor 2
HGF	Hepatocyte growth factor
IGF1	Insulin-like growth factor 1
KCl	Potassium Chloride
kDA	Kilodaltons
LB agar	Luria-Bertani agar
LB broth	Luria-Bertani broth
LIMK	LIM kinase
MAPK	Mitogen-activated protein kinase

$MgCl_2$	Magnesium chloride
mDia	Diaphanous-related formin
MMPs	Matrix metalloproteases
MLC	Myosin-light chain
MLCK	Myosin-light chain kinase
mRNA	Messenger RNA
MS222	Ethyl 3-aminobenzoate methanesulfonate
mTOR	Mammalian target of rapamycin
Na_3VO_4	Sodium orthovanadate
NaCl	Sodium chloride
NaF	Sodium fluoride
NaOH	Sodium hydroxide
Nck	Non-catalytic region of tyrosine kinase adaptor protein
NHEJ	Non-homologous end joining
PAK	p21-activated kinase
PBS	Phosphate buffered solution
PCR	Polymerase chain reaction
PDK1	3-phosphoinositide-dependent kinase 1
PFA	Paraformaldehyde
PIP2	Phosphatidylinositol-4,5-bisphosphate
PIP 5-kinase	Phosphatidylinositol-4-phosphate 5-kinase
PIX	PAK1-interacting exchange factor
PKA	Protein kinase A
PMSF	Phenylmethylsulfonyl fluoride
POPX1	Partner of PIX 1
POPX2	Partner of PIX 2
PP2A	Phosphatase type 2A
PR	Progesterone receptor
PTU	N-Phenylthiourea

PVP	Polyvinylpyrrolidone solution
RFP	Red fluorescent protein
ROCK	Rho-associated, coiled-coil containing protein kinase 1
RNA	Ribonucleic acid
RPMI	Roswell Park Memorial Institute
SCAR/WAVE	Suppressor of cAMP receptor/WASP verprolin-homologous
SDS	Sodium dodecyl sulphate
SDS-PAGE	Sodium dodecyl sulphate-polyacrylamide gel electrophoresis
SEM	Standard error of the mean
sgRNA	Short guide RNA
shRNA	Short hairpin RNA
TBS	Tris buffered saline
TBST	Tris buffered saline tween
TEMED	Tetramethylethylenediamin
TNBC	Triple negative breast cancer
WASP	Wiskott-Aldrich Syndrome Protein

Chapter 1

Introduction

Chapter 1 Introduction

1.1 Breast cancer

Breast cancer is one of the most commonly diagnosed cancers with females having a 12.3% lifetime probability of developing the disease (Rojas and Stuckey, 2016). Despite recent medical advances, it is the primary cause of cancer lethality in women (Jemal et al., 2010). Five-year survival rates highlight the ongoing challenge of treating late stage diagnoses, with a survival rate of almost 100% of patients diagnosed with early stage breast cancers which is dramatically reduced to 21% for patients diagnosed with advanced disease (Hayat et al., 2007). Environmental factors such as obesity, alcohol consumption, cigarette smoking, oral contraceptives and increasing age can all influence the development of breast cancer (Rojas and Stuckey, 2016, Althuis et al., 2004). Genetic factors are also implicated in the development of the disease, with germline mutations in the BRCA1 and BRCA2 tumour suppressor genes being associated with a high lifetime risk of 60-85% for developing breast cancer (Ripperger et al., 2009).

As breast cancer is a very heterogeneous disease, it is classified into distinct subtypes by specific molecular markers and clinical treatments (Banin Hirata et al., 2014). The human epidermal growth factor 2 (HER2) receptor is amplified in 30% of breast cancers and is associated with aggressive disease and therefore poor clinical outcomes (Banin Hirata et al., 2014). Although the development of trastuzumab, a monoclonal antibody which targets the HER2 receptor, has significantly improved outcomes (Banin Hirata et al., 2014). Hormone receptor positive tumours overexpress the oestrogen (ER) and progesterone (PR) receptors (Althuis et al., 2004). As these tumours are regulated by hormones, they respond to drugs which target the ER such a tamoxifen (Althuis et al., 2004). Tumours lacking the presence of both hormone and HER2 receptors are known as triple negative breast cancer (TNBC) (Foulkes et al., 2010).

1.1.1 Triple negative breast cancer

Of all breast cancer cases diagnosed 10-20% are TNBC (Costa and Gradishar, 2017). TNBC has a higher incidence in younger, obese and African American women (Lebert et al., 2018).

TNBC are highly heterogeneous and several attempts to classify TNBC into subtypes have been attempted however they are yet to deliver clinical utility (Bianchini et al., 2016). Chemotherapy is the mainstay treatment for TNBC as there is a distinct lack of targeted therapies available for this type of breast cancer (Hudis and Gianni, 2011) highlighting the need for the identification of new therapeutic targets. TNBC are associated with poor prognosis, short progression free and overall survival (Costa and Gradishar, 2017). In fact, on diagnosis TNBC have often already metastasised to the surrounding lymph nodes and are more likely to be diagnosed at a later stage than other forms of breast cancer, due to their more aggressive nature (Dent et al., 2007).

1.1.2 Tumour metastasis

Metastatic disease is the leading cause of cancer mortality (Jemal et al., 2010) and is responsible for approximately 90% of cancer deaths despite the improvements in cancer diagnosis, chemotherapies and surgical techniques (Valastyan and Weinberg, 2011). This highlights the need to develop a clinical strategy to supress metastasis. The metastatic cascade's multistep nature offers various molecular opportunities for pharmacological intervention, however understanding the molecular mechanisms is crucial to identify novel therapeutic targets (Palmer et al., 2011).

Metastatic disease is the dissemination of cancer cells from the primary site of origin to distant non-native tissue. Cancer cells invade into the surrounding stroma and neighbouring tissues, leading to intravasation into the bloodstream. These cells are then transported via the circulation, extravasate out of the bloodstream and proliferate to form distant metastases (Valastyan and Weinberg, 2011) **(Figure 1.1)**. This process, known as the metastatic cascade, involves the tight co-ordination of cell motility and invasion away

from the primary tumour, cell survival in non-permissive environments and proliferation at distant sites.

Epithelial to mesenchymal transition (EMT) is associated with metastasis as non-invasive cancer cells from the primary tumour transform into migratory and motile cells. SNAIL, TWIST and TGFβ signalling are key inducers of EMT as they regulate early events of the transition such as loss of E-cadherin expression and apicobasal cell polarity (Thiery et al., 2009). The mesenchymal phenotype characterised by front to rear polarity is established by the RhoGTPases when induced by extracellular signals such as hepatocyte growth factor (HGF), epidermal growth factor (EGF) and Insulin- like growth factor 1 (IGF1) (Lamouille et al., 2014). Once EMT has occurred, invasive cancer cells need to penetrate the basement membrane, this is achieved by secretion of matrix metalloproteases (MMPs), enzymes which degrade the extracellular matrix (ECM) (Kessenbrock et al., 2010). Increased expression of MMP9 is found to correlate with higher rates of metastasis in aggressive HER2 positive and triple negative breast cancers (Yousef et al., 2014). In animal models, inhibition of MMPs have been shown to prevent cancer cell invasion however they failed to improve clinical outcomes in human clinical trials (Kessenbrock et al., 2010). It is speculated that this is due to MMP function being more complex then degradation enzymes, as they also play a role in signalling pathways to regulate proliferation and apoptosis (Kessenbrock et al., 2010). Finally, once the invading cancer cells have penetrated the basement membrane, they interact with the tumour supporting stroma containing further environmental cues and a variety of cells including macrophages, adipocytes and endothelial cells, which further enhance invasive behaviour (Valastyan and Weinberg, 2011).

Breast cancer is able to metastasise to other organs, most commonly the lungs, liver and bone (Weigelt et al., 2005). Different subtypes of breast cancer preferentially metastasise to different non-native sites. The bone is the most common site of hormone receptor positive breast cancers metastasis (Lorusso and Ruegg, 2012) whereas triple negative breast cancers rapidly spread to visceral organs such as the liver and lungs (Dent et al., 2009). Only 6% of breast cancer patients initially present with metastatic disease at

diagnosis however 30% of patients diagnosed with early stage breast cancers will develop metastatic disease (O'Shaughnessy, 2005).

Recently, a new term ‘migrastatics’ has been coined which specifically refers to drugs that interfere with all modes of cancer cell migration and invasion (Gandalovicova et al., 2017). Using antimetastatic drugs alongside antiproliferative therapy could prevent both the growth and spread of cancer to prevent metastasis occurring.

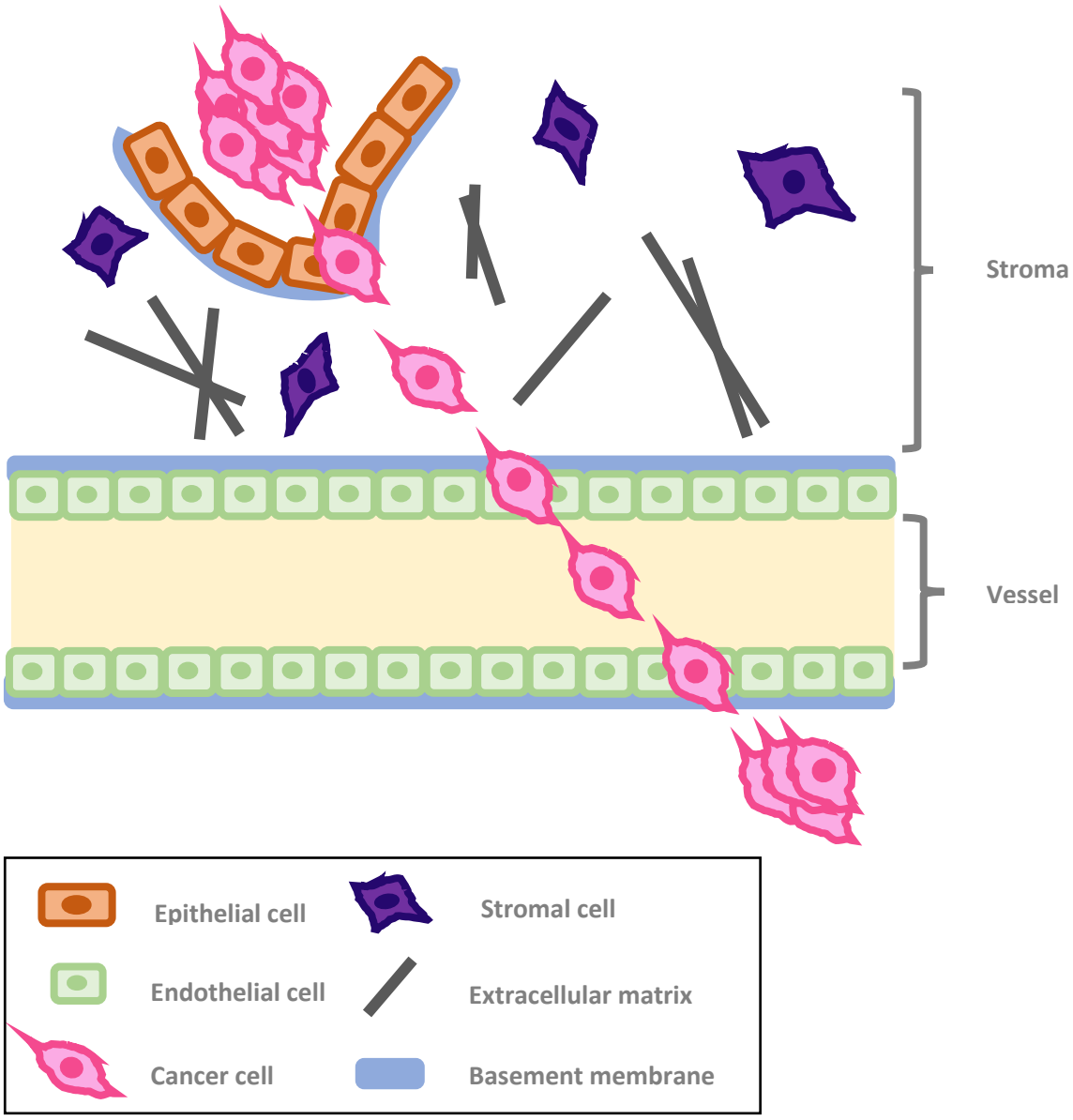

Figure 1.1 Schematic diagram of the metastatic cascade. Cells from the primary tumour penetrate the basement membrane and invade into the surround stromal tissue. Cells are then able to intravasate into the vasculature and lymphatic systems where they travel around the body. Cancer cells can then extravasate, colonise and proliferate at non-native sites to form metastases.

1.2 The importance of cell migration

Cell migration is an essential process which plays a vital role in morphogenesis, wound healing, tissue repair and immune surveillance (Ridley et al., 2003). It's a complex multi-step and highly coordinated process that in the context of cancer can result in the formation of metastases (Valastyan and Weinberg, 2011). Understanding the mechanisms involved in cell migration and the metastatic cascade could provide novel therapeutic targets to prevent cancer metastasis.

1.2.1 Modes of Cell migration

In normal cells, migration can be grouped into mechanically distinct stages due to the regulation of the cytoskeleton, cell-cell adhesions and cell-matrix adhesions. Cells become polarised and produce broad protrusions and finger-like protrusions at the leading edge, termed lamellipodia and filopodia respectively. New cell-matrix adhesions are formed to anchor the cell to the ECM. This produces traction forces allowing cell body contraction (Friedl and Alexander, 2011). This coupled with the membrane retraction and degradation of cell adhesions at the rear of the cell results in forward movement and cell migration (Friedl and Alexander, 2011, Ridley, 2011).

Cancer cells can migrate through the ECM during the metastatic cascade as either individual cells or as a group, termed single cell and collective migrations respectively (Friedl and Wolf, 2003, Sanz-Moreno and Marshall, 2010) **(Figure 1.2)**. There are two methods of single cell migration, mesenchymal and amoeboid.

Mesenchymal cells have a fibroblast-like elongated and polarised morphology and migrate in the multistep process similar that of normal cells. However mesenchymal migration relies on the secretion of MMPs form invadopodia, actin rich protrusions from the plasma membrane which degrade the ECM and permit invasion (Murphy and Courtneidge, 2011). Amoeboid migration occurs when cells of a spherical morphology, characterised by rapid deformability, squeeze through strands in the ECM. High intracellular hydrostatic pressure allows membrane blebs to form which sense the surrounding ECM. Amoeboid cells also

possess high actin myosin contractility and low adhesion forces meaning cell migration is driven by a propulsive mechanism (Friedl and Wolf, 2003).

Collective cell migration occurs when multiple cells migrate as a group, this can be within sheets, clusters or streaming (Friedl and Wolf, 2010). During collective cell migration cell-cell adhesions (such as cadherins) and cell-matrix adhesions (such as integrins) are not degraded (Sahai, 2005). Both types of cell migration, single and collective, are not mutually exclusive and can occur simultaneously in cancer migration (Friedl and Wolf, 2003). For example, in collective cell migration, migration tracks are formed by the presence of one or multiple leader cells with utilise a mesenchymal-like mode of migration to degrading the ECM ahead of the collective cell mass (Friedl, 2004).

Cellular plasticity refers to the ability of a cell to modulate its phenotype based on its surrounding environment, this concept allows cancer cells to not only survive in but migrate through different tissues (Friedl and Alexander, 2011). Cellular morphology and mode of migration can differ greatly based on extracellular matrix properties and the adhesive and proteolytic capabilities of a cell (Friedl and Wolf, 2010). For example, cells in soft matrices favour an amoeboid-like mode of migration (Krakhmal et al., 2015) whereas a matrix of an increased stiffness in 3D migration promotes formation of focal adhesions and cell elongation which are both characteristics of mesenchymal-like migration (Friedl and Wolf, 2010).

Furthermore, studies into breast cancer cells have demonstrated the ability of cells to adapt their mode of migration based on their proteolytic capacities. Untreated MDA-MB-231 cells display a mesenchymal-like mode of migration, generating proteolytic degradation tracks in 3D collagen matrices, however when treated with protease inhibitors the cells migrate by propulsive squeezing between pre-existing gaps in the matrix, an amoeboid-like mode of migration (Wolf et al., 2003).

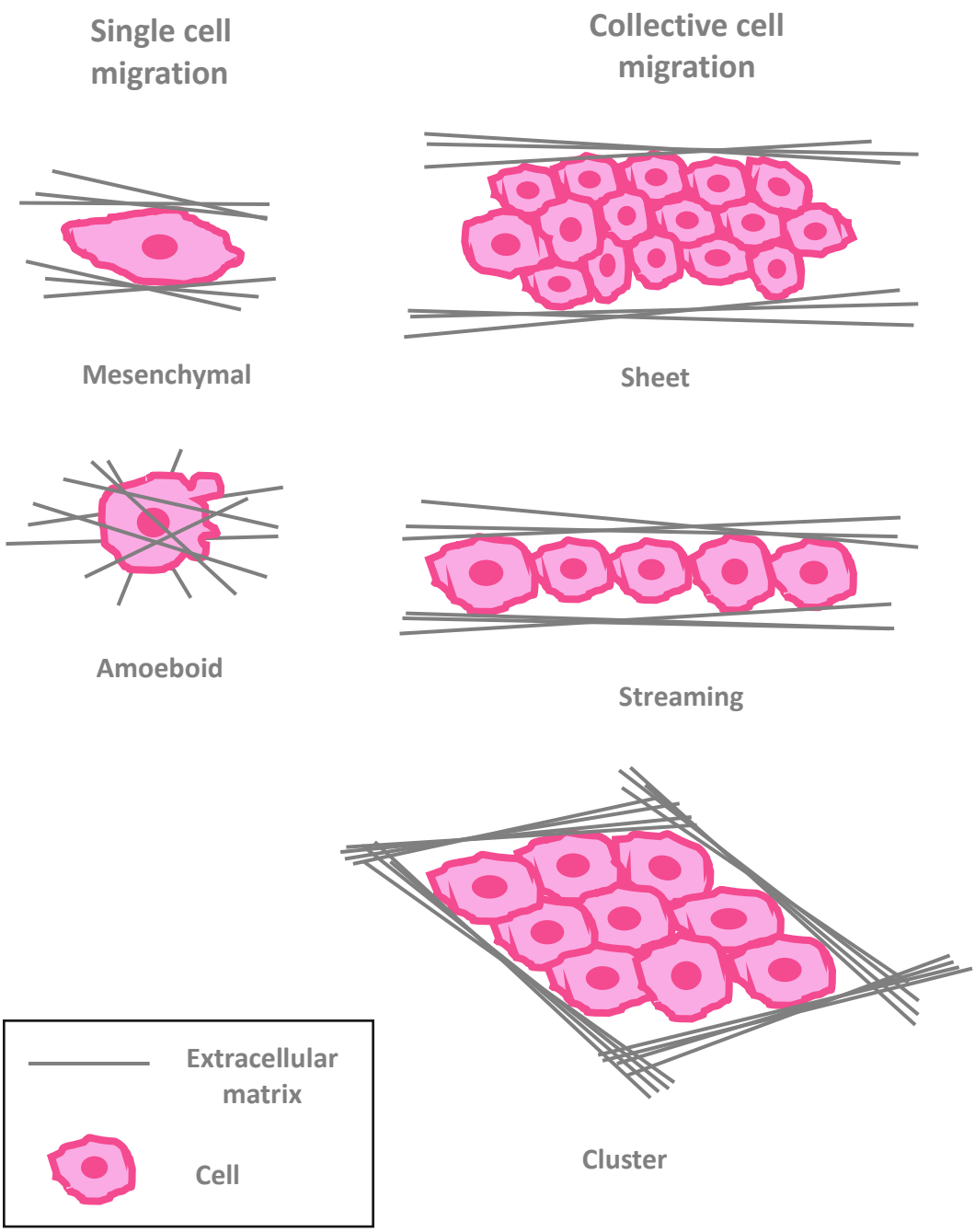

Figure 1.2 A schematic diagram of the modes of cancer cell migration. Cells can invade by single cell or collective cell migration. Single cell migration consists of both mesenchymal and amoeboid modes of migration, characterised by elongated cells and matrix degradation, and rounding blebbing cells with high contractility respectively. In collective cell migration, cells migrate with cell-cell adhesions intact in sheets, files or clusters.

1.2.2 The role of cell spreading in cell migration

Two distinct types of cell spreading occur and are reportedly studied in the literature; these are known as early and late spreading. Early spreading, also termed nascent spreading, refers to the initial attachment of a cell to a matrix or coverslip. Whilst both early cell spreading and cell migration require the deformation of the plasma membrane and formation of cell-matrix adhesions they are thought to be two distinct phenomena (McGrath, 2007). Fundamental differences between early and late spreading have been identified. Early cell spreading is a passive process while late cell spreading is an active process (McGrath, 2007).

Early cell spreading can be grouped into three stages- the initial stage where the cell body attached to its substrate, the flattening and spreading of the cell body, and finally the formation of focal adhesions between the cell and its substrate and the organisation of the actin cytoskeleton (Khalili and Ahmad, 2015). When integrins, transmembrane proteins, are active they can bind components of the ECM to initiate the formation of cell-matrix adhesions (Khalili and Ahmad, 2015). These initial integrin-mediated adhesions attach the cell actin cytoskeleton to the ECM and stimulate bidirectional signalling pathways (Khalili and Ahmad, 2015). A major group of proteins activated downstream of integrin and ECM binding are the Rho GTPases (Hall, 1998). Activation of Rho GTPases results in the organisation of the actin cytoskeleton, stabilisation of cell-ECM adhesions and cell spreading (Khalili and Ahmad, 2015).

Late cell spreading involves actin polymerisation and myosin contraction causing polarised cells to crawl, a process that is essential at the leading edge of a migratory cell (McGrath, 2007, Dobereiner et al., 2004, Dubin-Thaler et al., 2004). The Rho GTPases are known to play a critical role in late cell spreading during cell migration (Sit and Manser, 2011). Cell migration and therefore cancer metastasis is powered by the constant turnover and reorganisation of the actin cytoskeleton (Yamaguchi and Condeelis, 2007).

1.2.3 Actin dynamics in cell migration

Cell migration is dependent on the dynamic processes of the actin cytoskeleton (Ridley et al., 2003). The actin cytoskeleton is comprised of filamentous actin (F-actin) which are thin flexible polymeric fibres made up of individual monomers of globular actin (G-actin) (Jiang et al., 2009). In an adenosine triphosphate (ATP) dependent manner, G-actin is added to the fast-growing barbed end (+) of F-actin. Simultaneously, at the slow-growing pointed end of F-actin, hydrolysis of ATP on the G-actin monomers to adenosine diphosphate (ADP) causes these monomers to dissociate creating a functional polarity for F-actin (Jiang et al., 2009). The continuous assembly, disassembly and reorganisation of actin filaments is modulated by regulatory proteins, such as the actin-related proteins 2/3 (Arp2/3) complex and capping proteins. The Arp2/3 complex is a seven-subunit protein complex which allows branching of F-actin by creating new nucleation cores ensuring continuous assembly of F-actin at the leading edge of a migratory cell (Welch et al., 1997). Capping proteins, such as CapZ and gelsolin, ensure a defined cell shape for migration as they bind the barbed ends of F-actin to prevent the association and dissociation of G-actin (Cooper and Sept, 2008).

Different geometric organisation of F-actin allows the formation of various architectural structures which influence cell migration. For example, branched and cross-linked filaments constitute lamellipodia formation whereas parallel actin filaments constitute filopodia formation (Blanchoin et al., 2014). Finally, a network of cross-linked actin filaments causes the formation of stress fibres, an entity which provides the structural basis for maturation of focal adhesions, another important regulator of cell migration (Blanchoin et al., 2014).

1.2.4 Focal adhesions in cell migration

Focal adhesions allow attachment of the cell to the ECM and are essential for many processes such as cellular proliferation, survival, differentiation, cellular morphology and migration (Nagano et al., 2012). Tight control of their assembly and disassembly is crucial

for efficient cell migration. Firstly, the protrusions forming at the leading edge of a migrating cell need to be stabilised. Nascent adhesions form under the lamellipodia which activate proteins to cause actin polymerisation resulting in subsequent protrusions. Failure of adhesion formation at the leading edge results in membrane ruffle formation without distinct polarity (Parsons et al., 2010). The nascent adhesions mature and generate tension forces to enable cell contractility. In contrast, adhesions at thea rear of the cell must dissociate for cell retraction to occur, allowing movement in the direction of migration (Nagano et al., 2012).

Focal adhesions form when transmembrane integrins cluster at the site of cell-ECM contact. The intracellular domains of the integrins recruit scaffold/adaptor which connect the focal adhesions to the cell's actin cytoskeleton. Important adaptor proteins are talin, paxillin, vinculin, zyxin, tensin and α-actinin (Huttenlocher and Horwitz, 2011) . The linkage of focal adhesions and actin cytoskeleton generates tension and traction forces necessary for cell morphology and migration respectively (Nagano et al., 2012).

Integrins also recruit signalling proteins which transmit extracellular signals to their downstream effectors resulting in cellular responses such as proliferation, survival and migration (Huttenlocher and Horwitz, 2011). Integrins have no enzymatic activity and therefore rely on signalling proteins to transmit signals to cellular machinery via signalling cascades. One of the most noted and important signalling proteins in focal adhesions is focal adhesion kinase (FAK) (Huttenlocher and Horwitz, 2011).

1.2.5 Focal adhesion kinase

FAK is a cytoplasmic tyrosine kinase heavily implicated in the turnover of focal adhesions and therefore cell migration (Nagano et al., 2012). Cells from FAK knockout mice have an increase number of focal adhesions and reduced mobility (Ilic et al., 1995). Furthermore, both cancer cells and fibroblasts with FAK depletion have higher numbers of larger peripheral adhesions with impaired turnover and reduced migration (Sieg et al., 2000, Hsia et al., 2003, Webb et al., 2004, Chan et al., 2009).

Multiple pathways implicate FAK in focal adhesion turnover. A downstream target of FAK, paxillin, is a key regulator of adhesion dynamics (Brown et al., 2005) as it is associated with many effector proteins, including GIT1, PAK1-interacting exchange factor (PIX) and p21-activated kinase (PAK), all of which have a known involvement of focal adhesion regulation (Ballestrem et al., 2006). Further, FAK is able to cause adhesion disassembly through interactions with cytoskeletal regulatory proteins or regulation of calpain, extracellular-signals regulated kinase (ERK) and myosin-light chain kinase (MLCK) (Webb et al., 2004, Carragher et al., 2003).

Although there are many ways in which FAK can influence focal adhesion turnover the most established and studied mechanism is by the ability of FAK to regulate the Rho GTPases. The scaffold function FAK possesses plays an important role in recruiting proteins which can activate or inhibit the Rho GTPases, which are the master regulators of cell migration (Huttenlocher and Horwitz, 2011).

1.3 The Rho GTPase family

The Rho GTPases form a subgroup of the Ras-like protein superfamily of GTPases. Twenty human Rho GTPases have been identified and are involved in a wide range of cellular processes such as cell division, transcriptional regulation, phagocytosis, vesicular trafficking, cytoskeletal regulation, cell migration and cell adhesions (Jaffe and Hall, 2005). The Rho GTPases are divided into two groups - classical and atypical Rho GTPases. Classical Rho GTPases are the best studied in actin cytoskeletal regulation and cell motility (Sit and Manser, 2011).

The classical Rho GTPases act as molecular switches that cycle between an inactive GDP-bound conformation and an active GTP-bound conformation. In this active conformation the Rho GTPases can interact with their downstream target proteins to induce cellular responses **(Figure 1.3)**. There are three types of protein that can regulate classical Rho GTPases. GTPase-activating proteins (GAPs) enhance the intrinsic GTP hydrolysis activity of the Rho GTPases rendering them inactive whereas guanine nucleotide exchange factors (GEFs) activate the Rho GTPases by promoting the exchange of GDP to GTP (Bos et al., 2007). Finally, Rho guanine-nucleotide-dissociation inhibitors (GDIs) bind the GDP-bound Rho GTPase proteins sequestering the inactive protein in the cytosol extracting them from cellular membranes and preventing downstream signalling (Fukumoto et al., 1990, Leonard et al., 1992). The most studied role of the RhoGTPases is their ability to regulate cell migration. This concept stems from observations that the Rho GTPase proteins can mediate the formation of specific actin-containing structures.

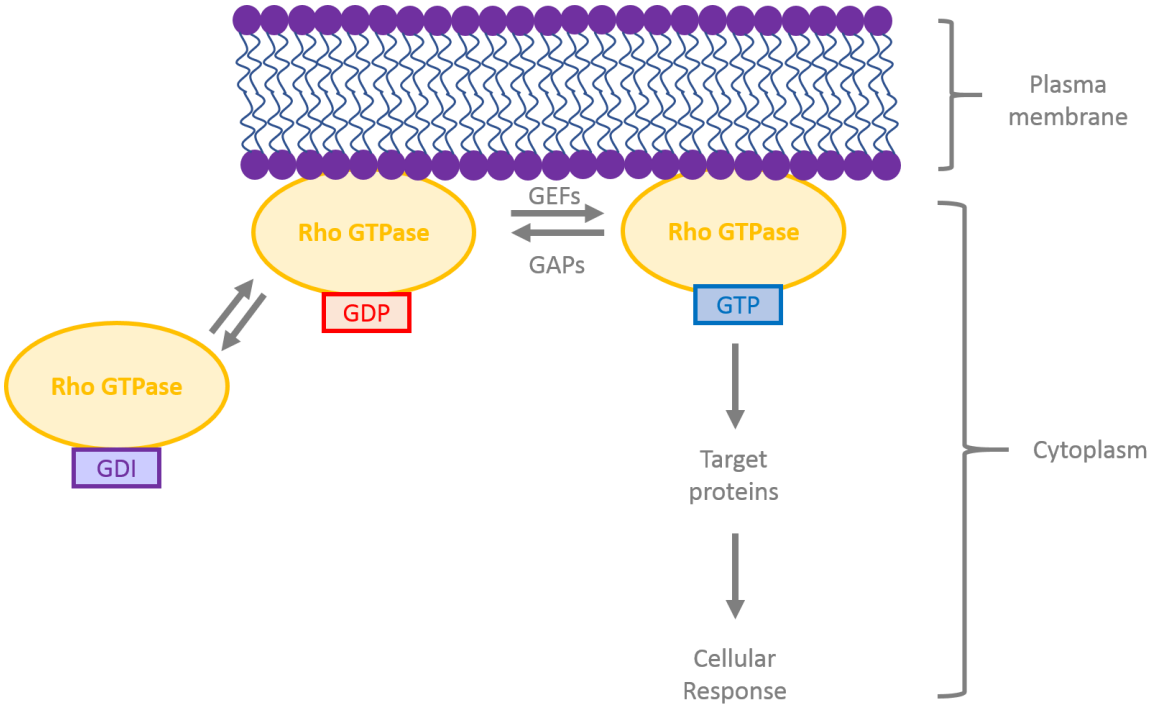

Figure 1.3 Regulation of the Rho GTPases. GDIs sequester Rho GTPases in the cytoplasm, away from sites of activation and prevents their downstream signalling. At the plasma membrane inactive GDP-bound Rho GTPases are activated by GEFs allowing signalling to downstream proteins causing cellular responses. GAPs inactive active GTP-bound Rho GTPases.

1.3.1 Rho GTPases in cell migration

The three most characterised Rho GTPases in cell motility and organisation of the actin cytoskeleton are Ras homolog gene family member A (RhoA), Ras-related C3 botulinum toxin substrate 1 (Rac1) and cell division control protein 42 (Cdc42) and will therefore be discussed herein (Sit and Manser, 2011). Both Rac1 and Cdc42 drive cell migration as they aid the formation of actin based protrusive structures at the cells leading edge. Rac1 activity is required for the formation of lamellipodia whereas Cdc42 activity is associated with the formation of filopodia (Nobes and Hall, 1995). Interestingly Cdc42 and Rac are also implicated in the formation of filopodia and lamellipodia in nascent cell spreading (Price et al., 1998). Initial studies of RhoA highlight its importance in cell body contraction however the recent development of RhoA biosensors have indicated a role for RhoA in the formation of membrane ruffles at the cells' leading edge (Donnelly et al., 2014).

Rac1, Cdc42 and RhoA's downstream targets and their roles in cytoskeletal regulation have been well studied. Rac1 and Cdc42 can initiate the formation of SCAR/WAVE (suppressor of cAMP receptor/WASP verprolin-homologous) and WASP (Wiskott-Aldrich Syndrome Protein) respectively (Parsons et al., 2010) **(Figure 1.4)**. The formation of SCAR/WAVE and WASP activates the Arp2/3 complex allowing actin nucleation and branching to occur (Parsons et al., 2010). Rac1 also plays a role in the removal of capping proteins from the barbed ends of F-actin, allowing actin polymerisation. Phosphatidylinositol-4,5-bisphosphate (PIP2) can remove capping proteins such as gelsolin when synthesised on Rac1 binding to phosphatidylinositol-4-phosphate 5-kinase (PIP 5-kinase) (Tolias et al., 2000) **(Figure 1.4)**.

Rac1, Cdc42 and RhoA are all able to regulate cofilin via LIM kinase (LIMK). Rac1 and Cdc42 activate PAK1 which in turn phosphorylates and activates LIMK (Edwards et al., 1999) **(Figure 1.4)**. RhoA activates ROCK (Rho-associated, coiled-coil containing protein kinase 1) which is also able to activate LIMK (Ohashi et al., 2000) **(Figure 1.4)**. Once activated, LIMK can phosphorylate cofilin to inactivate and inhibit its actin severing activity allowing actin filament stabilisation and growth (contractility, as ROCK can directly phosphorylate

myosin-light chain (MLC) and also inhibit MLC phosphatase (Fukata et al., 2001, Parri and Chiarugi, 2010) **(Figure 1.4)**. A formin, Diaphanous-related formin (mDia), also activated downstream of RhoA, enables the addition of G-actin monomers to the barbed end of F-actin allowing actin polymerisation (Jaffe and Hall, 2005) **(Figure 1.4)**.

Rac1, Cdc42 and RhoA are implicated in the formation of focal adhesions which play an essential role in cell migration. ROCK and mDia activation downstream of RhoA promotes the formation of dorsal stress fibres (Le Clainche and Carlier, 2008) **(Figure 1.4)**. Focal adhesions associate to the end of stress fibres at the plasma membrane during cell motility (Ridley and Hall, 1992). This connection enhances cell contractility (Huttenlocher and Horwitz, 2011). RhoA also plays a role in the maturation of focal contacts, whilst Rac1 and Cdc42 are responsible for the formation of initial focal attachments to the ECM (Nobes and Hall, 1995, Ridley and Hall, 1992, Rottner et al., 1999).

The Rho GTPases also regulate focal adhesion turnover, another vital process required for efficient cell migration. Upon Rac1 induced activation, PAK1 can interact with paxillin to cause the disassembly of focal adhesions (Zhao et al., 2000, Ridley, 2001). Further to its role in cell contractility, RhoA is responsible for focal adhesion disassembly at the rear of the cell causing cell retraction in the direction of migration (Huttenlocher and Horwitz, 2011).

As the Rho GTPases have differing roles in cell migration there is tight spatial and temporal regulation of the proteins which in part is maintained by significant cross talk between these three Rho GTPases. RhoA and Rac1 have an antagonistic relationship. RhoA can inhibit Rac1 activity by activating the Rac-GAP, ARHGAP22 (Parri and Chiarugi, 2010) **(Figure 1.4)**. However, Rac1 can inhibit RhoA activity by activation of a Rho GAP called p190RhoGAP (Mammoto et al., 2007) **(Figure 1.4)**. This results in a bistable relationship between the two Rho GTPases ensuring efficient cell migration as high Rac1 and low RhoA activity is required for cells to protrude whereas low Rac1 and high RhoA activity is required for cell contraction (Byrne et al., 2016). Interestingly FAK plays a role in interplay between RhoA and Rac1 in adhesion turnover. FAK deficient fibroblasts exhibit

constitutively active RhoA activity which stabilises adhesions (Ilic et al., 1995). However, FAK signalling can also activate p190RhoGAP to inhibit Rho activity and recruit and activate a Rac containing complex (Schober et al., 2007).

Cdc42 can also regulate the activity of both RhoA and Rac1. The Cdc42-ßPIX complex formed at the cells leading edge during cell motility binds to srGAP1, a protein which suppresses RhoA activity (Kutys and Yamada, 2014) **(Figure 1.4)**. Interestingly ßPIX is a Rac-GEF which is activated by Cdc42. Cdc42's ability to activate the Rac-GEFs such as ßPIX and TIAM1, in turn activates Rac1 and recruits it to the front of the cell to maintain cell polarity and directional migration (Cau and Hall, 2005) **(Figure 1.4)**.

The Rho GTPases have many downstream effectors influencing cell migration. The most notably downstream effectors of Rac1 and Cdc42 are the PAK family which also play an important role in the regulation of the cytoskeleton and focal adhesions during cell motility (King et al., 2014).

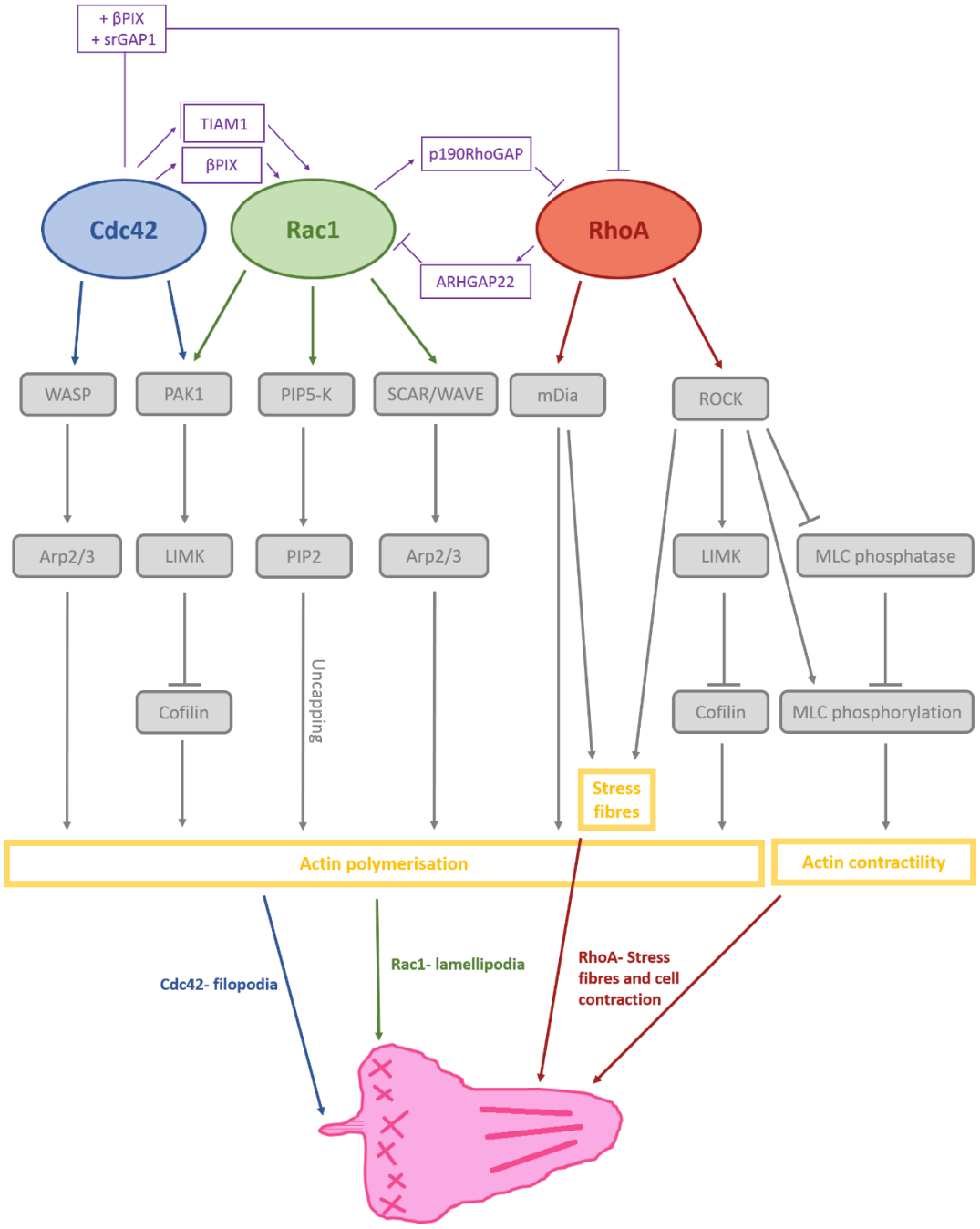

Figure 1.4 Rho GTPase effector pathways that regulate cytoskeletal dynamics. Cdc42 and Rac1 are predominantly associated with filopodia and lamellipodia formation respectively. This occurs by the activation of LIMK via PAK1 to inhibit cofilin's actin severing abilities and by promoting the formation of the Arp2/3 complex via WASP for Cdc42 and SCAR/WAVE for Rac1. Rac1 is also implicated in the PIP5-PIP2 signalling pathway which results in uncapping of actin filaments. RhoA signals to mDia and ROCK causing formation of stress fibres and actin polymerisation, as ROCK can inhibit cofilin via LIMK. RhoA signalling via ROCK also causes an increase in MLC phosphorylation inducing actin contractility. Cross talk between the RhoGTPases ensures efficient cell migration. Cdc42 can enhance Rac1 activation via TIAM1 and βPIX and inhibit RhoA activity via βPIX and srGAP1. RhoA activates ARHGAP22 to inhibit Rac1, and Rac1 activates p190RhoGAP to inhibit RhoA.

1.4 The p-21 activated kinase family

The PAK family is a family of serine/threonine kinases involved in a wide range of cellular processes such as cell survival, proliferation, motility and gene transcription (King et al., 2014). There are six members of the family, divided into two groups, PAK1-3 (group I) and PAK4-6 (group II) based on similarities in their sequences, domains and regulation (Arias-Romero and Chernoff, 2008) **(Figure1.5)**. The PAK proteins are highly conserved in a wide range of organisms including yeast, *Caenorhabditis elegans*, *Drosophila melanogaster* and humans (Bokoch, 2003).

All group I PAKs exhibit high expression in the brain, especially PAK3 where this protein is predominantly expressed (Arias-Romero and Chernoff, 2008). Indeed, the PAK3 knockout mouse model exhibits abnormalities in synaptic plasticity and defects in learning and memory (Kelly and Chernoff, 2012). PAK2 is ubiquitously expressed and the PAK2 knockout mouse model is lethal at E8 due to developmental defects (Kelly and Chernoff, 2012). PAK1 is found at high levels in the heart, liver, spleen and muscle. The PAK1 mouse knockout model is viable but exhibits immune, glucose homeostasis and neuronal defects, and cardiac hypertrophy on pressure overload (Kelly and Chernoff, 2012). PAK4 is expressed highly throughout development and knock out of the protein is embryonically lethal at E11.5 in mice, owing to foetal heart defects, such as enlargement of the right atria and ventricle and thinning of the myocardium (Qu et al., 2003). In adulthood is it thought to be ubiquitously expressed with high levels present in the colon, prostate and testis (Kelly and Chernoff, 2012). PAK6 is also found at high levels in the prostate and testis, as well as the placenta, breast, brain and kidney (Kelly and Chernoff, 2012). Finally, PAK5 is expressed in the pancreas, testes, prostate and adrenal gland. Both the PAK5 and PAK6 knockout mouse models are healthy and viable (Kelly and Chernoff, 2012).

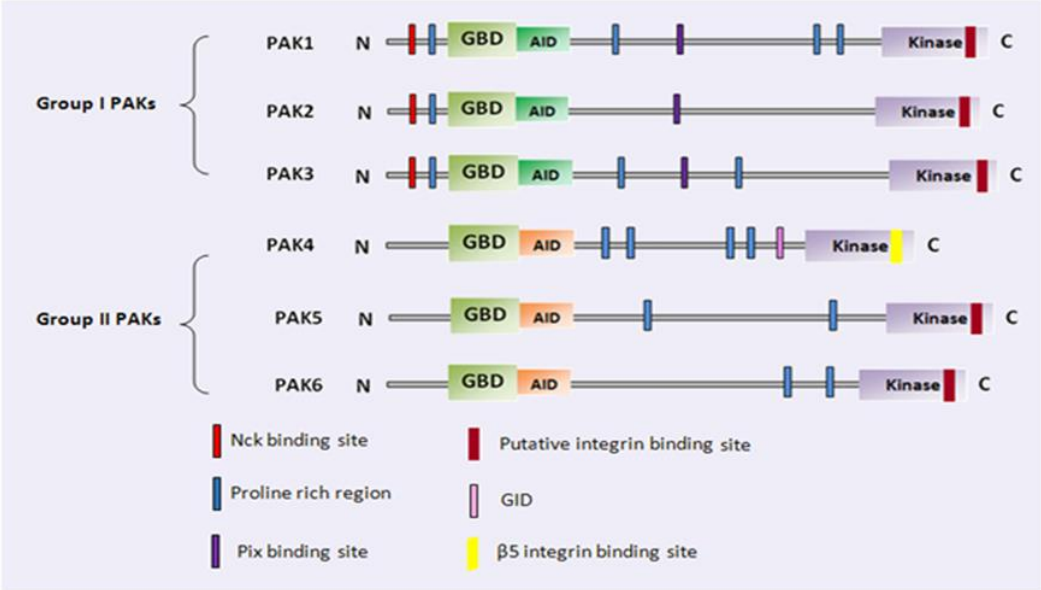

Figure 1.5 p21-activated kinase family structures. The structures of group I (PAK1-3) and group II (PAK4-6) PAKs. All PAKs have an N-terminal p21-GTPase binding domain (GBD) and a C-terminal kinase domain. Group I PAKs also contain an autoinhibitory domain (AID), a PIX binding site (purple), a putative integrin binding site (dark red) and variable numbers of proline rich regions (blue). The group II PAKs all also contain variable numbers of the proline rich regions and a putative AID. PAK3 and 4 contain, like the group I PAKs, a putative integrin binding site (dark red). PAK4 contains a GEF/GRB2-associated-binding protein 1 (Gab1) interacting domain (GID) (pink) and the β5 integrin binding site (yellow).

1.4.1 PAK domain structure and regulation

All six PAK proteins possess an N-terminal p21-GTPase-binding domain (GBD) and a highly conserved C-terminal serine/threonine kinase domain (Arias-Romero and Chernoff, 2008) **(Figure 1.5)**. However intervening sequences differ between group I and group II PAKs leading to differences in regulation.

Group I PAKs have an autoinhibitory domain (AID) which overlaps the N-terminal GBD, blocking protein activation (Lei et al., 2000). Inactive group I PAKS form inhibitory *trans*-homodimers where an AID of one protein will inhibit the kinase domain of another (Parrini et al., 2002). The main method of activation for group I PAKs is the binding of the RhoGTPases, Cdc42 and Rac1, to the GBD **(Table 1.1)**. This releases the dimer and allows the PAK to autophosphorylate itself at threonine 423, threonine 402 and threonine 421 for PAK1, PAK2 and PAK3 respectively, rendering the proteins active (Zenke et al., 1999, Arias-Romero and Chernoff, 2008) **(Figure 1.6)**. The ability of PAK2 and PAK3 to form homodimers has not previously been investigated however due to their high sequence homology within the binding sites to PAK1 it is assumed they are capable of dimerization (Combeau et al., 2012). Interestingly the PAK3 gene can produce spliced variant of the protein that are constitutively active. These variants favour heterodimerisation with PAK1 rather than homodimers (Kreis et al., 2008, Combeau et al., 2012).

Many proteins including the Rho GTPases can influence PAK1 activity by protein-protein interactions. Group I PAKs have N terminal non-catalytic region of tyrosine kinase adaptor protein (Nck) binding sites **(Figure 1.5) (Table 1.1)**. On Nck binding to PAK1 it is localised to the plasma membrane where Rho GTPases can activate it (Lu and Mayer, 1999). Other adaptor proteins such as growth factor receptor-bound protein 2 (Grb2) can influence PAK1 activity **(Table 1.1)**. On PAK1 and Grb2 binding, via the N terminal proline region of PAK1 and an SH3 domain on Grb2, the PAK1/Grb2 complex localises to the plasma membrane. Here PAK1 can be activated by the epidermal growth factor receptor (EGFR) (Puto et al., 2003). Active 3-phosphoinositide-dependent kinase 1 (PDK1) in the presence

of sphingosine can also activate PAK1 by phosphorylating it at threonine 423, its autophosphorylation site (King et al., 2000) **(Table 1.1)**.

PAK1 can also be negatively regulated by protein-protein interactions. Many proteins such as PKA (protein kinase A), PP2A (phosphatase type 2A) and POPX1 and POPX2 (partner of PIX 1 and 2) can dephosphorylate PAK1 rendering it inactive (Howe and Juliano, 2000, Koh et al., 2002) **(Table 1.1)**. Proteins which directly bind the N-terminus of PAK1 can cause an inhibitory effect on PAK1 activity such as human PAK1-interacting protein, CRIPak (cysteine rich inhibitor of PAK1) and merlin (Talukder et al., 2006, Xia et al., 2001, Kissil et al., 2003) **(Table 1.1)**. Finally, a microRNA (miR-7) targets the 3'-untranslated region of PAK1 mRNA inhibiting its translation into the PAK1 protein (Reddy et al., 2008).

The method of regulation of group II PAKs remains controversial. It was previously thought PAK4 activity was dependent on phosphorylation at serine 474 however this site has been demonstrated to be constitutively phosphorylated (Ha et al., 2012). Two proposed mechanisms of PAK4 activation exist. The first mechanism asserts it is in a very similar manner to how group I PAKs are regulated. It is thought there is an N-terminal region, an AID at amino acids 20-68, binds the GBD and holds PAK4 in an inactive form. Upon Cdc42 binding to the GBD, there is a conformational change which allows PAK4 to become active (Baskaran et al., 2012) **(Figure 1.6)**. The second mechanism asserts an N-terminal pseudosubstrate motif with a crucial proline residue (R^{49}PKPLV) inhibits the kinase domain and subsequently the kinase activity of PAK4. Activation occurs when a protein containing an SH3 domain binds PAK4, allowing the autoinhibition to be relieved (Ha et al., 2012) **(Figure 1.6)**.

Being the most notable downstream effectors of Cdc42 and Rac1 the PAKs, like the RhoGTPases, play a key role in proliferation, the cell cycle, cell movement and apoptosis. As these cellular processes are heavily involved in cancer survival and progression, it is not surprising the PAKs are implicated in many cancer types. The PAK1 isoform is the most implicated of the PAK family members in cancer (King et al., 2014).

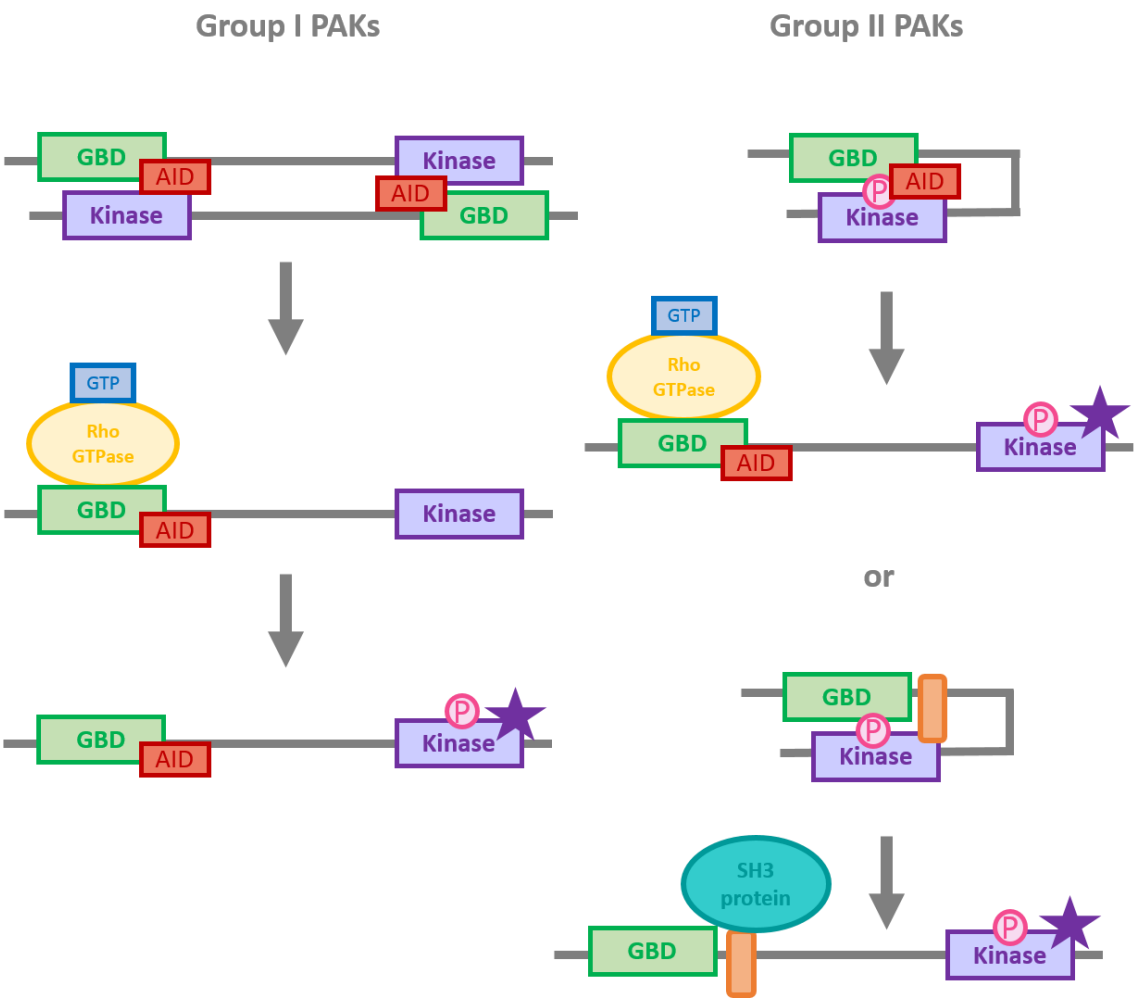

Figure 1.6 Regulation of group I and group II PAKs. Inactive group I PAKs form homodimers where the AID of one monomer inhibits the kinase activity on the opposing monomer, and visa versa. The homodimers dissociate on Rho GTPase binding to the GBD domain. This allows autophosphorylation to occur and therefore the activation of the group I PAKs. Phosphorylation of the kinase domain is indicated by a P (pink) and an active kinase domain is indicated by the presence of a star (purple). There are two proposed mechanisms for group II PAK activation. First, the AID of the PAK inhibits the kinase domain on the same protein. On Rho GTPase binding to the GBD the AID domain releases the kinase domain rendering it active. The second group II activation mechanism places an N terminal psuedodomain (orange) in the kinase cleft causing kinase inactivity. On binding on an SH3 domain containing protein the psudeosubstrate releases the kinase domain rendering it active.

Protein	Regulator/effector of PAK1	Function	Reference
Cdc42	Regulator	Activates PAK1 by binding to the GBD and relieving PAK1 heterodimerisaton	King et al. (2014)
Rac1	Regulator	Activates PAK1 by binding to the GBD and relieving PAK1 heterodimerisaton	King et al. (2014)
Nck	Regulator	Binds and translocates PAK1 to the plasma membrane	Lu and Mayer. (1999)
Grb2	Regulator	Binds and translocates PAK1 to the plasma membrane	Puto et al. (2003)
PDK1	Regulator	Phosphorylate and activate PAK1	King et al. (2000)
PKA	Regulator	Dephosphorylation and inactivation of PAK1	Howe and Juliano. (2000)
PP2A	Regulator	Dephosphorylation and inactivation of PAK1	Koh et al. (2000)
POPX1 POPX2	Regulator	Dephosphorylation and inactivation of PAK1	Koh et al. (2000)
CRIPak	Regulator	Binds N terminal of PAK1 inhibiting its activation	Talukder et al. (2006)
Merlin	Regulator	Binds N terminal of PAK1 inhibiting its activation	Kissil et al. (2003)
ER	Effector	PAK1 phosphorylates to promote ER signalling	Holm et al. (2006)
LIMK	Effector	PAK1 phosphorylates to activate thus causing downstream inhibition of cofilin allowing actin polymerisation	Edwards et al. (1999) Arber et al. (1998)

Myosin light chain	Effector	PAK1 phosphorylates to induce cellular contractility and stress fibre formation	Stockton et al. (2004)
Filamin A	Effector	PAK1 binds to induce membrane ruffling	Vadlamudi et al. (2002)
P41-Arc	Effector	PAK1 phosphorylates to promote formations of the Arp2/3 complex	Vadlamudi et al. (2004)
PDK1	Effector		
Raf	Effector	PAK1 phosphorylates to promote MAPK signalling	Aksamitiene et al. (2011)
Mek	Effector	PAK1 phosphorylates to promote MAPK signalling	Aksamitiene et al. (2011)
Paxillin	Effector	PAK1 phosphorylates to promote GIT1 binding causing translocation to focal adhesions	Nayal et al. (2006)
Snail	Effector	PAK1 phosphorylates causing translocation to the nucleus inhibiting e-cadherin expression	Whale et al. (2011) Elloul et al. (2010)
CRKII	Effector	PAK1 phosphorylates to cause a downstream decrease in p120-catenin expression	Rettig et al. (2012)

Table 1.1 PAK1 regulators and effectors

1.4.2 PAK1 in cancer

PAK1 is thought to be involved in multiple aspects of cancer, including cell proliferation and survival, as well as resistance to apoptosis and cell migration due to three different alterations (King et al., 2014) **(Table 1.2)**. PAK1 overexpression has been linked to breast, colorectal, endometrial, gastric, lung, melanoma, ovarian, pancreatic, prostate and squamous cell carcinomas (King et al., 2014) **(Table 1.2)**. PAK1 sits at 11q13 in the genome, an area which is often amplified in breast cancer (Bekri et al., 1997). Genomic amplification of PAK1 is also present in bladder, melanoma, ovarian, and T cell lymphomas (King et al., 2014) **(Table 1.2)**. Finally, increased phosphorylation of PAK1 is associated with breast, glioblastoma, kidney and ovarian cancers (King et al., 2014) **(Table 1.2)**.

These aberrations of PAK1 expression results in higher PAK1 activity in many cancer cell types. PAK1 is implicated in many of these tumour types due to its ability to aid the development and progression of cancers (King et al., 2014).

Interestingly the localisation of PAK1 influences cancer progression. An increased level of phosphorylated PAK1 in the cytoplasm is correlated with a reduced survival time in patients with glioblastoma patients (Aoki et al., 2007). When under the control of a ß-lactoglobulin promoter in mice, a constitutive active PAK1 mutant induced mammary gland tumours, demonstrating PAK1's role in breast cancer formation (Wang et al., 2006). In this mouse mammary tumour model nuclear localisation of PAK1 is correlated with the progression of ductal hyperplasia to adenocarcinoma (Wang et al., 2006). Nuclear localisation of PAK1, in the form of phosphorylated PAK1, is able to phosphorylate the ER at serine 305, which has also been linked to tamoxifen resistance in ER positive breast cancer patients (Holm et al., 2006, Rayala and Kumar, 2007).

PAK1 has a particular importance in breast cancer as it is reported to be implicated in over 50% of breast cancers (Ong et al., 2011). Whilst linked to other aspects of cancer growth and development, PAK1 is important in cancer metastasis due to its role in cell migration.

Cancer Type	Alteration in cancer	References
Bladder	Genomic amplification	Ito et al. (2007)
Breast	Protein overexpression	Balasenthil et al. (2004)
	Genomic amplification	Ong et al. (2011)
	Increased phosphorylation	Bostner et al. (2007) Stofega et al. (2004) Vadlamudi et al. (2000)
Colorectal	Protein overexpression	Carter et al. (2004)
Endometrial	Protein overexpression	Lu et al. (2013)
Gastric	Protein overexpression	Wu et al. (2014)
Glioblastoma	Increased phosphorylation	Aoki et al. (2007)
Kidney	Increased phosphorylation	O'Sullivan et al. (2007)
Lung	Protein overexpression	Ong et al. (2011)
Melanoma	Genomic amplification	Ong et al. (2013)
	Protein overexpression	Ong et al. (2013)
Ovarian	Genomic amplification	Brown et al. (2008) Schraml et al. (2003)
	Protein overexpression	Davidson et al. (2008) Siu et al. (2010)
	Increased phosphorylation	Siu et al. (2010)
Pancreatic	Protein overexpression	Zhou et al. (2014)
Prostate	Protein overexpression	Goc et al. (2013)
Squamous cell carcinoma	Protein overexpression	Chow et al. (2012)
T -cell lymphoma	Genomic amplification	Mao et al. (2003)

Table 1.2 PAK1 alterations in human cancers.

1.4.3 PAK1 in cell motility and cancer cell migration

PAK1 was first identified in 1994 due to its activation by the Rho GTPases (Manser et al., 1994). In non-cancerous cells PAK1 has been found to localise to the leading cell edge of migrating cells (Dharmawardhane et al., 1999, Nayal et al., 2006, Parrini et al., 2009, Sells et al., 2000), cell-cell junctions (Zegers et al., 2003) and focal adhesions (Delorme-Walker et al., 2011). It is therefore not surprisingly that PAK1 is able to influence cell migration due to its capabilities to regulate the actin cytoskeleton, focal adhesions and cell-cell junctions Studies of PAK1 in cancer cell lines also highlight the importance of its function in cell migration and invasion. It has previously been demonstrated to play a role in melanoma (Pavey et al., 2006), prostate (Goc et al., 2013), breast (Adam et al., 2000) and ovarian cancer (Siu et al., 2010) cell migration.

Studies in both non-cancerous and cancerous cell types have elucidated the mechanisms by which PAK1 can influence cell migration. PAK1 can regulate the actin cytoskeleton via several different signalling pathways and localises to cortical actin structures on PDGF stimulations (Dharmawardhane et al., 1997). As previously mentioned, it can phosphorylate LIMK when activated by Cdc42 and Rac1 resulting in inhibition of cofilin's actin severing function allowing the formation of membrane protrusions due to actin polymerisation (Edwards et al., 1999, Arber et al., 1998, Yang et al., 1998) **(Table 1.1)**. PAK1 can also phosphorylate myosin light chains directly, inducing cellular contractility and stress fibre formation (Stockton et al., 2004) **(Table 1.1)**. PAK1 is also able to influence the cytoskeleton by interactions with actin binding proteins. PAK1 is able to induce membrane ruffling by interacting with filamin A (Vadlamudi et al., 2002) and is able to promote the formation of the Arp2/3 complex by phosphorylating the p41-Arc a subunit (Vadlamudi et al., 2004) **(Table 1.1)**. This results in enhanced actin polymerisation in breast cancer cell migration (Vadlamudi et al., 2004).

PAK1 has also been implicated in Akt signalling and cell migration (Huynh et al., 2010). When activated by Rac1, PAK1 acts as a scaffold to induce Akt stimulation via PDK1. PAK1 is also able to recruit Akt to the membrane in motile cells (Higuchi et al., 2008) and can enhance migration and invasion of colon cancer cells (Huynh et al., 2010).

In addition to Akt signalling, PAK1 is also involved in MAPK signalling. PAK1 is able to phosphorylate Raf1 and MEK1 on sites serine 338 and serine 298 respectively (King et al., 2014). Phosphorylation of these sites increases the association of Raf with MEK and MEK with ERK thus further stimulating MAPK signalling (Aksamitiene et al., 2012) **(Table 1.1)**. Expression of constitutively active PAK1 results in MAPK signalling and anchorage independent growth in breast cancer cells (Vadlamudi et al., 2000). Further to this, activation of HER2 in ER positive breast tumours results in PAK1 activation, via Rac1, causing epithelial breast cells to proliferate and transform via the MAPK pathway (Arias-Romero et al., 2010). PAK1 signalling via the MAPK cascade can induce the formation of lamellipodia (Smith et al., 2008). Finally, PAK1 signalling has also been shown to enhance the formation of invadopodia, protrusions formed by cancer cells (Ayala et al., 2008, Nicholas et al., 2016) and induce them to secrete MMPs (Rider et al., 2013).

PAK1 is also able to regulate the disassembly of focal adhesions, an important part of cell migration. Expression of constitutively active PAK1 causes a reduction in the number of focal adhesions (Manser et al., 1997) and focal adhesions turnover is disrupted upon the inhibition of PAK1 (Delorme-Walker et al., 2011). Group I PAKs have a PIX binding domain (Manser et al., 1998) **(Figure 1.5)**. This binding localises PAK1 to focal adhesions where it can bind paxillin, one of the major components of focal adhesions (Brown et al., 2002). The binding of PAK1 with paxillin is thought to play a role in the dissolution of focal adhesions (Ridley, 2001, Zhao et al., 2000). Phosphorylation of paxillin at serine 273 by PAK1 causes GIT1 binding to paxillin. The GIT1-PIX-PAK1 complex is recruited to the cells leading edge promoting focal adhesion turnover and Rac induced protrusions (Nayal et al., 2006) **(Table 1.1)**. However, PAK1 phosphorylation of paxillin at serine 273 has been disputed (Dart et al., 2015).

As well as focal adhesions, PAK1 has also been shown to regulate cell-cell adhesions and therefore influence cancer cell migration. Interestingly depletion of PAK1 in prostate cancer cells inhibits the disassembly of cell-cell junctions (Bright et al., 2009). PAK1 can phosphorylate and translocate the zinc finger protein Snail to the nucleus. Snail is then able to prevent E-cadherin expression causing a decrease in E-cadherin cell to cell

junctions, which promotes cell to cell dissociation (Whale et al., 2011, Elloul et al., 2010) **(Table 1.1)**. In ovarian cancer cell lines this has been shown to promote EMT (Elloul et al., 2010). PAK1 also influences E-cadherin as it is required for E-cadherin disassembly at cell junctions downstream of Rac1 (Lozano et al., 2008). PAK1 can also cause a reduction in E-cadherin and other cell to cell junction proteins, such as p120-catenin by phosphorylation of CRKII which is able to downregulate these junctional proteins **(Table 1.1)**. Silencing PAK1 in nonsmall cell lung cancer cells increases the p120-catenin levels and decreases the motility and invasiveness of these cells (Rettig et al., 2012). It is therefore thought PAK1 can promote cell motility and invasiveness of nonsmall cell lung cancer cells by down regulating p120-catenin via CRK-II phosphorylation (Rettig et al., 2012).

1.5 Project aims

The aim of this project was to investigate the importance of PAK1 kinase activity during breast cancer cell spreading and migration and identify potential downstream signalling pathways involved in these processes. Specific objectives comprise the following:

- Assess the effect of perturbation, via depletion and pharmacological inhibition, of PAK1 on cell morphology and 2D migration
- Access the requirement for PAK1 kinase activity in *in vitro* cell invasion and *in vivo* cell migration
- Utilise an inducible PAK1 model system to monitor PAK1 specific cellular responses and identify potential downstream signalling pathways and effectors.

Chapter 2

Materials and methods

Chapter 2 Materials and methods

2.1 Materials

2.1.1 General materials

Reagent	Company
4-(2-hydroxyethyl)-1-piperazineethanesulfonic acid (HEPES)	A&E scientific
4',6-diamidino-2-phenylindole (DAPI)	Sigma-Aldrich, UK
Acetic acid	Sigma-Aldrich, UK
Acrylamide (30%)	Severn Biotech Ltd, UK
Agarose	Invitrogen, UK
Alexa Fluor® 488 Phalloidin	Invitrogen, UK
Ammonium persulfate (APS)	Sigma-Aldrich, UK
Aprotinin	Sigma-Aldrich, UK
Beta (β)- mercaptoethanol	Sigma-Aldrich, UK
Borosilicate glass capillary, 1.0mm outer diameter x 0.58mm inner diameter	Harvard Apparatus, USA
Borosilicate glass capillary, 1.0mm outer diameter x 0.78mm inner diameter	Harvard Apparatus, USA
Bovine serum albumin (BSA)	VWR International, UK
Bromophenol blue	Bio-Rad
Calcium chloride ($CaCl_2$)	Sigma-Aldrich, UK
Calcium phosphate transfection kit	Invitrogen, UK
Cell dissociation buffer	Sigma-Aldrich, UK
CellTracker™ Green CMFDA Dye	ThermoFisher Scientific, USA
Corning® Collagen I, Rat Tail	Corning, USA
Coverslips 13mm	Scientific Laboratories Supplies
Cytoskeleton phospho antibody array	Full moon biosystems, USA
DH5α™ competent *Escherichia coli* (*E.coli*) cells	Invitrogen, Uk
Dimethyl sulfoxide (DMSO)	Sigma-Aldrich, UK
Dithiothreitol (DTT)	Sigma-Aldrich, UK
Dulbecco's Modified Eagle's Medium (DMEM) (5x)	PAA, UK
Doxycycline hyclate	Sigma-Aldrich, UK
DMEM	Sigma-Aldrich, UK
Dulbecco's phosphate-buffered saline without calcium and magnesium	LONZA, UK

Epidermal growth factor (EGF)	ThermoFisher Scientific, USA
Ethanol	BDH Laboratory Supplies, UK
Ethyl 3-aminobenzoate methanesulfonate (MS222)	Sigma-Aldrich, UK
Ethylenediaminetetraacetic acid (EDTA)	Sigma-Aldrich, UK
Fibronectin	Sigma-Aldrich, UK
FluorSave™ Reagent	Calbiochem, UK
Foetal bovine serum (FBS)	Gibco®, Invitrogen, UK
Gel Cassettes	Invitrogen, UK
Gel loading dye (6x)	New England Biolabs, UK
Glycerol	Sigma-Aldrich, UK
Glycine	Sigma-Aldrich, UK
Hank's balanced salts solution	Sigma-Aldrich, UK
Hydrochloric acid (HCl)	VWR International, UK
Hepatocyte growth factor (HGF)	PeproTech, UK
IPA-3	Sigma-Aldrich, UK
Kanamycin	Invitrogen, UK
Leupeptin	Sigma-Aldrich, UK
Low melting point agarose	Invitrogen, UK
Luria-Bertani (LB) Agar	Sigma-Aldrich, UK
Luria-Bertani (LB) broth tablets	Sigma-Aldrich, UK
Magnesium chloride ($MgCl_2$)	Sigma-Aldrich, UK
Methanol	VWR International, UK
Methylene blue	ThermoFisher Scientific, USA
Milk powder	Marvel, UK
Nitrocellulose membrane	PerkinElmer, UK
Nonidet P-40	Sigma-Aldrich, UK
N-Phenylthiourea (PTU)	Sigma-Aldrich, UK
OptiMEM	Invitrogen, UK
Paraformaldehyde (PFA)	Sigma-Aldrich, UK
Penicillin-streptomycin	Sigma-Aldrich, UK
Phenylmethylsulfonyl fluoride (PMSF)	Sigma-Aldrich, UK

Phosphate buffered solution (PBS) tablets	Oxoid Limited, UK
Pierce™ ECL western blotting substrate	ThermoFisher Scientific, USA
Polybrene	Sigma-Aldrich, UK
Polyvinylpyrrolidone solution (PVP)	Sigma-Aldrich, UK
Potassium Chloride (KCl)	Sigma-Aldrich, UK
Precision Plus Protein™ dual color standards	Bio-Rad, UK
PureLink® HiPure plasmid maxiprep kit	Invitrogen, UK
Puromycin	Sigma-Aldrich, UK
Rapamycin	Calbiochem, UK
Rhodamine Phalloidin	ThermoFisher Scientific, USA
Roswell Park Memorial Institute (RPMI)-1640 medium	Sigma-Aldrich, UK
Sodium chloride (NaCl)	Sigma-Aldrich, UK
Sodium dodecyl sulfate (SDS)	Sigma-Aldrich, UK
Sodium fluoride (NaF)	Alfa Aesar, UK
Sodium hydroxide (NaOH)	Sigma-Aldrich, UK
Sodium orthovanadate (Na_3VO_4)	New England Biolabs, UK
Sodium pyrophosphate ($Na_4O_7P_2$)	BDH Chemicals, UK
Tetramethylethylenediamine (TEMED)	Sigma-Aldrich, UK
Tris-base	Sigma-Aldrich, UK
Triton X-100	VWR International, UK
Trypsin	Gibco®, Invitrogen, UK
Tween® 20	VWR International, UK
ViaFect™ transfection reagent	Promega, UK
Virkon Powder Disinfectant	DuPont, USA
X-ray film	Scientific Laboratories Supplies
Zebrafish channel device	MMB Foundry, USA

Table 2.1 General materials

2.1.2 Buffers and solutions

Buffer/solution	Composition
Blocking solution	5% w/v milk powder or 5% w/v BSA in tris buffered saline (TBS)-tween (TBST)

Cell lysis buffer	0.5% NP-40, 30mM $Na_4O_7P_2$, 50mM Tris-HCl pH7.6, 150mM NaCl, 0.1mM EDTA, 1mM DTT, 10µg/ml leupeptin, 1µg/ml aprotinin, 10mM PMSF, 10mM NaF, 1mM Na_3VO_4
E3 Media	5mM NaCl, 0.17mM KCl, 0.44mM $CaCl_2$, 0.68mM $MgSO_4$ in H_2O
FACS buffer	1% FBS, 1mM EDTA, 25mM HEPES in $PBS^{-/-}$
Gel sample buffer (6x)	375mM Tris-HCl pH 6.8, 10% w/v SDS, 30% v/v glycerol, 6% β-mercaptoethanol, 0.2% w/v bromophenol blue
SDS-PAGE running buffer (10x)	250mM tris-base, 1.92M glycine, 1% w/v SDS
SDS-PAGE transfer buffer (10x)	250mM tris-base. 1.92M glycine
Stripping buffer	25mM glycine pH2, 1% w/v SDS
TBST	25mM tris-HCl pH7.6, 50mM NaCl, 0.1% v/v tween 20
Type I Collagen mix	1.5mg/ml type I collagen, 20% 5X DMEM (containing 10% FBS) and 1% 1mM NaOH in sterile H_2O

Table 2.2 Buffers and solutions

2.1.3 Primary antibodies

Antibody	Species	Company	Dilution for WB
GAPDH	Mouse	Santa Cruz Biotechnology	1:5000
PAK1	Rabbit	Cell Signalling Technology	1:1000
Phospho-PAK1/PAK2 (Thr423/Thr402)	Rabbit	Cell Signalling Technology	1:1000
Phospho- LIMK1/2 (Thr508/Thr505)	Rabbit	Cell Signalling Technology	1:1000
LIMK1	Mouse	BD Transductions Laboratories	1:1000
LIMK2	Rabbit	Cell Signalling Technology	1:1000
Phospho-CRKII (Tyr221)	Rabbit	Cell Signalling Technology	1:1000
FAK	Rabbit	Santa Cruz Biotechnology	1:1000
Phospho-FAK (Ser910)	Rabbit	ThermoFisher Scientific	1:1000
Vinculin	Mouse	Sigma-Aldrich	1:5000
ERK1/2 (p44/42 MAPK)	Rabbit	Cell Signalling Technology	1:1000
Phospho-ERK1/2 site (p44/42 MAPK) (Thr202/Tyr204)	Rabbit	Cell Signalling Technology	1:1000
ERK3 (MAPK6)	Mouse	Abnova	1:1000

Phospho-ERK3 (MAPK6) (Ser189)	Sheep	An in-house antibody kindly gifted by Professor Ole Morten Seternes, University of Tromsø, Norway	1:1000

Table 2.3 Primary antibodies used

2.1.4 Secondary antibodies

Antibody	Species	Company	Dilution for WB	Dilution for IF
HRP conjugated anti-mouse	Goat	DAKO	1:2000	-
HRP conjugated anti-rabbit	Goat	DAKO	1:2000	-
HPR conjugated anti-sheep	Donkey	R&D systems	1:2000	-
Alexa Fluor® 488 Phalloidin	-	Invitrogen	-	1:300
Rhodamine phalloidin	-	Invitrogen	-	1:1000

Table 2.4 Secondary antibodies used

2.1.5 shRNA sequences

shRNA	Target Sequence (5'-3')	Company
Control shRNA (pGIPz)	CTTACTCTCGCCCAAGCGAGAG	Open Biosystems, ThermoFisher Scientific, UK (RHS4346)
PAK1 shRNA 1 (pGIPz)	GCCTAGACATTCAAGACAA	Open Biosystems, ThermoFisher Scientific, UK (V2LHS_152618)
PAK1 shRNA 2 (pGIPz)	TATTGTCACTCTTGATGTC	Open Biosystems, ThermoFisher Scientific, UK (V2LMM_68590)

Table 2.5 shRNA constructs used

2.1.6 CRIPSPR constructs

CRISPR	Target Sequence (5'-3')	Company
PAK1_105909	TTATTTGACATTGTCACCAC	Horizon Discovery
PAK1_105910	GCTGGTATTTCTCATCGGAG	Horizon Discovery
PAK1_105911	GGTTCCAGCATCTTTGCTGC	Horizon Discovery
PAK1_105912	GAGGCAGAGGTTTAGAACCA	Horizon Discovery
PAK1_105913	TTATTTGCTGCAAGAGAAAC	Horizon Discovery

Table 2.6 CRISPR constructs used

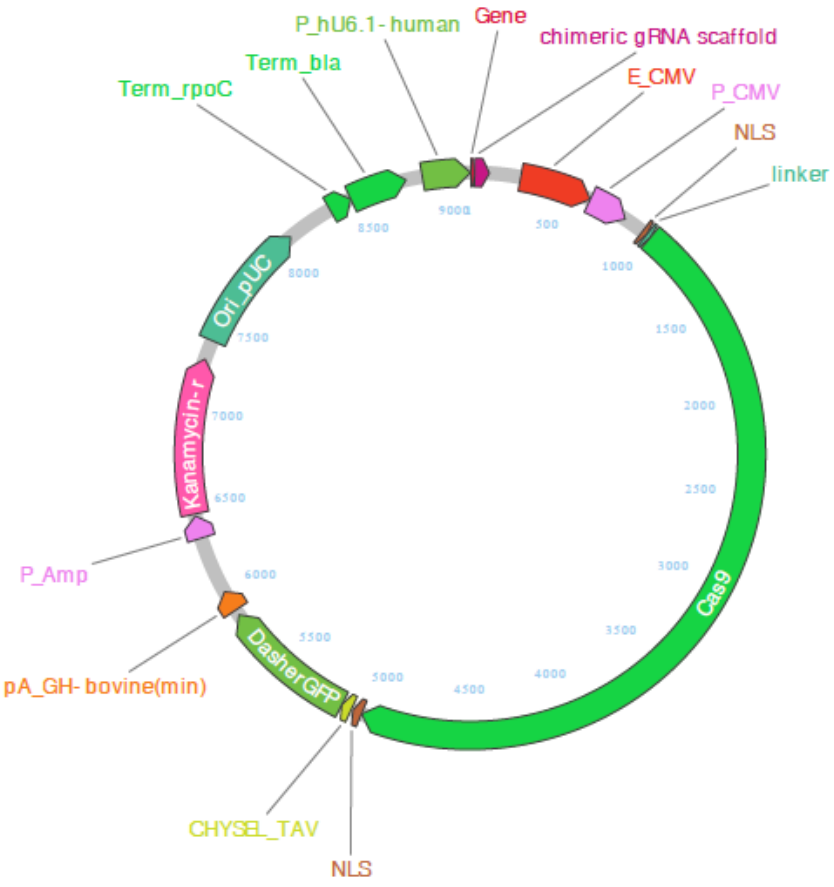

Figure 2.1 Schematic diagram of CRISPR constructs. The plasmid DNA for the CRISPR-Cas9 constructs. Detailed are the GFP tag, kanamycin resistance gene and guide RNA scaffold are indicated. The plasmid name is PAK1_105909, a pD1301- AD:154977 plasmid from horizon discovery.

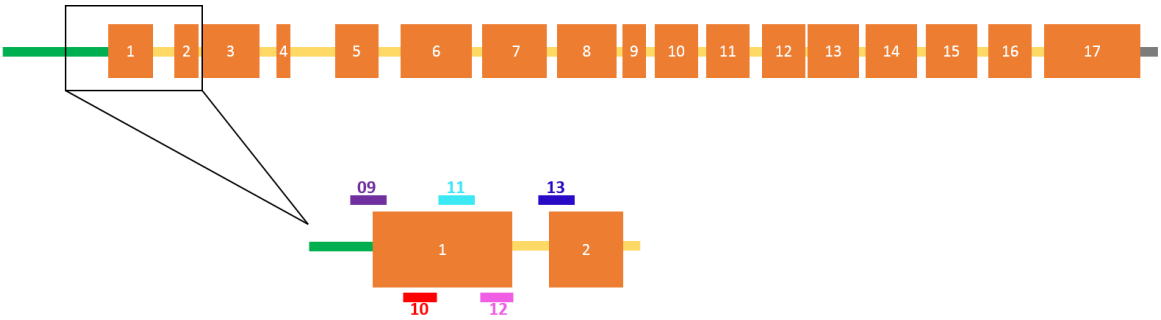

Figure 2.2 Schematic diagram of PAK1 CRISPR target sites on the PAK1 gene. The 5'UTR (green), exons (orange), introns (yellow) and 3'UTR (grey) of the PAK1 gene are all shown. The target sites of the five PAK1 CRISPR constructs are shown in purple (PAK1_105909, 09 on figure), red (PAK1_105910, 10 on figure), turquoise (PAK1_105911, 11 on figure), pink (PAK1_105912, 12 on figure) and blue (PAK1_105913, 13 on figure).

2.2 Methods

2.2.1 Transformation of competent *E.coli* cells

DH5α™ competent *E.coli* cells were removed from the -80°C freezer and thawed on ice. 2ng of the required DNA plasmid was added to 20µl of competent cells and incubated on ice for 30 minutes. The cells were then heat shocked for 30 seconds in a 42°C water bath and returned to ice for two minutes. 500µl of warm LB broth was added to the cells which were then shaken at 225rpm for one hour at 37°C. 100µl of the transformed bacteria was spread on an LB agar plate containing appropriate antibiotic before the plates were inverted and incubated at 37°C overnight. The following morning a single colony was picked from the agar plate using a sterile pipette tip. The colony was grown in 200ml of LB broth containing the appropriate selection antibiotic for 24 hours. The following day a small amount of the bacterial culture was used to make a glycerol stock and the rest was used to purify the plasmid DNA.

2.2.2 DNA plasmid purification

Isolation and purification of the plasmid DNA from the *E.coli* cultures was performed using the Invitrogen PureLink® HiPure plasmid maxiprep kit according to the manufacturers' protocol. The DNA was then ruspended in TE buffer and the DNA concentration was measured in ng/µl using a nano-drop. Purified DNA plasmids were stored at -20°C.

2.2.3 Cell culture

All cell lines were kept at 37°C with 5% atmospheric CO_2 in a humidified tissue culture incubator (referred to as 37°C from here on). Cells were passaged regularly to ensure they did not reach confluency. To passage cells, the growth media was aspirated off and the cells were washed with phosphate buffered saline (PBS). Cells were then incubated with trypsin/EDTA at 37°C for five minutes to detach them from the flask/plate. Once detached, growth media was added to deactivate the trypsin before the cell suspension was

centrifuged at 1200rpm in an Eppendorf 5702 centrifuge with a A-8-17 rotor for four minutes to pellet the cells. The cell pellet was then resuspended in an appropriate volume of growth media and cells were then seeded at an appropriate density and dilutions into the plates and flasks required.

Human embryonic kidney HEK293 cells, human pancreas adenocarcinoma PaTu-8988t cells and PaTu-8902 cells and human breast cancer MDA-MB-231 cells were obtained from Claire Wells, King's College London and grown in Dulbecco's Modified Eagle's Medium (DMEM) supplemented with 10% v/v FBS, 100U/ml penicillin and 100µg/ml streptomycin. The media of MDA-MB-231 cells with PAK1 knockdown (sh1 and sh2 cells) and control cells were supplemented with 1µg/ml puromycin to select for cells containing the sh constructs **(Table 2.5)**.

Human prostate cancer PC3 cells were obtained from Claire Wells, King's College London and grown in Roswell Park Memorial Institute (RPMI) 1640 supplemented with 10% v/v FBS, 100U/ml penicillin and 100µg/ml streptomycin. Human pancreatic cancer AsPC-1 cells were obtained from Dr Stéphanie Kermorgant, Barts Cancer Institute and grown in RPMI 1640 supplemented with 10% v/v FBS, 100U/ml penicillin and 100µg/ml streptomycin. BT-549 cells were obtained from Dr Phillippe Chavrier, Centre de Recherche Institut Curie and were grown in RPMI 1640 supplemented with 10% v/v FBS, 100U/ml penicillin, 100µg/ml streptomycin and 10µg/ml insulin.

Human breast cancer MDA-MB-231 cells (UNC-WT) and MDA-MB-231 stably expressing a Rap-PAK1 construct (S44) cells were obtained from Dr Klaus Hahn, University of North Carolina. The UNC-231 cells were grown in DMEM supplemented with 10% v/v FBS and 1mM penicillin-streptomycin. The S44 cells were also grown in this media but additionally supplemented with 1µg/ml puromycin to select for the cells containing the Rap-PAK1 construct and 10µg/ml doxycycline as the Rap-PAK1 construct operates as a Tet-off system. Two days before using the S44 cells in an experiment the cells were passaged, as written above, and media containing no doxycycline was added to the cells. Six hours after passaging the media was aspirated off, cells were washed with PBS and fresh media

containing no doxycycline was added to ensure that doxycycline was not present in the media thus allowing the Rap-PAK1 construct to be expressed.

2.2.4 Cell storage and recovery

To recover cells, cryovials, kept in the liquid nitrogen, were place in a 37°C water bath and allowed to thaw. Growth medium was added to the cell suspension which was then centrifuged for four minutes at 1200 rpm using an Eppendorf 5702 centrifuge with a A-8-17 rotor. Cells were then resuspended in fresh growth medium and seeded into a flask or plate. The medium was changed the next day.

To store cells, they were passaged as normal but resuspended in 90% FBS and 10% DMSO instead of normal growth medium. The cell solution was then transferred into cyrovials and placed into a cyro-freezing box in a -80°C freezer to ensure slow freezing. The vials were then transferred to liquid nitrogen at a later date for long term storage.

2.2.5 Transfection of HEK293 with calcium phosphate

HEK293 cells were seeded in a 2cm tissue culture dish at a density of 1 x 10^5 cells/ml and incubated overnight at 37°C. The following day the media was removed and replaced with fresh media. The transfection mixes are described in **table 2.7**.

	2cm tissue culture dish (2ml)
Tube A	6µl 2M $CaCl_2$ (final concentration 60mM) 4µg plasmid DNA Make up to 60µl with sterile H_2O
Tube B	60µl HEPES buffered saline

Table 2.7 Calcium phosphate kit transfection mix

Once prepared, tube A was added to tube B with aeration and left at room temperature for 30 minutes. The transfection mix was then added drop wise onto the cells which were then left at 37°C. The following day fresh media was replenished. Cells were then left for a further 48 hours before being harvested.

2.2.6 Transfection of MDA-MB-231 with viafect

MDA-MB-231 cells were seeded in a 10cm plate at density of 1 x 10^5 cells/ml and incubated overnight at 37°C. The following day the media was removed and replaced with fresh media. The transfection mixes are described in **table 2.8**.

10cm tissue culture dish (10ml)
470µl optiMEM
30µl viafect
10µg DNA

Table 2.8 Viafect transfection mix

Once prepared the transfection mix was incubated at room temperature for 17 minutes before being added drop wise onto the cells. The cells were then incubated for 24 hours at 37°C before the media was changed. The cells were then left for a further 24 hours at 37°C before being harvested.

2.2.7 Generation of stable fluorescent LifeAct cells

Lentiviral vectors containing LifeAct-RFP was kindly gifted by Prof Maddy Parsons, King's College London. The virus was packaged and harvested by Dr Jeremy Carlton. MDA-MB-231 cells were plated at an appropriate density in a 6 well plate and kept at 37°C for 24 hours. The following day fresh media was replenished and the viral construct was added drop wise to the media with 0.8 µg/ml polybrene. 24 hours later the media was replenished again. Cells were then passaged, as described in 2.2.3, four times in the virus tissue culture room before moving to the normal tissue culture room. Virus waste was left in 10% virkon for 24 hours before being disposed of. The virally infected cells subject to fluorescence-activated cell sorting (FACS) (as described in 2.2.9) to ensure all cells were expressing the LifeAct construct.

2.2.8 Single cell cloning

To single cell clone a population of cells, the cells were passaged (as described in 2.2.3) and once resuspended in fresh growth media the cells were counted, and a series of dilutions were made to give a suspension where there was appropriately one cell for every 100µl. To each well of a 96 well plate 100µl was added and incubated at 37°C for two weeks. After two weeks cells were screened at regular intervals to note in which wells a population of cells appeared to be growing from a single cell. When a high enough confluency was reached cells were passaged and moved to a 24 well plate, then a 6 well plate and then finally a T25 flask. Cells were the frozen down (2.2.4) or lysed (2.2.10).

2.2.9 Fluorescence-activated cell sorting

To perform FACS, cells were passaged (as described in 2.2.3) but resuspended in FACS buffer **(Table 2.2)** instead of growth media. A cell suspension of 0.5 x 10^6 cells per ml was prepared and sorted with a BD FACSAriall SORP sorter using a 100nm nozzle, gated on forward and side scatter parameters, singlet discrimination and 488nm or 561nm lasers when selecting for GFP or RFP positive cells respectively. Doublets were excluded by FSC area vs FCS height. The selected cells were then placed in a suitable plate or flash depending on cell number and allowed to recover in growth media in a 37°C incubator. FACS was performed by Yasmin Sfy.

2.2.10 Cell lysis

Cells were seeded at an appropriate density in 6 well plates. Cells were washed twice with PBS and then 100µl of cell lysis buffer **(Table 2.2)** was added to each well for five minutes whilst the cells were placed on a rocking table on ice. Cells were then scraped off and pipetted into eppendorf tubes. The tubes were then centrifuged for ten minutes at 4°C at 13,0000xg. The supernatant was then pipetted off and placed in a clean eppendorf. 20µl of 6x gel sample buffer **(Table 2.2)** was added and the eppendorf were boiled for five minutes and stored at -20°C.

2.2.11 Gel electrophoresis and immunoblotting

Lysates were boiled and loaded onto 10% acrylamide gels. Proteins were separated by sodium dodecyl sulphate-polyacrylamide gel electrophoresis (SDS-PAGE) at 130V for one and a half hours in 1x running buffer **(Table 2.2)**. The proteins were then transferred onto a nitrocellulose membrane for one hour at 100V in 1x transfer buffer **(Table 2.2)**. The membranes were the blocked for one hour at room temperature in either 5% milk in TBST or 5% BSA in TBST. The membranes were then placed in an appropriately diluted primary antibody **(Table 2.3)** in the same solution as used for blocking and placed on a tube roller over night at 4°C. The following day the membranes were washed three times in TBST **(Table 2.2)**. They were then placed in the appropriately diluted secondary antibody **(Table 2.4)** in the same solution as used for blocking for one hour at room temperature. The membranes were then washed three times in TBST. The probed proteins were the visualised using Pierce™ ECL western blotting substrate.

2.2.12 Stripping nitrocellulose membranes

Where appropriate, membranes were re-probed. To strip the membrane mild stripping buffer was used. Membranes were placed in this buffer two times for 15 minutes each time on a rocking table. The membranes were then washed in PBS ready to be blocked and re-probed with an appropriate primary antibody (as described in 2.2.11).

2.2.13 Densitometry

ImageJ was used to perform densitometry analysis on protein bands. A mean grey value was attributed to each band based on its intensity. The mean grey values were then normalised to background noise and the loading control used for that experiment, and where appropriate were made relative to a control condition.

2.2.14 Coverslip preparation

13mm coverslips were acid treated to prepare them for immunofluorescence. The coverslips were placed in a beaker containing 40% of 70% ethanol and 60% 1M hydrochloric acid (HCl) for 24 hours. This solution was then replaced with dH_2O which was then boiled. The coverslips were the rinsed in dH_2O six times before being placed on whatman paper to dry. The coverslips were then transferred into a glass bottle and autoclaved to complete sterilisation.

2.2.15 Collagen coating of coverslips

Coverslips were placed in a desired plate. Type I collagen was diluted to 50 µg/ml in filter sterilised 0.02M glacial acetic acid (GAA). This solution was added to the coverslips and incubated for 60 minutes at room temperate. The collagen solution was removed, and the coverslips were washed three times with PBS. Cells were then seeded onto the coated coverslips.

2.2.16 Fibronectin coating of coverslips

Coverslips were placed in a desired plate and 10µg/ml human fibronectin solution in PBS was added. The plate was then placed in a 37°C incubator for 30 minutes. The fibronectin solution was removed and the coverslips were washed three times with PBS. Cells were then seeded onto the coated coverslips.

2.2.17 Immunofluorescent staining and imaging

Immunofluorescent staining was performed on cells seeded at an appropriate density on either glass, collagen coated or fibronectin coated coverslips. The coverslips were washed three times in PBS before being fixed in 4% paraformaldehyde (PFA) for 20 minutes at room temperature. For inhibitor experiments the cells were incubated with a final concentration IPA-3 or DMSO of 1µM for two, four or six hours prior to fixation. Once

fixed, the cells were washed a further three times and incubated in 0.2% X-triton for five minutes to permeabilised the cell membrane. The cells were then washed a further three times before being incubated in PBS containing phalloidin and DAPI at appropriate concentrations for 60 minutes in the dark. Cells were then washed a further two times in PBS and twice in ddH_2O. The coverslips were then mounted onto glass slides using FluroSave and left in the dark at room temperature overnight. The slides were stored at 4°C. Coverslips were imaged using an Olympus IX71 microscope with either Image ProPlus AMS software or micromanager2.0beta depending on the camera installed at the time of imaging.

2.2.18 Image processing and cell morphology analysis

Images were opened in ImageJ. Cells were manually drawn around and parameters such as cell area and perimeter were measured for each cell.

2.2.19 2D migration random migration assay and analysis

Cells were seeded at an appropriate density in full growth medium on 50µg/ml type I collagen six well plate and placed in a 37°C incubator overnight. The next day the medium was replaced with 2ml of fresh medium containing 40µl of HEPES buffer, and where appropriate IPA-3 or DMSO was added to give a final concentration of 1µM two hours prior to the start of imaging. The plate was then sealed with parafilm and images were taken every five minutes for 16 hours at 37°C using an Olympus IX71 microscope and Image ProPlus AMS software. The images were extracted and saved as AVI files. These were then opened in ImageJ where the manual tracking plugin in was used to map both X and Y coordinates of a cell in each frame. This data was then analysed in Ibidi Chemotaxis and Migration Tool, version 2.

2.2.20 Spheroid assay and analysis

Spheroids were made by seeding 1000 cells in 100µl of full growth medium into a Corning black walled 96-well clear black round bottom ultra-low attachment spheroid microplate. The plate was then kept in a 37°C incubator for five days. After the five days the medium was removed and replaced with type I collagen mix **(Table 2.2)**. The plate was the placed back in the incubator for two hours to allow the collagen to set. 100µl of full growth medium was then gently added on top of the collagen, for the inhibitor experiments either 5µM of IPA-3 or DMSO was added to the media. The spheroids were then imaged using an Olympus IX71 microscope and micromanager2.0beta software. The plate was then placed back in the incubator for 24 hours before the spheroids were imaged again.

Spheroid images were analysed in ImageJ. The initial and final spheroid sizes were measured and the number of cells that invaded outside of a defined area were counted using the ImageJ cell counter function.

2.2.21 Zebrafish embryo maintenance

All zebrafish work completed was approved by the King's College Ethical Review committee and performed under the UK Home Office licence PPL 70/7912.

Zebrafish were collected from zebrafish facility and separated into multiple 10cm dishes with 1X E3 media with 0.0002% methylene blue and kept at 28°C. At 6-8 hours post fertilisation (hpf) any debris and unfertilised cells were removed from the dishes. At 1-day post fertilisation the chorion of the zebrafish was removed from each embryo to allow the embryos to straighten during development. At 6dpf or the end of an experiment, whichever was sooner, embryos were culled by exposure to an anaesthetic overdose of 15mM ethyl 2-aminobenzoate methanesulfonate (MS222) for 60 minutes.

2.2.22 Zebrafish yolk invasion assay and imaging

Needles were pulled using a P-87 Flaming/Brown Micropipette Puller. The glass capillaries were pulled at both ends away from the heating element to create two fine needles.

The AsPC-1 cells were washed with PBS and incubated at 37°C for 10 minutes in cell dissociation buffer. Once detached from the flask media was added and the cells were centrifuged for four minutes at 1200rpm using an Eppendorf 5702 centrifuge with a A-8-17 rotor to form a cell pellet. The pellet was then resuspended and incubated in a mix of PBS and CellTracker™ Green CMFDA Dye (final concentration 5µM) for 30 minutes at 37°C. The cells were then centrifuged again for four minutes at 1200rpm using an Eppendorf 5702 centrifuge with a A-8-17 rotor. The cell pellet was then resuspended in PBS-/- and a 50µl solution containing $2.1x10^7$ cells/ml and 10% PVP. The cells were stimulated with 50ng/ml HGF prior to injection.

The virally infected MDA-MB-231 cells were and incubated at 37°C for 10 minutes in cell dissociation buffer. Once detached from the flask media was added and the cells were centrifuged for four minutes at 1200rpm using an Eppendorf 5702 centrifuge with a A-8-17 rotor to form a cell pellet. The cell pellet was then resuspended in PBS-/- and a 50µl solution containing either 1.6 x 10^4cells/µl, 2.1 x 10^4cells/µl or 3.2 x 10^4cells/µl and 10% PVP. The cells were stimulated with 50ng/ml EGF prior to injection.

Zebrafish embryos at 2dpf were placed in E3 media containing 3.5mM of MS222 and 1% penicillin-streptomycin. They were then placed in a V shape grooved 2% agarose (in H_2O) mould. The cells were loaded into the glass capillary needle and approximately 200-500 cells were injected into the yolk sac of the zebrafish using a Nikon SMZ-U zoom 1:10 Picospritzer II microinjection station. Embryos were then placed back in E3 media containing 3.5mM of MS222 and 1% penicillin-streptomycin and allowed recover for one hour at 28°C. They were then transferred to 33°C for the remainder of the experiment.

For AsPC-1, two hours post injection embryos which lacked a tumour mass in the yolk sac or had cells outside of the yolk sac were removed and humanely killed using 15mM MS222.

The percentage of embryos with tail fish invasion was calculated 24 hours post injection. For MDA-MD-231 cells, 24 hours post injection embryos which lacked a tumour mass in the yolk sac or had cells outside of the yolk sac were removed and humanely killed using 15mM MS222. For inhibitor experiments either IPA-3 or DMSO was added to the post injected water at a final concentration of 5µM until the end of the experiment. The percentage of embryos with tail fish invasion was calculated four days post injection (dpi). They embryos were then humanely killed using 15mM MS222.

2.2.23 Rapamycin experiments

For the rapamycin morphology experiments an appropriate number of cells were seeded onto glass, collagen or fibronectin coated coverslips in full growth medium and kept in a 37°C incubator for 24 hours. Rapamycin in FBS free medium was added to the cells at 0, 5, 20 and 60 minutes so the final concentration of rapamycin was 500nM. At these time points cells were fixed and stained (as described in 2.2.17).

For the rapamycin western experiments an appropriate number of cells were seeded onto collagen coated six well plates in full growth medium and kept in a 37°C incubator for 24 hours. Rapamycin in FBS free medium was added to the cells at 0, 5, 20 and 60 minutes so the final concentration of rapamycin was 500nM. At these time points cells were lysed (as described in 2.2.10).

2.2.24 Cytoskeleton phospho antibody array

1 X 10^6 cells were seeded on two collagen coated 10cm tissue culture plates. Rapamycin in FBS free medium was added to one plate, the final concentration of rapamycin was 500nm. The same volume of in FBS free medium not containing rapamycin was added to the other plate. Both plates were then incubated at 37°C for five minutes. Cells were lysed and the Full Moon BioSystems cytoskeleton phospho antibody array was performed according to the manufacturer's protocol and returned to Full Moon BioSystems to be scanned and imaged.

Once received the phosphoarray images were analysed using ImageJ. Each circle was attributed a mean grey value score which was then normalised to background noise and the loading marker. A value was calculated for each protein on the array and the fold change in signal for each protein was calculated between the plus and minus rapamycin conditions.

2.2.25 Statistical analysis

GraphPad Prism was used to perform an unpaired t-test on datasets generated from three independent experiments. A P value of ≤0.05 (95% confidence interval), ≤0.01 (99% confidence interval) and ≤0.001 (99.9% confidence interval) are indicated by *, ** and *** respectively. Error bars represent the standard error of the mean (SEM).

Chapter 3

Investigating the effect of PAK1 perturbation on cell morphology and migration

Chapter 3 The effect of PAK1 perturbation on cell morphology and migration

3.1 Introduction

Cells remodel their cytoskeletons to regulate cell movement and migration (Yilmaz and Christofori, 2009). One of the key family of proteins involved in this process are the Rho GTPases (Vega and Ridley, 2008). Cdc42 and Rac1, two of the most widely studied Rho GTPases, are key regulators of cell motility due to their ability to control the polymerisation, depolymerisation and branching of actin filaments (Vega and Ridley, 2008). The p21 activated kinase (PAK) family are the most well characterised downstream effectors of Cdc42 and Rac1 (Bishop and Hall, 2000).

The PAKs are a family of serine/threonine kinases that are involved in a wide range of cellular processes, many of which are important in cancer (King et al., 2014, Radu et al., 2014). There are six PAK family members which are divided into two groups – PAK1-3 (group I) and PAK4-6 (group II) – based on similarities in their sequences, domains and regulation (Arias-Romero and Chernoff, 2008). The involvement of the PAK family in cancer formation, progression and metastasis has been widely noted due to their roles in cellular processes such as proliferation, apoptosis and cell migration (King et al., 2014). PAK1 is the member of the PAK family which is most studied and associated with cancer.

PAK1 has been shown to play a role in, but not limited to, bladder, colorectal, endometrial, kidney, liver, lung, melanoma, prostate and ovarian cancers (King et al., 2014). A multitude of studies have also demonstrated PAK1 contributes to breast cancer formation, development and metastasis (King et al., 2014).

PAK1 is implicated in breast cancer due to its overexpression, genomic amplification and increased phosphorylation (Balasenthil et al., 2004, Holm et al., 2006, Bostner et al., 2007, Stofega et al., 2004, Vadlamudi et al., 2000). PAK1 has also been linked to tamoxifen resistance in the treatment of ER positive breast cancers (Holm et al., 2006).

As PAK1 is a downstream effector of Cdc42 and Rac1 and is heavily involved in many cancer types, it is no surprise PAK1 has been heavily linked to cell migration of both cancerous and non-cancerous cell types. Active PAK1 has been shown to localise to leading edge of motile fibroblasts (Sells et al., 2000) and to lamellipodia and sites of membrane ruffling (Dharmawardhane et al., 1997).

Studies in downstream signalling from PAK1 also support an importance for PAK1 in cell motility; this is largely due to PAK1's ability to alter the cells cytoskeleton. PAK1 can phosphorylate LIMK downstream of Cdc42 and Rac1 which induces cytoskeletal changes (Edwards et al., 1999). Once phosphorylated, LIMK1 is able to phosphorylate cofilin, resulting in the inhibition of its actin severing functions. This leads to growth of actin fibres which can form plasma membrane protrusions (Arber et al., 1998, Yang et al., 1998).

PAK1 also plays a role Akt signalling and cell migration (Huynh et al., 2010). When activated by Rac1, PAK1 acts as a scaffold to induce Akt stimulation via PDK1. PAK1 is able to recruit Akt to the membrane in motile cells (Higuchi et al., 2008) and can enhance migration and invasion of colon cancer cells (Huynh et al., 2010).

PAK1 can also influence the cytoskeleton by interacting with actin binding proteins. PAK1 induces membrane ruffling when it interacts with filamin A (Vadlamudi et al., 2002) and can promote the formation of the Arp2/3 complex by phosphorylating the p41-Arc- a subunit, this results in enhanced actin polymerisation in breast cancer cell migration (Vadlamudi et al., 2004). Whilst the role of PAK1 in cell migration has been studied, the requirement of PAK1 in MDA-MB-231 cell migration has not previously been assessed by depletion studies. In addition to this, very little is known about the role of PAK1 in spreading, and the specific role of PAK1 in MDA-MB-231 cell morphology is currently unknown.

Interestingly, recent studies have highlighted the PAK family also exhibit kinase independent functions (Wang et al., 2013, Dart et al., 2015, Thullberg et al., 2007). As PAK1 is heavily implicated in breast cancer and plays an important role in cell motility, this

chapter aims to investigate the role of PAK1 and its kinase activity on breast cancer cell morphology and migration by modulating PAK1 expression levels and kinase activity.

3.2 Results

3.2.1 PAK1 is expressed in breast, pancreatic and prostate cancer cell lines

As PAK1 is reportedly expressed in a wide range of cancers (Kichina et al., 2010), a panel of cancer cell lines were studied to determine their level of PAK1 expression. Two breast cancer cell lines (MDA-MB-231 and BT-549 cells), a prostate cancer cell line (PC3) and two pancreatic cancer cell lines (PaTu-8902 and PaTu-8988T) were assessed.

Both breast cancer cell lines are from TNBC. The MDA-MB-231 cell line was originally isolated from a pleural effusion from a breast cancer patient suffering widespread metastasis (Cailleau et al., 1974). BT-549 cells are derived from the primary tumour of an invasive ductal carcinoma (Littlewood-Evans et al., 1997). PC3 cells were isolated from a bone metastasis from a patient suffering from prostatic adenocarcinoma (Kaighn et al., 1979). PaTu-8902 cells were derived from a primary grade II pancreatic ductal adenocarcinoma (Elsasser et al., 1993). The PaTu-8988T cells were isolated from a liver metastasis from a patient suffering with pancreatic adenocarcinoma (Elsasser et al., 1992). These cell lines were selected as they all exhibit mesenchymal cell migration, a mode of migration where PAK1's importance has been previously reported (Al-Azayzih et al., 2015).

All five cancer cell lines assessed express PAK1 **(Figure 3.1)**. PAK1 expression was highest in the PaTu-8988T cells and MDA-MB-231 cells, these both being cell lines derived from metastatic sites. BT-549, PC3 and PaTu-8902 cells all have a lower level of PAK1 expression. The MDA-MB-231 cell line has significantly higher PAK1 expression than the BT-549 cell line. It is for this reason the MDA-MB-231 cell line will be used for subsequent experiments.

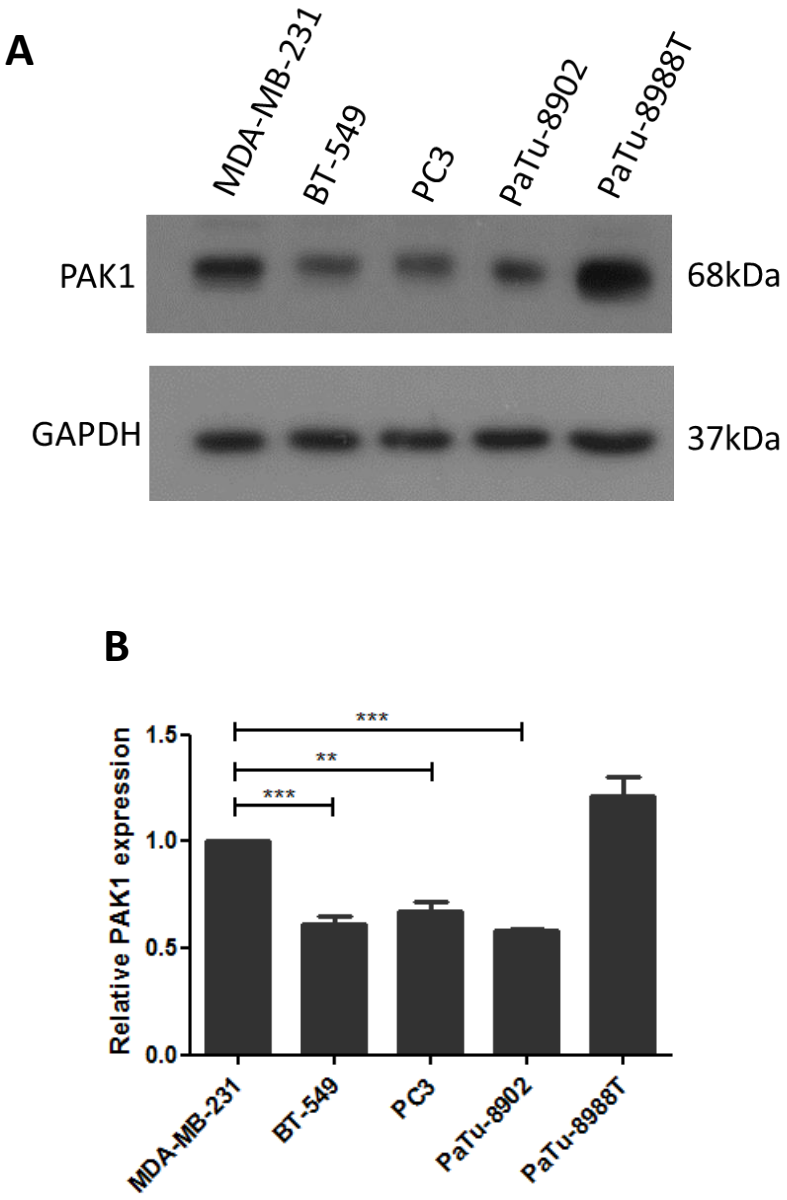

Figure 3.1 PAK1 expression in cancer cell lines.**(A)** Cell lysates from breast (MDA-MB231 and BT-549), prostate (PC3) and pancreatic (PaTu-8092 and PaTu-8988T) cancer cells were probed for PAK1. Glyceraldehyde 3-phosphate dehydrogenase (GAPDH) was used as a loading control. **(B)** Densitometric analysis on ImageJ was used to compare the expression levels of PAK1, normalised to the loading control and background noise. Error bars represent the SEM for three independent experiments. Statistical analysis was carried out using t-tests (** $p<0.01$, *** $p<0.001$).

3.2.2 Knockdown of PAK1 impacts cell morphology and migration

Having confirmed the expression of PAK1 in MDA-MB-231 cells, the effect of reducing PAK1 expression levels on cell morphology and migration was investigated. To achieve this objective stable PAK1 depleted cell lines were generated using two different PAK1 specific short hairpin ribonucleic acid (shRNA) constructs. In parallel a control shRNA line was also generated. Analysis of cells lysates derived from these lines revealed a significant knockdown in PAK1 expression compared to the wild-type cells, with approximately a 45% and 70% reduction for sh1 and sh2 constructs respectively **(Figure 3.2)**. No significant change of PAK1 expression in the control shRNA construct and wild-type cells was observed **(Figure 3.2)**. These established MDA-MB-231 cell lines containing the sh1, sh2 and control shRNA constructs alongside the wild-type untransfected control cells were subsequently used to investigate the effect of PAK1 knockdown in cell morphology and migration.

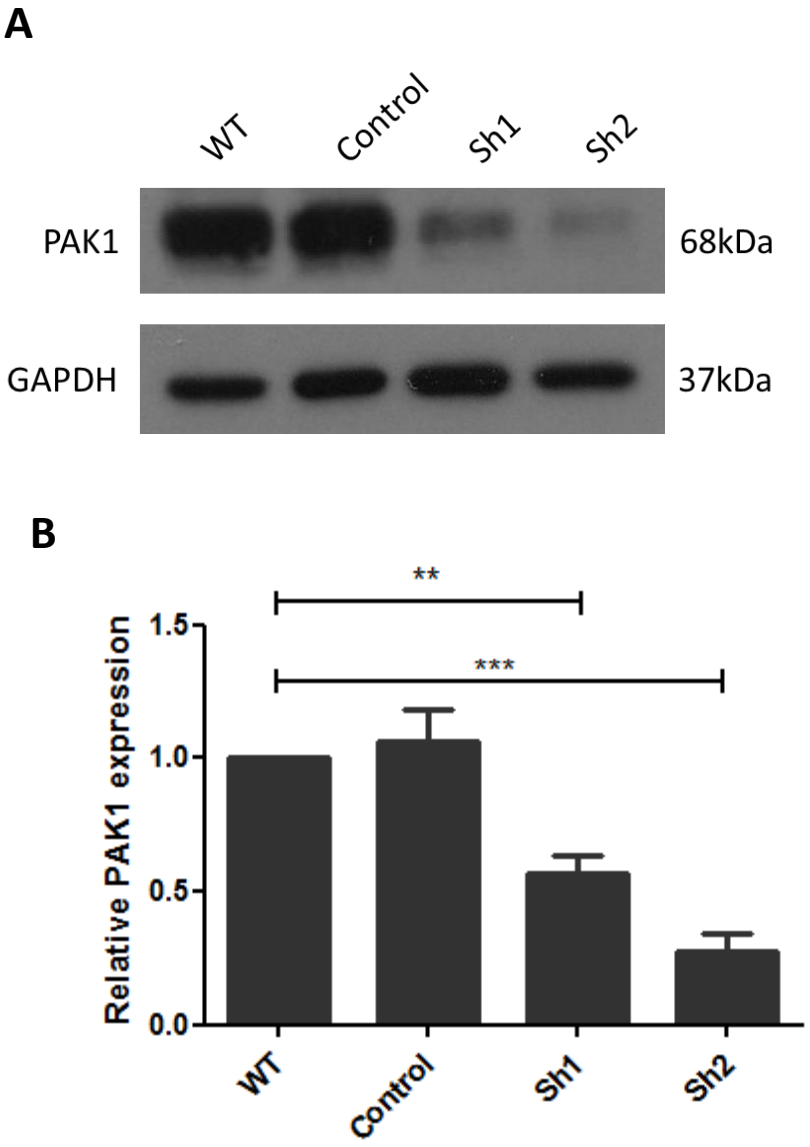

Figure 3.2 shRNA knockdown of PAK1 in MDA-MB-231 cells. Whole cell lysates were prepared from MDA-MB-231 cells transfected with two shRNA PAK1 constructs and an shRNA control construct. A wild-type untransfected control was also used. **(A)** Representative western blot indicating a knockdown of PAK1 expression with both PAK1 shRNA constructs (sh1 and sh2) but not the shRNA control (control) construct compared to the wild-type control. GADPH was used as the loading control. **(B)** Densitometric analysis on ImageJ was used to compare the expression levels of PAK1, normalised to the loading control and background noise. Error bars represent SEM for three independent experiments. Statistical analysis was carried out using t-tests (** $p<0.01$, *** $p<0.001$).

The cells were characterised for changes in cell morphology and migration potential on type I collagen, as this is more physiologically relevant than plastic or glass.

Differences in morphology following PAK1 knockdown could imply changes in a cell's ability to migrate and invade. Morphological analysis revealed a significant decrease in cell spread area and perimeter for both shRNA PAK1 knockdown cell lines (sh1 and sh2) compared to wild-type cells **(Figure 3.3)**. No significant difference in these measurements were observed for the shRNA control cells compared to the wild-type cells **(Figure 3.3)**.

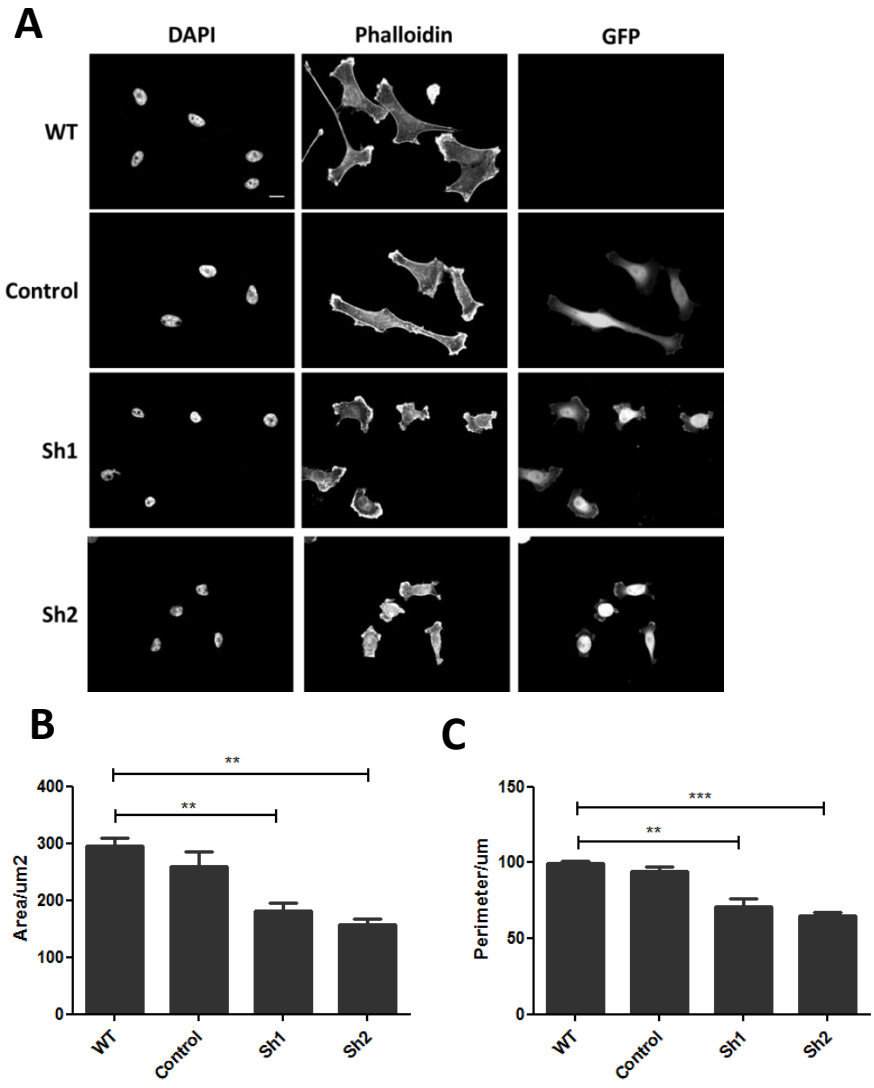

Figure 3.3 Morphology of shRNA PAK1 knockdown MDA-MB-231 cells. (A) shRNA PAK1 knockdown cells (sh1 and sh2), shRNA control cells (control) and wild-type cells (WT) were seeded onto collagen coated coverslips, fixed and stained for DAPI and phalloidin. A GFP signal is used to confirm presence of the shRNA constructs. Cells were then subject to morphological analysis using ImageJ. The scale bar represents 10µm. **(B and C)** Graphical representation of cell area (B) and perimeter (C) for knockdown and control cells. Error bars represent SEM for three independent experiments, 30 cells per experiment. Statistical analysis was carried out using t-tests (** $p<0.01$, *** $p<0.001$).

The phenotypic morphology of cancer cells has been widely linked to their ability to migrate (Clark and Vignjevic, 2015). Having observed shRNA induced knockdown of PAK1 in MDA-MB-231 cells causes a decrease in cell spread area **(Figure 3.3)**, the cells ability to migrate was assessed.

Cells depleted of PAK1 show a significantly reduced mean cell speed on type I collagen compared to control cells **(Figure 3.4)**, indicating an importance for PAK1 in 2D cell migration.

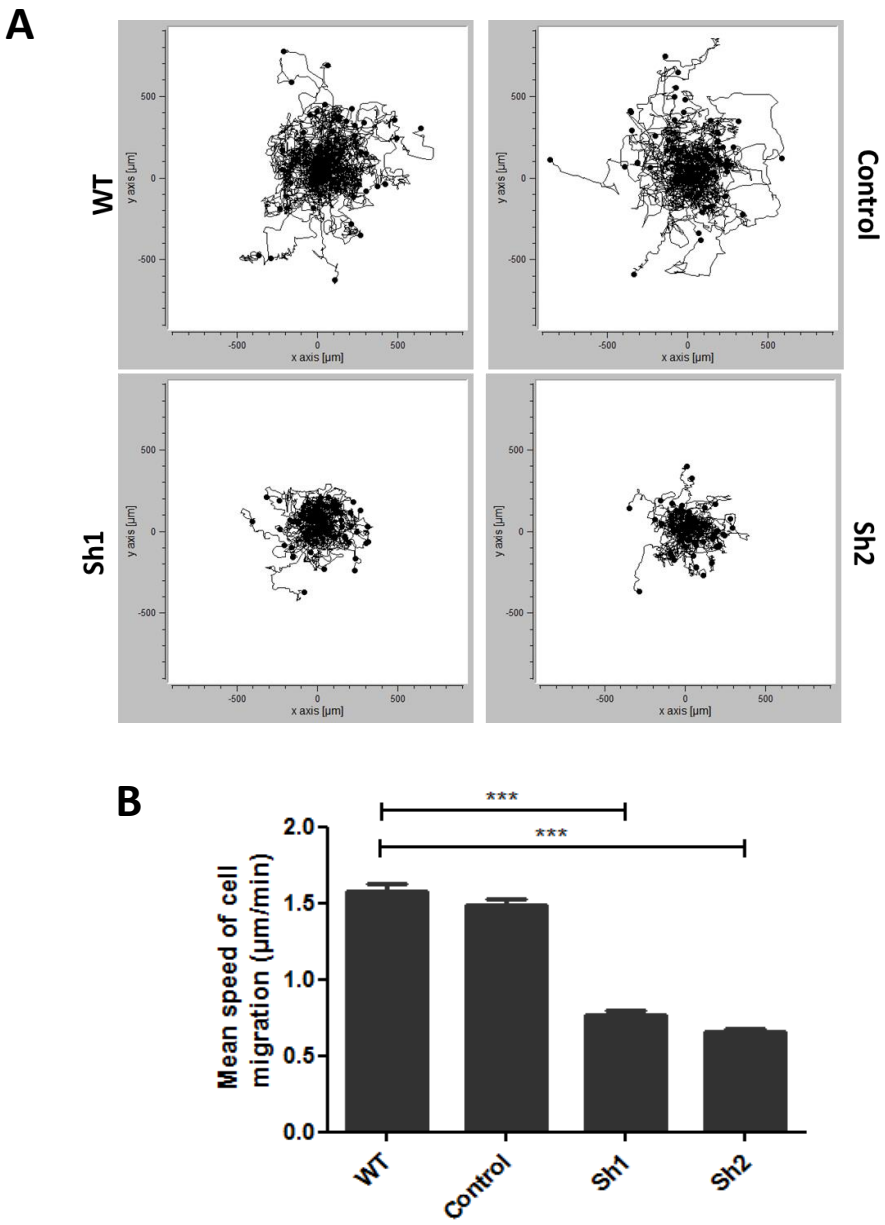

Figure 3.4 2D migration of shRNA PAK1 knockdown MDA-MD-231 cells. (A) shRNA PAK1 knockdown and control cells were seeded onto type I collagen and imaged for 16 hours. ImageJ was used to manually track the cells and cell speeds and plots were obtained using ibidi chemotaxis and migration tool. **(B)** Graphical representation of shRNA PAK1 knockdown and control cells. Error bars represent SEM for three independent experiments, 20 cells per experiment. Statistical analysis was carried out using t-tests (*** $p<0.001$).

3.2.3 CRISPR of PAK1 impacts cell morphology and behaviour

To complement shRNA knockdown of PAK1 an alternative approach to perturbing PAK1 expression was attempted using CRISPR-Cas9 technology. Potential genomic alteration is produced when a short guide RNA (sgRNA) specific to a region of the target gene guides the Cas-9 deoxyribose nucleic acid (DNA) nuclease to the target site in the genome. Cas-9 will then cleave the genomic DNA in site specific manner. Once damaged, the cell will repair the DNA by either non-homologous end joining (NHEJ) or homologous directed repair (HDR) which often lead to insertion or deletion mutations. These mutations are likely to cause a frame-shift or premature stop coding thus a functioning protein is not produced due to an alteration at the genomic level (Hsu et al., 2014).

Five PAK1 CRISPR constructs were available from Horizon Discovery **(Table 2.6)**. All five constructs target before or within exon two of the PAK1 gene **(Figure 2.2)**. To validate and select the most efficient construct HEK293 cells were used as they have a high transfection efficiency which would result in an increased likelihood of a CRISPR event occurring. It was not expected to see a total knockout of PAK1 in this experiment as not all cells would be transfected with the construct, and a CRISPR event would not take place in all the transfected cells, therefore the reduction in PAK1 expression was used as a measure of efficiency for the different CRISPR constructs. The PAK1 expression level was assessed by western blotting. All CRISPR constructs, except for CRPISPR 13, show a significant knockdown of PAK1 expression compared to wild-type cells **(Figure 3.5)**. CRISPR 9 induced the greatest reduction in PAK1 expression **(Figure 3.5)** and was selected as the construct to use for generating a complete knockout of PAK1 in the MDA-MB-231 cell line.

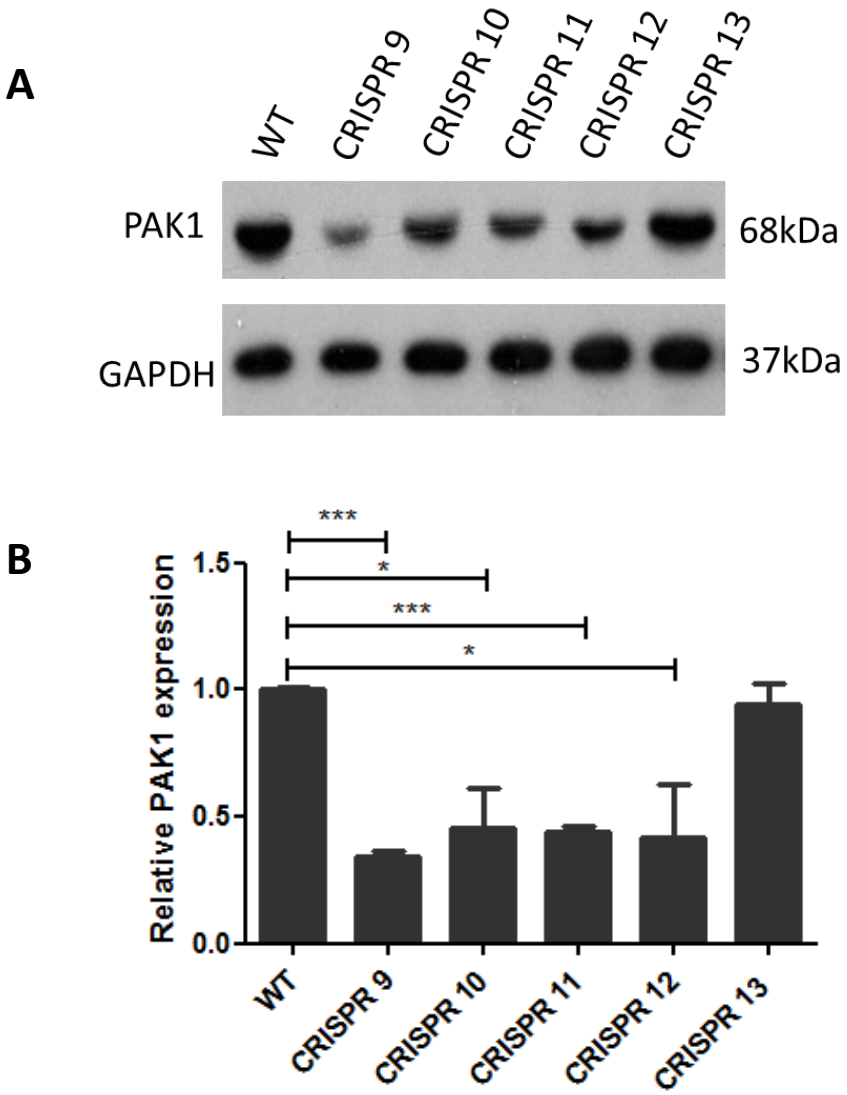

Figure 3.5 Validation of PAK1 CRISPR constructs in HEK293 cells. Whole cell lysates were prepared from HEK293 cells transfected with different PAK1 CRISPR constructs (CRISPR 9-13). **(A)** Representative western blot indicating the level of PAK1 expression with each different CRISPR construct and the wild-type untransfected control. GADPH was used as the loading control. **(B)** Densitometric analysis on ImageJ was used to compare the expression levels of PAK1, normalised to the loading control and background noise. Error bars represent SEM for three independent experiments. Statistical analysis was carried out using t-tests (* $p<0.05$, *** $p<0.001$).

To generate an MDA-MB-231 PAK1 knockout cell line a CRISPR protocol was designed **(Figure 3.6)**. MDA-MB-231 cells were seeded onto dishes and transfected with the CRISPR 9 construct. As the plasmid encoding the CRISPR sequence and Cas-9 contains a GFP tag **(Figure 2.1)**, 48 hours after transfection the cells were FACS sorted to select GFP positive cells, thus ensuring all cells used from now on had been transfected with the plasmid. The cells were allowed to recover and were then single cell cloned to ensure, if a CRISPR event had occurred on all copies of the PAK1 gene, all cells within the population would have no PAK1 expression. The single cell clones were expanded and either cell lysates prepared for western blotting or DNA extraction was performed for polymerase chain reaction (PCR).

PCR primers were designed to bind the genomic DNA over the target site of the CRISPR9 construct. This would allow PCR amplicons of the PAK1 gene to be generated from unsuccessful CRISPR and wildtype clones but no PCR product would be generated from clones which had complete PAK1 knockout. Unfortunately, despite multiple strategies and extensive optimisation of a PCR protocol, generation of specific amplicons without non-specific bands of the PAK1 gene on wildtype DNA was unsuccessful. Therefore, western blotting was used to identify any potential PAK1 knockout clones, which offers the advantage of direct identification of total knockout at the protein level.

Lysates from 68 different single cell populations were subject to western blotting and probed for PAK1 to identify any clones with a loss of PAK1 expression.

Western blots revealed cell populations with varying levels of PAK1 expression, as shown in the representative blot **(Figure 3.7).** Two single cell populations, 2.10 and 1.22 were identified as a potential PAK1 knockout cell population as no PAK1 band appeared on the western blot **(Figure 3.7)** despite prolonged exposure to autoradiographs. These two cell populations were therefore subject to further validation.

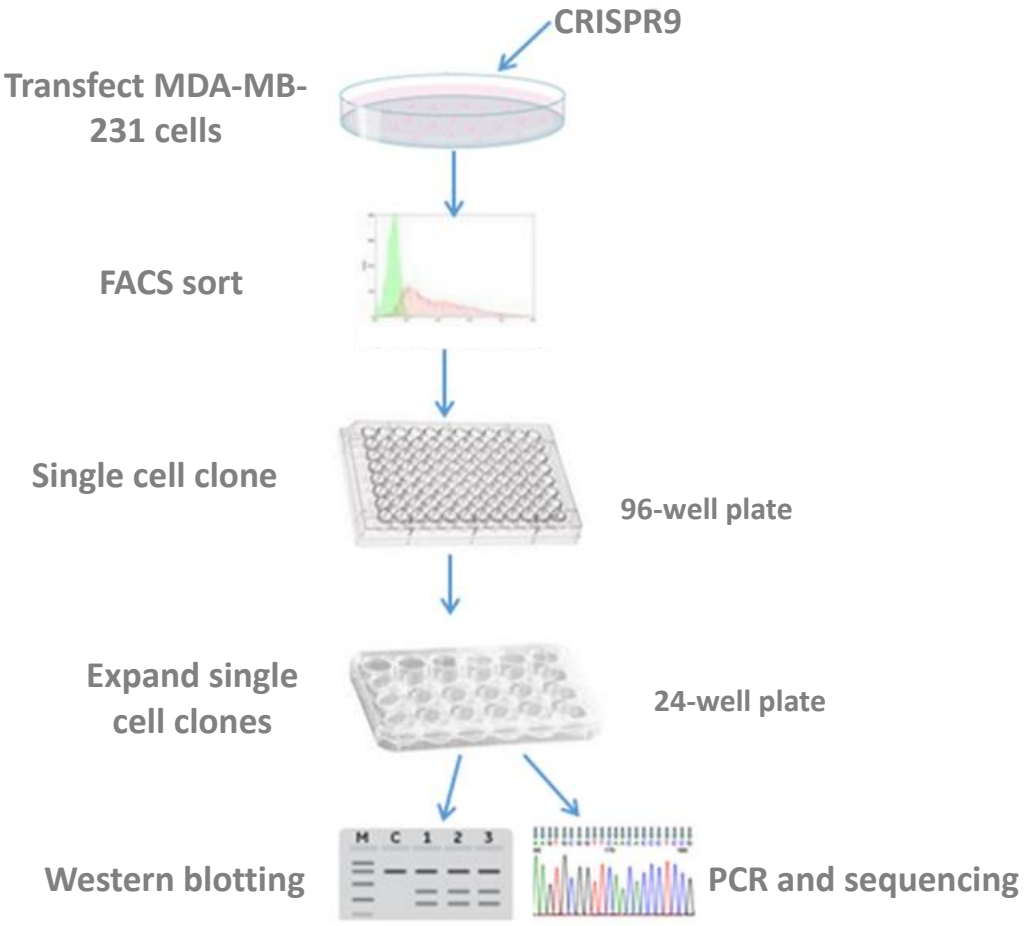

Figure 3.6 Flow diagram of CRISPR protocol. A flow diagram explaining the steps used to develop an MDA-MB-231 PAK1 knockout cell line. Adapted from Dharmacon.

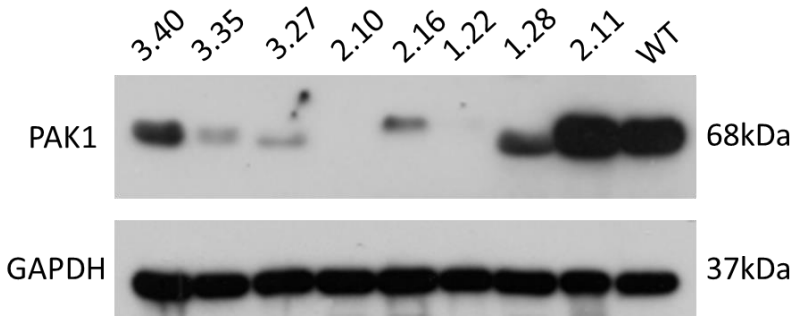

Figure 3.7 CRISPR screening using western blotting. Whole cell lysates were prepared from MDA-MB-231 single cell populations transfected with PAK1 CRISPR construct, CRISPR9. A representative western blot indicating the level of PAK1 expression in eight different single cell populations. An untransfected wild-type cell population was also included. GADPH was used as the loading control (n=1).

For both 1.22 and 2.10 cell clones, when first recovered into culture from liquid nitrogen at passage number zero (P+0), no PAK1 expression was detected in the cell lysates. Lysates were made after two weeks in culture at passage number four (P+4), after four weeks in culture at passage number eight (P+8) and after six weeks in culture at passage number 12 (P+12). It was observed that as the cells were continuously cultured, PAK1 expression levels increased relative to their passage number **(Figure 3.8)**. Although PAK1 levels were now detectable, up to passage number eight (P+8) the 1.22 and 2.10 cell clones still had a significant reduction in PAK1 expression levels, with a 48% and 57% knockdown respectively, compared to the wild-type control. **(Figure 3.8)**. The initial aim of generating a complete PAK1 knockout MDA-MB-231 cell line was unsuccessful however two MDA-MB-231 cell clones with a significantly reduced level of PAK1 had been generated provided the passaged number was less than eight.

Thus clones 1.22 and 2.10 are PAK1 depleted and can be directly compared with the behaviour of PAK1 shRNA cells. Such comparison has not been previously reported.

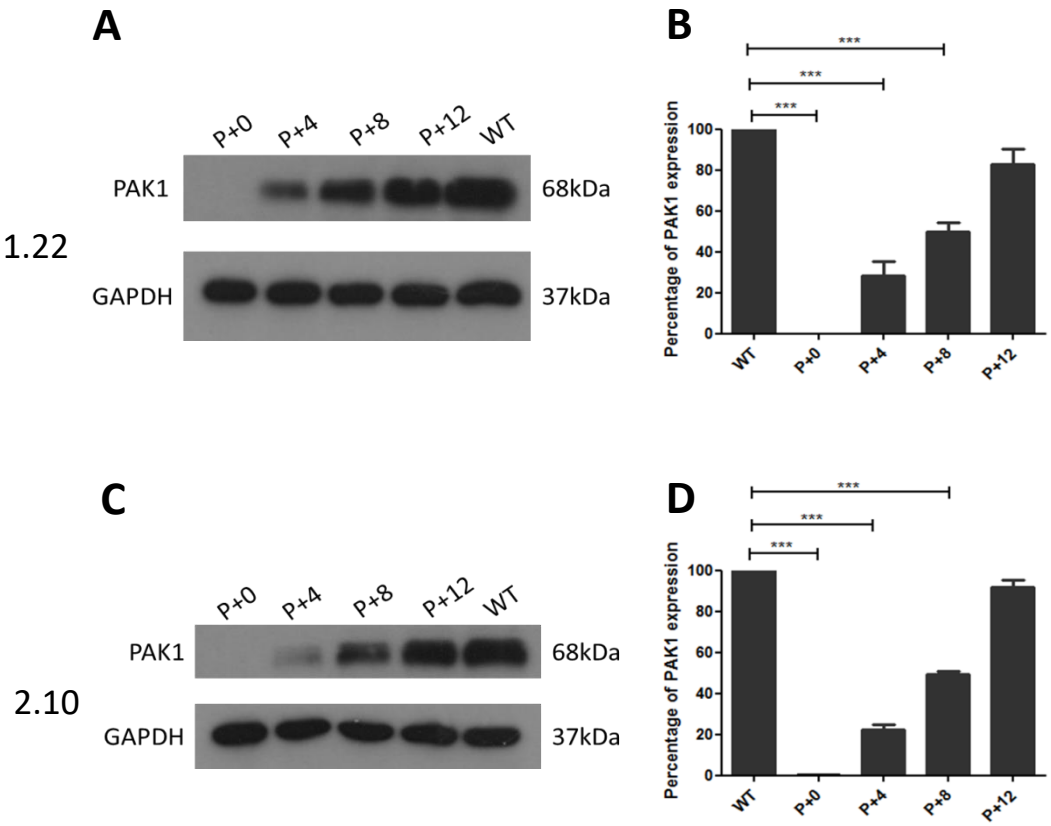

Figure 3.8 PAK1 expression in CRISPR PAK1 knockdown cells. Whole cell lysates prepared from two different MDA-MB-231 cells clones, 1.22 and 2.10, which were previously identified as being a potential PAK1 knockout. **(A and C)** Representative western blots showing PAK1 expression of cell clones 1.22 and 2.10 respectively at different passage numbers. A wild-type control is also present, GAPDH was used as the loading control. **(B and D)** Densitometric analysis on ImageJ was used to compare the expression levels of PAK1 normalised to the loading control and background noise, in 1.22 and 2.10 cell clones respectively. Error bars represent SEM for three independent experiments. Statistical analysis was carried out using t-tests (*** $p<0.001$).

Thus, as PAK1 reduction using shRNA showed a significant reduction in cell spread area **(Figure 3.3)** the CRISPR PAK1 knockdown cells area was quantified.

CRISPR PAK1 knockdown cells, 1.22 and 2.10, and wild-type control cells were seeded on rat tail type I collagen coated coverslips, fixed and stained with DAPI and rhodamine phalloidin as before **(Figure 3.3)**. Cells were then subject to morphology analysis in ImageJ. This analysis revealed a significant decrease in cell area and perimeter of both 1.22 and 2.10, the CRISPR PAK1 knockdown cells, compared to the wild-type cells (**Figure 3.9)** reminiscent of PAK1 shRNA cells **(Figure 3.3)**.

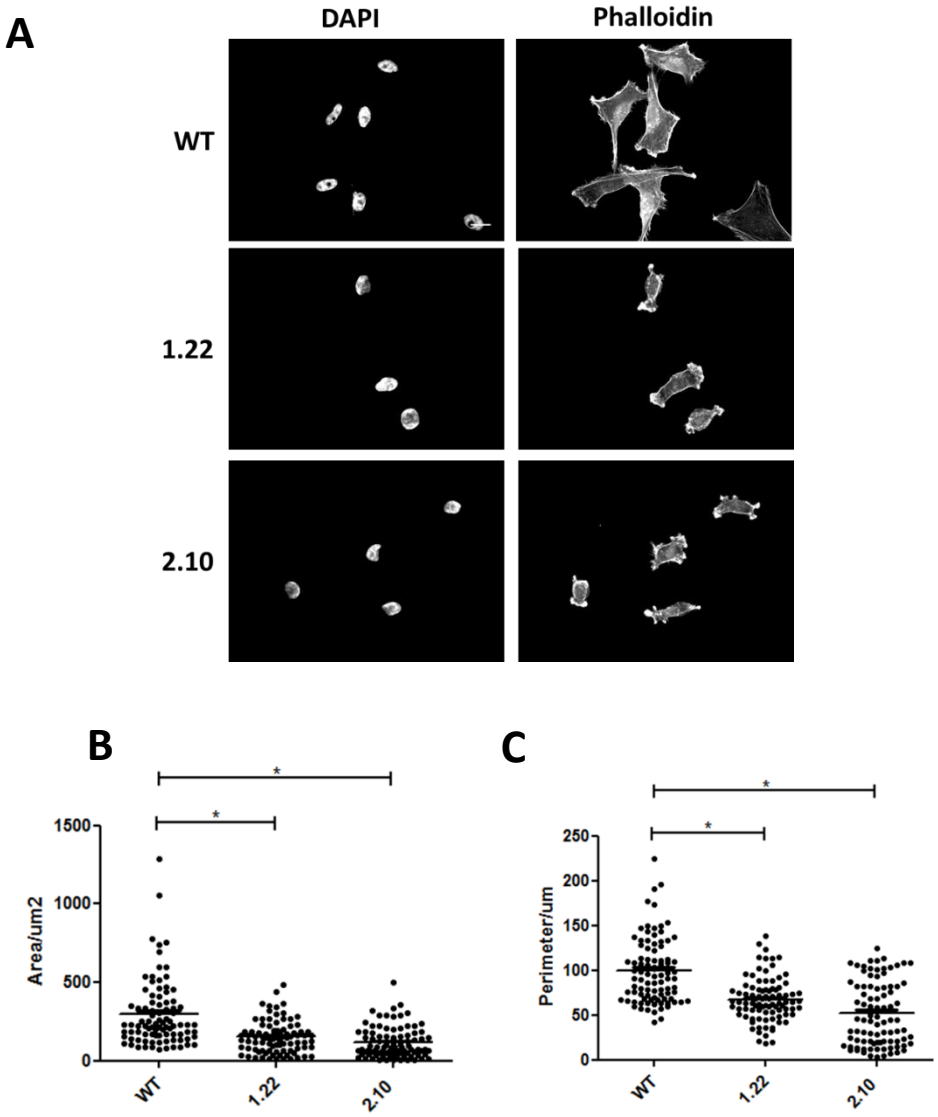

Figure 3.9 Morphology of CRISPR PAK1 knockdown MDA-MB-231 cells. (A) CRISPR PAK1 knockdown cells (1.22 and 2.10) and wild-type cells (WT) were seeded onto collagen coated coverslips, fixed and stained for DAPI and phalloidin. Cells were then subject to morphological analysis using ImageJ. The scale bar represents 10µm. **(B and C)** Graphical representation of cell area (B) and perimeter (C) for knockdown and wild-type cells. Error bars represent SEM for three independent experiments, 30 cells per experiment. Statistical analysis was carried out using t-tests (* $p<0.05$).

Both the CRISPR PAK1 knockdown cells and the shRNA PAK1 knockdown cells show a decreased in cell spread area compared to wild-type and control cells **(Figure 3.3 and 3.9).** Therefore, CRISPR PAK1 knockdown cells were assessed to examine if this change in morphology also caused a reduction in mean speed of cell migration, as seen in the shRNA PAK1 cells **(Figure 3.4)**.

The two CRISPR PAK1 knockdown cell populations show a significantly reduced mean cell speed compared to wild-type cells **(Figure 3.10)**, consistent with the PAK1 shRNA knockdown data **(Figure 3.4)**.

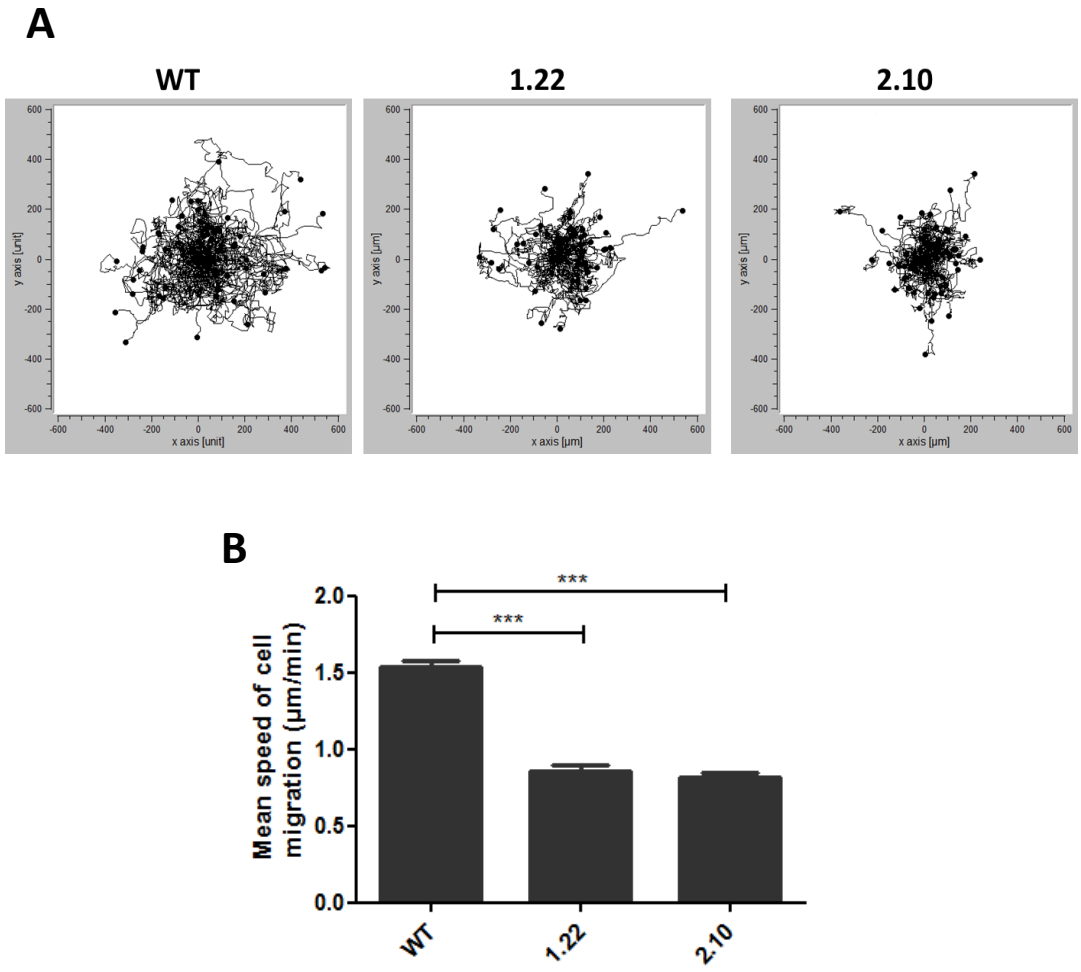

Figure 3.10 2D migration of CRISPR PAK1 knockdown MDA-MD-231 cells. (A) CRISPR PAK1 knockdown and wild-type cells were seeded onto type I collagen and imaged for 16 hours. ImageJ was used to manually track the cells and cell speeds and plots were obtained using ibidi chemotaxis and migration tool. **(B)** Graphical representation of CRISPR PAK1 knockdown and wild-type cells. Error bars represent SEM for three independent experiments, 20 cells per experiment. Statistical analysis was carried out using t-tests (*** $p<0.001$).

3.2.4 Pharmacological inhibition of PAK1 impacts cell morphology and migration

Depleting PAK1 protein levels using shRNA and CRISPR technology results in a decrease in cell area and perimeter and a decrease in mean speed of cell migration. This highlights the importance that PAK1 plays in both cell morphology and migration. Whilst it is clear PAK1 plays a role in the morphology and migration of MDA-MD-231 cells it was unclear if this was in a kinase dependent manner. It was therefore decided to further investigate whether these phenotypes were dependent on the kinase activity of PAK1.

To explore the relationship between observed phenotypes in a PAK1 depleted background and kinase activity a widely employed PAK1 specific inhibitor was utilised. IPA-3 is a non-ATP competitive inhibitor of PAK1 activation; it targets the autoregulatory mechanism PAK1 possesses by covalently binding to its regulatory domain (Deacon et al., 2008, Viaud and Peterson, 2009). If the morphological and migratory phenotype seen in knockdown PAK1 cells is due to a kinase dependent function of PAK1, the same phenotype should be observed with IPA-3 treated cells.

To investigate the effects IPA-3 had on cell morphology, wild-type MDA-MB-231 cells were incubated with the inhibitor or a DMSO control for two, four or six hours. 1µM of IPA-3 was used based of previous publications (Wang et al., 2016). Morphological analysis was then performed on the cells. At all three-time points (two, four and six hours) IPA-3 treated MDA-MD-231 cells showed a significant decrease in cell area and size compared to the DMSO and wild-type controls **(Figure 3.11)**.

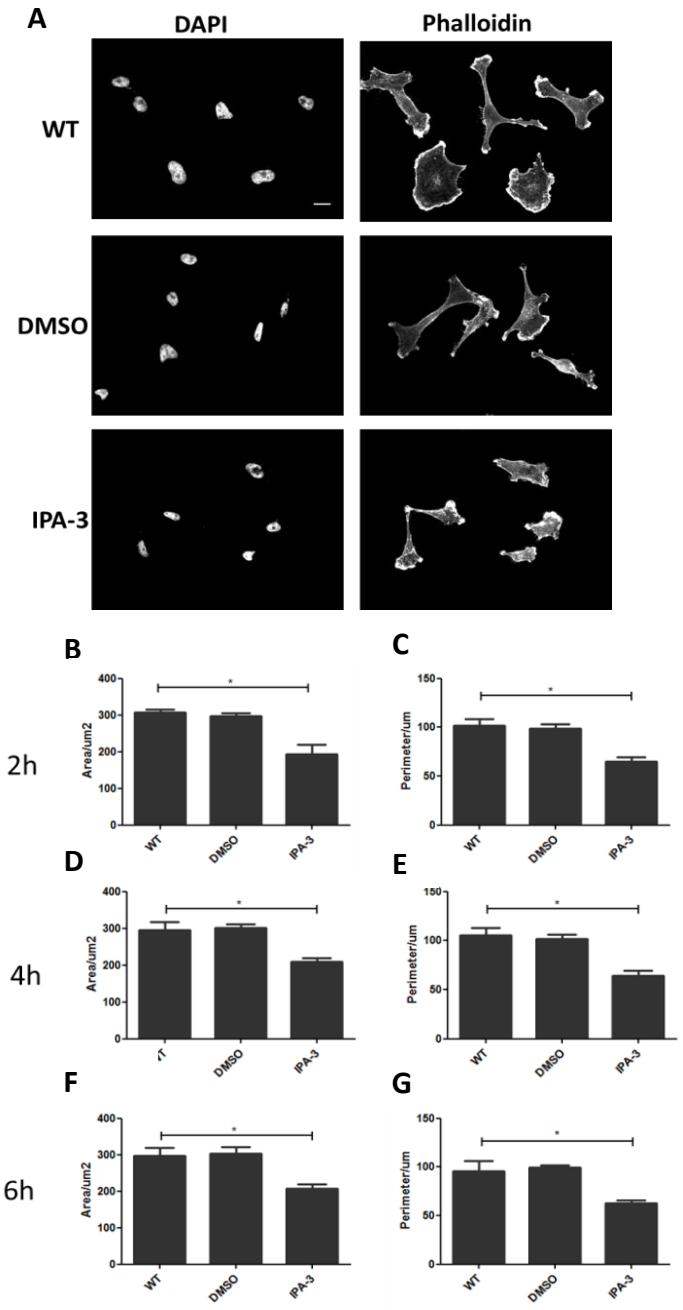

Figure 3.11 The effect of IPA-3 on MDA-MB-231 cell morphology. (A) Representative images of wild-type MDA-MB-231 cells when treated with IPA-3 and a DMSO control. Wild-type MDA-MD231 cells were seeded onto collagen coated coverslips and incubated with IPA-3 or DMSO for two, four and six hours. Cells were then fixed and stained for DAPI and phalloidin. Cells were then subject to morphological analysis using ImageJ. The scale bar represents 10µm. **(B, D and F)** Graphical representation of cell area after incubation for two hours (B), four hours (D) and six hours (F). **(C, E and G)** Graphical representation of perimeter after incubation for two hours (C), four hours (E) and six hours (G). Error bars represent SEM for three independent experiments, 30 cells per experiment. Statistical analysis was carried out using t-tests (* $p<0.05$)

Pharmacological inhibition of PAK1 rendered the same morphological phenotype, a reduced cell spread area, as PAK1 knockdown studies. Therefore, 2D cell migration of MDA-MB-231 cells treated with the PAK1 kinase inhibitor was investigated to examine if pharmacological inhibition also caused the same phenotype compared to the previous PAK1 knockdown data.

Wild-type MDA-MB-231 cells were incubated with IPA-3 or DMSO one hour prior to imaging. Cells treated with the IPA-3 inhibitor show a significantly reduced mean cell speed compared to DMSO control and wild-type cells **(Figure 3.12)**.

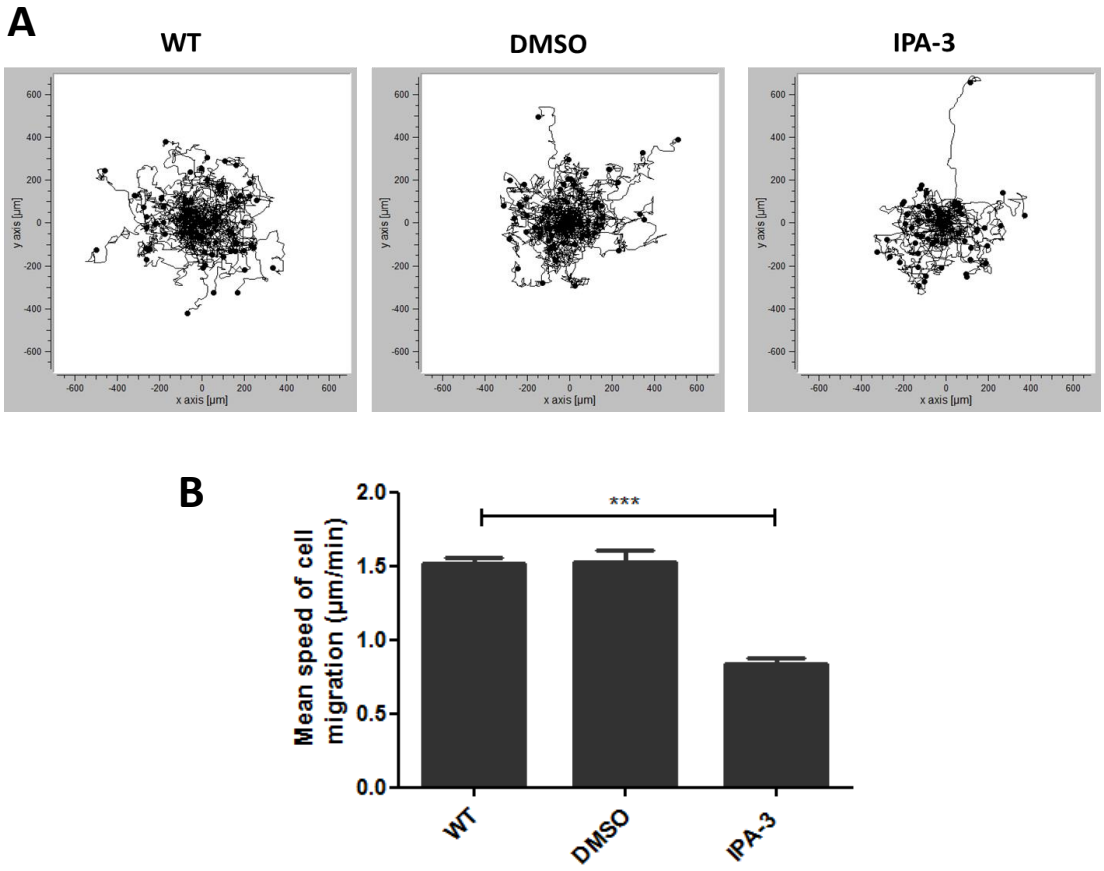

Figure 3.12 The effect of IPA-3 on MDA-MB-231 cells in 2D migration. (A) Wild-type MDA-MB-231 cells were seeded onto type I collagen and incubated with IPA-3, DMSO or nothing. The cells were then imaged for 16 hours. ImageJ was used to manually track the cells and cell speeds and plots were obtained using ibidi chemotaxis and migration tool. **(B)** Graphical representation of the mean speed of cell migration of wild-type cells alone or incubated with IPA-3 or a DMSO control. Error bars represent SEM for three independent experiments, 20 cells per experiment. Statistical analysis was carried out using t-tests (*** $p<0.001$).

3.3 Discussion

It has been well established that PAK1 plays a role in cell migration and is overexpressed in many breast cancers (Radu et al., 2014). However, it is not clear to what extent PAK1 has a role in influencing the morphology and migration of breast cancers, and whether this is a kinase dependent function. Establishing a role for PAK1 in breast cancer cell migration, if due to its kinase activity, could identify a new therapeutic target to prevent metastatic disease.

First, PAK1 expression was confirmed in the various cancer cell types and the breast cancer cell line with the highest PAK1 expression was identified as MDA-MB-231 cells. PAK1 expression was detected in breast cancer cell lines, MDA-MB-231 and BT-549 cells **(Figure 3.1)**. This is not surprising as PAK1 has been widely detected in both breast cancer cell lines and breast cancer tissue staining, with studies suggesting up to 55% of breast cancers have PAK1 overexpression (Balasenthil et al., 2004). Staining of human breast cancer tissue has also implicated PAK1 as an important factor in breast cancer cell migration. High PAK1 expression has been associated with lymph node metastasis and correlated with poor prognosis (Ong et al., 2011) .

Expression of PAK1 in both MDA-MB-231 and BT-549 cell lines have been previously reported (Zhan et al., 2017). MDA-MB-231 cells have been reported to express high levels of PAK1 when comparing them to other breast cancer cell lines. Ergun et al (2015) found that although all breast cancer cell lines assessed had PAK1 expression, MDA-MB-231 cells have the highest expression in PAK1 compared to four other breast cancer cell lines: SKBR3, MCF-7, HCC1500 and ZR-75-1. In this study the MDA-MB-231 cell line is shown to have a 2.1-fold increase in PAK1 expression compared with hTERT-HME1 cells, a human breast epithelial cell line (Ergun et al., 2015). It has also been shown that MDA-MB-231 cells have a higher PAK1 expression level than the MCF-7 breast cancer cell line (Morimura and Takahashi, 2011). Fewer studies regarding PAK1 in the BT-549 cell line have been published although previous expression has been noted (Zhan et al., 2017). In this chapter it is confirmed PAK1 is expressed in both MDA-MB-231 and BT-549 cells, in agreement

with existing literature, but also allows direct comparison of PAK1 expression between the two cell lines.

PAK1 expression was also observed in PC3, PaTu-8988T and PaTu-8902 cells **(Figure 3.1)**. PAK1 expression has previously been reported in PC3 cells (Al-Azayzih et al., 2015) and PaTu-8988T cells (King et al., 2017). However, PAK1 expression has not been reported in the pancreatic cell line PaTu-8902, although PAK1 expression has been noted in other pancreatic cell lines (Jagadeeshan et al., 2015, King et al., 2017).

Interestingly PAK1 knockdown using shRNA or CRISPR-Cas9 technology has not been reported in MDA-MB-231 cells. Unfortunately, an MDA-MB-231 cell clone with complete PAK1 knockout was not generated. Whilst initially no PAK1 protein is detected, as the passage number increases PAK1 expression is detectable although at lower levels than wildtype cells **(Figure 3.8)**. This is an interesting phenomenon as a CRISPR event occurs at the genomic level and therefore if completely successful re-expression of the targeted protein is not possible.

The number of PAK1 alleles present in the MDA-MB-231 genome could influence the outcome of generating a complete PAK1 knockout. If MDA-MB-231 cells have an increased number of PAK1 alleles, all copies of the gene would need to be altered by CRISPR-Cas9 technology, ensuring no PAK1 mRNA was transcribed, thus decreasing the likelihood of generating a full PAK1 knockout.

PAK1 is located at 11q13.5 in the genome, a region that is commonly amplified in breast cancer (Ong et al., 2011, Bekri et al., 1997). More often associated with hormone receptor and HER2 positive tumours; amplification of the gene has been demonstrated in TNBC, with a mean copy number of 2.8 and a PAK1 amplicon frequency of 18% in TNBC tissue (Ong et al., 2011). Although genomic amplification of PAK1 in MDA-MB-231 cells has not been identified (Shadeo and Lam, 2006), the cells have a mean chromosome number ranging from 65-69 (Cailleau et al., 1974) with four copies of chromosome 11 compared to two in normal breast epithelial cells (Yoon et al., 2002). This, taken with the reported

high expression of PAK1 in MDA-MB-231 cells (Ergun et al., 2015) and findings in this chapter suggests increased expression due to aneuploidy of chromosome 11 in this cell line.

Two potential theories could explain the re-expression of PAK1 in the MDA-MD-231 cell line. Firstly, as MDA-MB-231 cells are likely to have an increased number of PAK1 genes, due to aneuploidy of chromosome 11 (Yoon et al., 2002), there is a possibility not all PAK1 genes were actively being expressed, i.e. - some were silenced. As PAK1 expression is detected at later passage numbers not all the copies of PAK1 were subject to alteration by CRISPR-Cas9 technology. If the active copies of PAK1 were altered by CRISPR-Cas9 so they no longer expressed PAK1 mRNA, other silenced copies which were unaffected by CRISPR-Cas9 could be switched on to compensate for the loss of PAK1 expression. This could explain the absence of PAK1 expression initially but the return of expression to detectable levels as passage number increased. To validate this theory sequencing of PAK1 in the MDA-MB-231 cells would be necessary.

The second explanation relates to single cell cloning, performed manually, of the MDA-MB-231 cells once FACS sorted. Cell populations grown from a single cell clone were identified in wells of a 96 well plate using a microscope. A successful PAK1 knockout cell when single cell cloned would produce a cell population completely lacking PAK1 expression. However, if a cell population was falsely identified as originating from a single cell, i.e. - the cell population came from multiple cells, this could result in a mixed population of cells expressing different levels of PAK due to the success or failure of the CRISPR-Cas9 technology. If initially the PAK1 knockout cells grew quicker than the wildtype or knockdown cells this could lead to a very low level of PAK1 expression in the whole population of cells, potentially at undetectable levels. As passage number increased the PAK1 expressing cells could outcompete the PAK1 knockout cells causing a gradual increase in PAK1 expression overtime. This, although seems plausible, is unlikely to be the case.

The importance of PAK1 in breast cancer cell proliferation has previously been reported, notably in MDA-MB-231 cells (Zhan et al., 2017). Additionally, whilst culturing both the shRNA PAK1 knockdown cells and the CRISPR PAK1 knockdown cells no obvious differences in cell proliferation rate were noted compared to wild-type MDA-MB-231 cells. It is therefore improbable that a PAK1 knockdown cell population would proliferate at such an accelerated rate with regards to wild type cells and result in undetectable levels of PAK1 expression.

When assessing both morphological and migratory phenotypes, it would be expected that a population of cells containing PAK1 knockout and PAK1 expressing cells would give rise to two different phenotypes. However, in CRISPR PAK1 knockdown cells, 1.22 and 2.10, only one phenotype is observed for both morphological and migratory analysis **(Figure 3.8 and 3.9).** In addition to this comparisons of the shRNA PAK1 knockdown cells and CRISPR PAK1 knockdown cells exhibit similar phenotypes with regards to cell size **(Figure 3.3 and 3.8)** and mean speed of cell migration **(Figure 3.4 and 3.9)**. This would suggest the re-expression of PAK1 detected in the CRISPR PAK1 knockdown cells, 1.22 and 2.10, is not as a result of a mixed cell population.

Although a complete PAK1 knockout MDA-MB-231 cell line was not generated, two PAK1 knockdown cell line using CRISPR-Cas9 technology with an average knockdown of 48% and 57% respectively at passage eight were established. It is not surprising a depletion of PAK1 alters the cells area and perimeter as PAK1 has previously been reported to play a role in the cytoskeletal changes in many different cell types in overexpression studies. In both fibroblasts and HeLa cells expression of constitutively active PAK1 causes loss of stress fibres and focal adhesions (Manser et al., 1997). In Swiss 3T3 cells microinjection of PAK1 causes rapid formation of filopodia and membrane ruffles (Sells et al., 1997). It has also been demonstrated that PAK1 can induce cytoskeletal changes in breast cancer cells. Talukder et al., 2006 demonstrate than an increase in PAK1 activity, in in the MCF-7 breast cancer cell line, causes an increase in lamellipodia structures at the leading edge and a decrease in stress fibres and focal adhesions. Similarly, in MCF-7 cells overexpression of

PAK1 causes cell ruffling on stimulation with prolactin (Hammer et al., 2013). However, the effect of PAK1 depletion in the morphology of MDA-MB-231 cells has not previously been reported.

In this chapter it is demonstrated knockdown by both shRNA and CRISPR-Cas9 technology, and pharmacological inhibition of PAK1 causes a decrease in cell spread area. The average area of shRNA and CRISPR knockdown cells are comparable **(Table 3.1)**, with small differences most likely accounted for by varying levels of PAK1 knockdown. The IPA-3 treated cells showed a bigger cell spread area compared to both types of knockdown cells. This could indicate a role independent of PAK1 kinase activity, potentially as a scaffold protein. Although, as the IPA-3 treated cells have a significantly smaller area than the wildtype of DMSO controls **(Figure 3.11)** the majority of the decrease cell spread area phenotype which arises by manipulating PAK1 can probably be attributed to its kinase activity.

Cellular studies highlighting PAK1's ability to influence cell migration have been widely reported. Adam et al (1998) demonstrate a role for endogenous PAK1 in reorganising of the actin cytoskeleton, when stimulated with heregulin, to increase cell migration and invasion of MCF-7 cells. Additionally, in MCF-7, hyperactivation of PAK1 using a catalytically active mutant promotes cell migration of this non-invasive breast cancer cell line (Vadlamudi et al., 2000).

Studies also support the findings in this chapter that a decrease in PAK1 activity causes a decrease in cell migration, specifically in MDA-MB-231 cells. Overexpression of a kinase-dead PAK1 mutant in MDA-MB-231 causes enhanced stress fibres and a reduction in invasiveness (Adam et al., 2000). Stimulation studies also highlight a role for PAK1 in MDA-MB-231 cell migration. Yang et al (2011) demonstrate PAK1 activation on EGF stimulation which increased cell migration. They also find expression of a dominant negative PAK1 mutant largely abolishes EGF-induced cell migration (Yang et al., 2011). Furthermore, lysophosphatidic acid stimulation also induces PAK1 activation and increases cell migration, whilst an inactive mutant of PAK1 inhibits cell migration (Du et al., 2010). In this

chapter the mean cell speed of the shRNA PAK1 knockdown, CRISPR PAK1 knockdown and IPA-3 treated cells indicate the role of PAK1 is dependent on PAK1 kinase activity and cannot be attributed to kinase independent functions **(Table 3.2)**. This effect of IPA-3 on MDA-MB-231 cell migration has not previously been published and strongly indicated PAK1 kinase activity is important for cell migration.

This chapter highlights the importance of PAK1 kinase activity in breast cancer cell morphology and migration.

Cell type	Area ($\mu m^{2)}$	Cell type/ treatment	Area ($\mu m^{2)}$	Cell type/ treatment	Area (μm^2)
WT (shRNA)	297	Control	259	Sh1	181
				Sh2	156
WT (CRISPR)	294	-	-	1.22	165
				2.10	176
WT (IPA-3)	301	DMSO	303	IPA-3	203

Table 3.1 Area values for shRNA, CRISPR and IPA- 3 morphology.
shRNA and CRISPR cell values are an average of three independent experiments, 30 cells per experiment. IPA-3 values are an average of three time-points (2, 4 and 6 hours) assessed for independent experiments, 30 cells per experiment.

Cell type	Mean cell speed (µm/min)	Cell type/ treatment	Mean cell speed (µm/min)	Cell type/ treatment	Mean cell speed (µm/min)
WT (shRNA)	1.58	Control	1.48	Sh1	0.77
				Sh2	0.65
WT (CRISPR)	1.54	-	-	1.22	0.86
				2.10	0.82
WT (IPA-3)	1.50	DMSO	1.47	IPA-3	0.84

Table 3.2 Mean cell speed values for shRNA, CRISPR and IPA- 3 morphology. Values are an average of three independent experiments, 20 cells per experiment

3.4 Future work

This chapter describes the phenotypes that arose from depletion of PAK1 in MDA-MB-231 cells. PAK1 depletion causes altered morphology and motility of these breast cancer cells. Confirming these findings in other breast cancer cell lines would further highlight the importance that PAK1 plays in breast cancer cell migration. Comparing PAK1 depletion phenotypes in TNBC cell lines to hormone receptor and HER2 positive breast cancers would also assess the requirement for PAK1 in highly invasive breast cancers. Furthermore, it would also be noteworthy to see if these PAK1 kinase dependent functions were conserved to other cancer cell lines, for the example if the same phenotypes were observed in PaTu-8988T cells which also express PAK1 at high levels.

As a complete PAK1 knockout cell line would be beneficial to studying the role of PAK1 in morphology and migration, sequencing the CRISPR PAK1 knockdown cells to confirm if a successful CRISPR event had altered any of the PAK1 copies in these cell populations would aid the explanation of PAK1 re-expression. If the CRISPR construct had successfully altered one or multiple of the PAK1 copies, it would be appropriate to subject the CRISPR PAK1 knockdown cell populations to CRISPR-Cas9 technology again, to generate an MDA-MB-231 cell line with no PAK1 expression. A complete absence of PAK1 expression would need to be confirmed by assessing protein and mRNA levels.

A complete knockout PAK1 cell line would provide a useful tool to further study PAK1 activity and cell migration as constitutively active or kinase dead mutants could be knocked in using CRISPR-Cas9 technology. The role of PAK1 kinase activity could then be assessed when expression is at endogenous levels rather than an overexpression or depletion of the protein.

Chapter 4

Assess the requirement of PAK1 activity in *in vitro* invasion and *in vivo* cell migration

Chapter 4 Assess the requirement of PAK1 activity in *in vitro* invasion and *in vivo* cell migration

4.1 Introduction

Chapter 3 has highlighted a key role for PAK1 kinase activity in breast cancer cell 2D migration and morphology, which is supported in the literature. Whilst morphological analysis and 2D migration studies are useful for elucidating the importance of proteins in migration they are limited regarding their physiological relevance to cell migration and metastasis in patients. 3D *in vitro* systems, also termed spheroid assays, offer a bridge between 2D and *in vivo* studies.

Spheroid assays offer several advantages as they permit the study of cell migration and invasion in 3D, which allows further investigation of proteins thought to be important in cancer cell migration. Spheroid assays also allow drug screening in a more physiological environment in comparison to 2D migration studies (Rodrigues et al., 2018). It is therefore no surprise that 3D *in vitro* systems are becoming a popular method to study cancer cell invasion however they still offer less physiological relevance compared to *in vivo* cell assays which utilise model organisms such as mice and zebrafish to study cancer cell migration.

Zebrafish (*Danio rerio*) offer many advantages as an *in vivo* model and therefore they are becoming increasingly popular in many fields, including oncology research and the study of metastasis (Liu and Leach, 2011). Zebrafish embryos are optically translucent and are ideally suited to high resolution live imaging (Falenta et al., 2013). Zebrafish breed in large numbers so a single mating pair can produce hundreds of embryos in one spawn and develop rapidly *ex-utero* (Rubinstein, 2003). Comprising many advantages as a model for cancer metastasis, zebrafish offer a viable alternative to mouse studies to image cancer cell dissemination *in vivo* (Stoletov and Klemke, 2008, Amatruda et al., 2002).

Zebrafish embryos allow xenotransplantation assays using fluorescently labelled cancer cells at two days post fertilisation (dpf) when these cells are injected into the embryo,

usually into the yolk sac, and dissemination of the cancer cells to distant sites is detected using fluorescent microscopy. This assay allows the invasion, migration and micrometastasis formation of the injected cancer cells to be observed and studied. The zebrafish xenograft assay allows quick evaluation of metastasis formation, with dissemination and colonisation of cancer cells at distant sites occurring within 5 days of embryo injection. In comparison, *in vivo* mouse studies can take weeks until metastases can be detected. For this reason using the zebrafish xenograft model is becoming an increasingly popular method to study cancer cell invasion and metastasis with studies conducted in a range of cancer types such as melanoma (Lee et al., 2005), leukaemia (Pruvot et al., 2011), breast (Stoletov et al., 2010) and pancreatic cancer (Marques et al., 2009).

Despite the development of both these assays to study breast cancer cell invasion and migration, very little is reported about PAK1 in such assays, and the role of PAK1 kinase activity in assays which offer more physiological relevance is mostly unknown. This chapter therefore aims to examine if PAK1 plays a role in 3D invasion and *in vivo* cell migration by utilising spheroid and zebrafish xenograft assays, and if so whether this is a PAK1 kinase dependent function.

4.2 Results

4.2.1 PAK1 kinase activity plays a role in 3D cell invasion

Previously PAK1 knockdown cells were generated using shRNA technology **(Figure 3.2)** and were shown to have altered morphology **(Figure 3.3)** and slower migration **(Figure 3.4)** compared to wildtype and control cells. Initially, 3D spheroid invasion was investigated.

Wildtype, control and PAK1 knockdown cells were subjected to a 3D spheroid invasion assay. Cell spheroids are formed, embedded in a collagen matrix and allowed to invade for 24 hours. The number of cells invading into the collagen is calculated per quadrant. Both populations of PAK1 knockdown cells (sh1 and sh2) showed a decrease number of cells invading per quadrant compared to wildtype and control cells **(Figure 4.1)**

MDA-MB-231 cells depleted for PAK1 using CRISPR-cas9 technology were also generated **(Figure 3.8)** and displayed an altered morphology **(Figure 3.9)** and decrease migration **(Figure 3.10)** compared to wildtype controls. These cells were therefore utilised to investigate the role of PAK1 in cell invasion. All experiments using these cells occurred before passage number eight; therefore, ensuring significant PAK1 knockdown compared to wildtype cells **(Figure 3.8)**. Similarly, to the shRNA PAK1 knockdown cells, the CRISPR PAK1 knockdown cells also show a decrease in the number of cells invading per quadrant compared to wildtype controls **(Figure 4.2)**.

Previous experiments demonstrate that PAK1 kinase activity is important in cell morphology and migration as when IPA-3, a PAK1 kinase inhibitor, is employed cells have altered morphology **(Figure 3.11)** and impaired migration **(Figure 3.12)** compared to wildtype and DMSO control cells. The IPA-3 treated cells also show a reduction in the number of invading cells compared to wildtype or DMSO treated control cells **(Figure 4.3)** in the 3D spheroid assay.

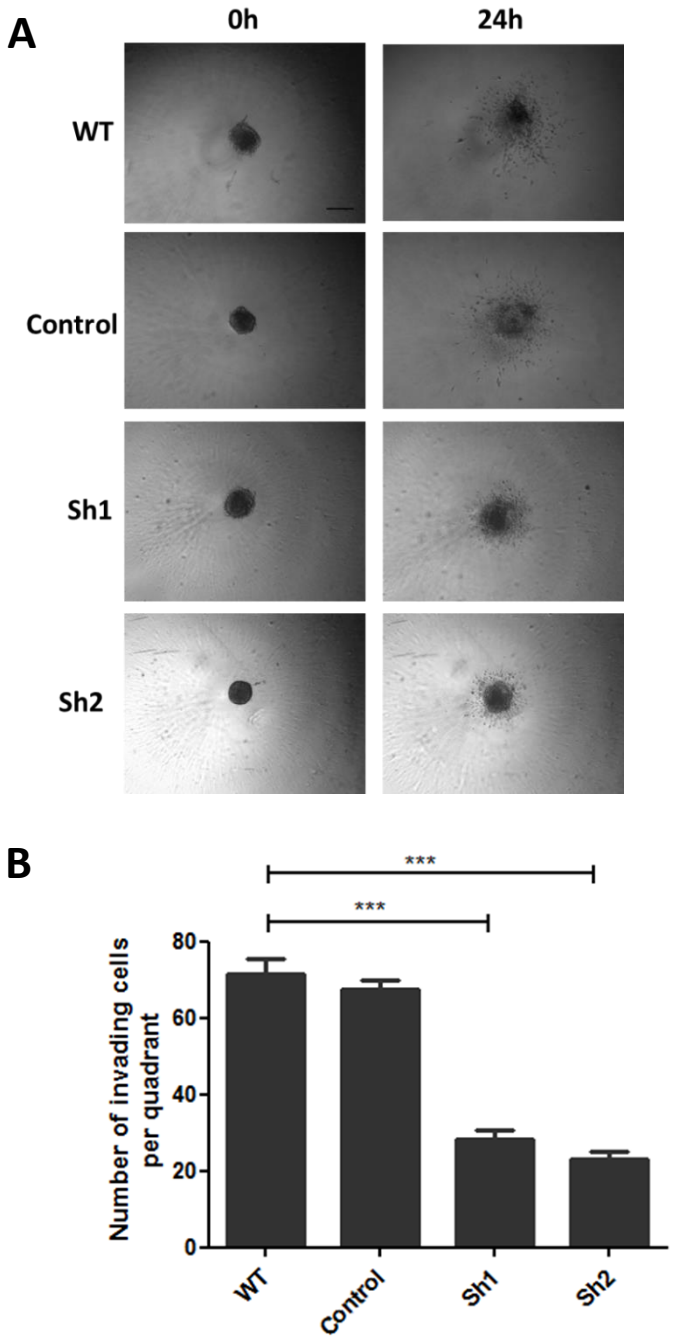

Figure 4.1 shRNA PAK1 knockdown leads to a decrease in cell invasion. Wildtype, control and PAK1 knockdown cells (sh1 and sh2) were seeded into non-adherent U-bottom 96 well plate and allowed to form spheroids. **(A)** Representative images of wildtype, control and PAK1 knockdown cells at 0h and 24h in a collagen matrix. Scale bar represents 300µm. **(B)** Graphical representation of the number of cells invading into the surrounding collagen per quadrant. Error bars represent SEM for three independent experiments, three spheroids analysed per condition, per experiment. Statistical analysis was carried out using t-tests (*** $p<0.001$).

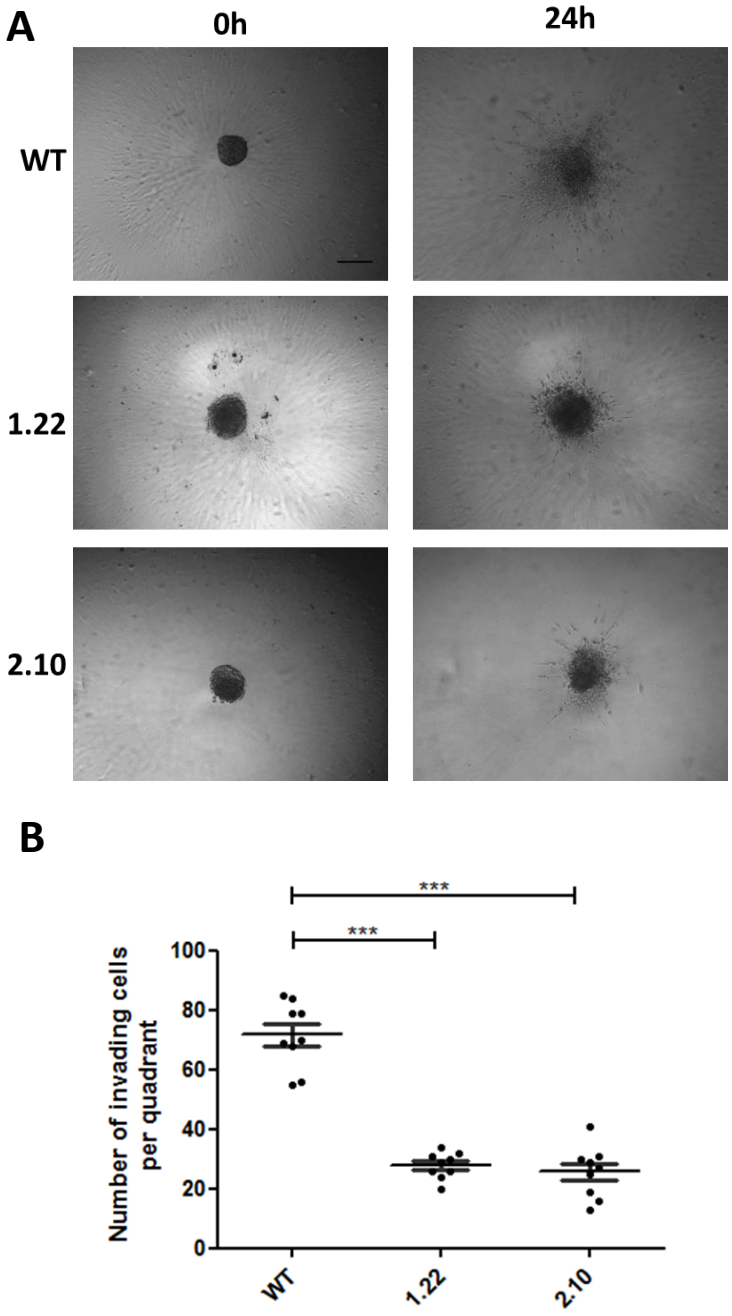

Figure 4.2 CRISPR PAK1 knockdown leads to a decrease in cell invasion. Wildtype and CRISPR PAK1 knockdown cells (1.22 and 2.10) were seeded into non-adherent U-bottom 96 well plate and allowed to form spheroids. **(A)** Representative images of wildtype and PAK1 knockdown cells at 0h and 24h in a collagen matrix. Scale bar represents 300µm. **(B)** Graphical representation of the number of cells invading into the surrounding collagen per quadrant. Error bars represent SEM for three independent experiments, three spheroids analysed per condition, per experiment. Statistical analysis was carried out using t-tests (*** $p<0.001$).

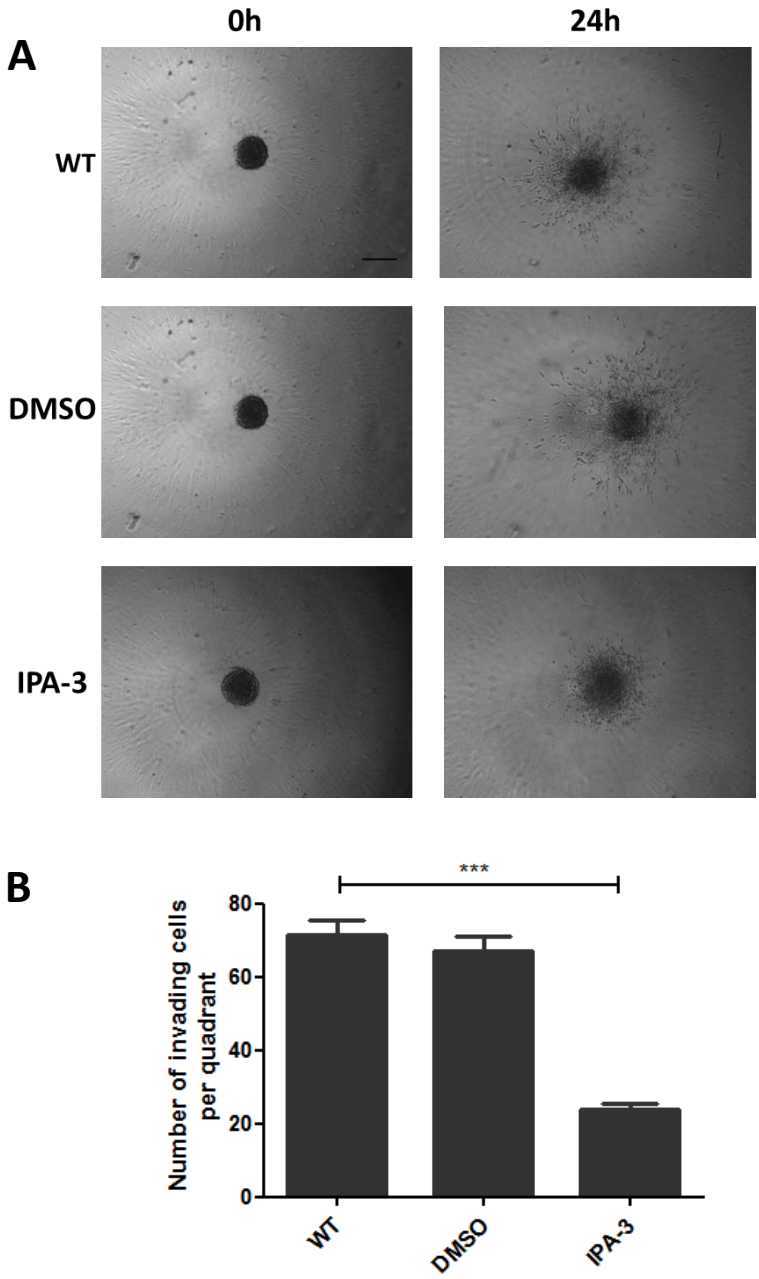

Figure 4.3 IPA-3 treatment leads to a decrease in cell invasion. Wildtype, DMSO treated and IPA-3 treated MDA-MB-231 cells were seeded into non-adherent U-bottom 96 well plate and allowed to form spheroids. **(A)** Representative images of wildtype, DMSO treated and IPA-3 treated cells at 0h and 24h in a collagen matrix. Scale bar represents 300µm. **(B)** Graphical representation of the number of cells invading into the surrounding collagen per quadrant. Error bars represent SEM for three independent experiments, three spheroids analysed per condition, per experiment. Statistical analysis was carried out using t-tests (*** $p<0.001$).

4.2.2 Zebrafish xenograft assay to study cancer cell migration

Having translated the 2D findings to 3D the next step was to investigate the requirement of PAK1 kinase activity in *in vivo* cell migration.

To gain the required technical skills for the zebrafish xenograft assay initial experiments were performed using AsPC-1 cells, a pancreatic cell line known to perform optimally in this assay (Teng et al., 2013).

AsPC-1 cells labelled with a fluorescent cell tracker dye were injected into the yolk sac of 2dpf zebrafish embryos. Two hours post injection the embryos were screened for the presence of fluorescence in the yolk sac **(Figure 4.4A)** and 24 hours after injected the embryos were screened for the presence of fluorescent deposits in the tail outside of the vasculature, indicating dissemination of AsPC-1 cells from the yolk sac to the tail **(Figure 4.4B)**. The percentage of embryos with dissemination was calculated **(Figure 4.4C)**.

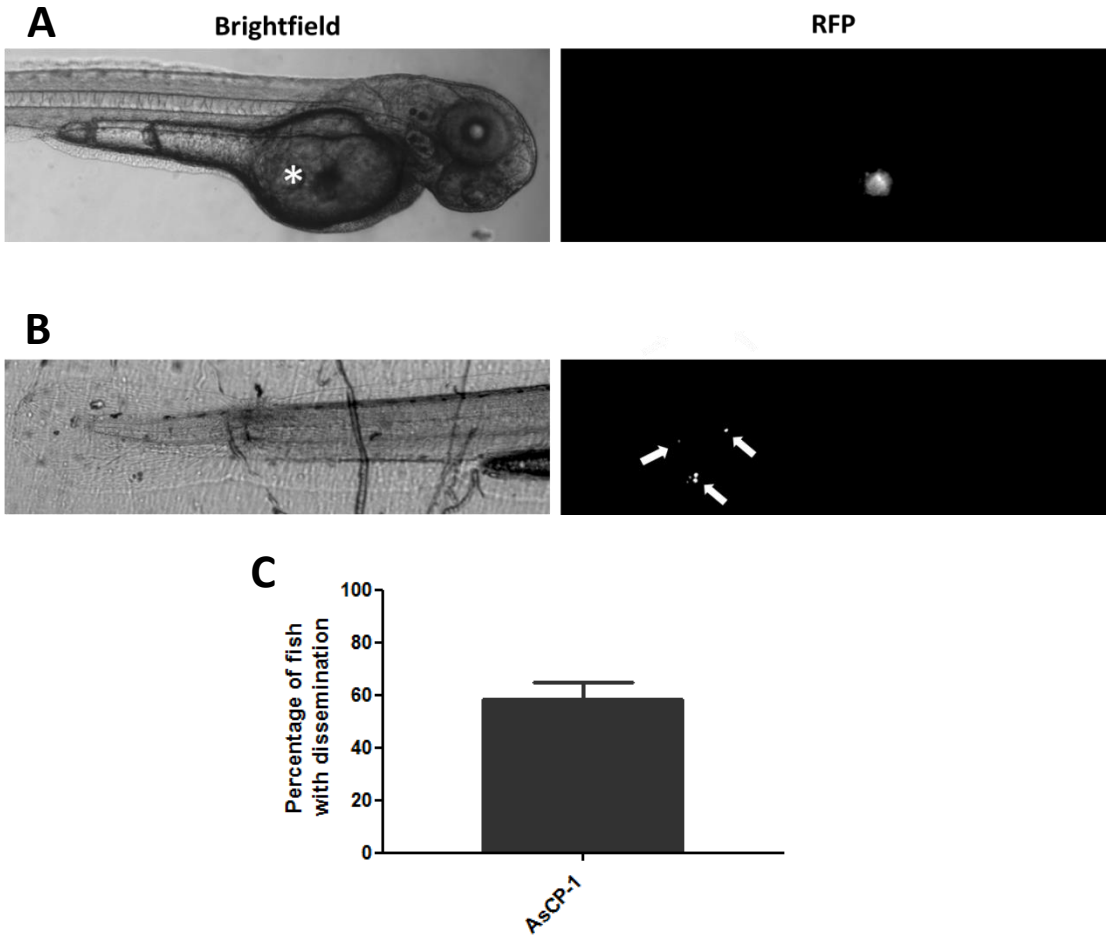

Figure 4.4 AsPC-1 cells dissemination in a zebrafish xenograft assay. Fluorescently labelled AsPC-1 cells were injected into 2dpf zebrafish embryos. **(A)** Representative image of an embryo with a positive fluorescent signal in the yolk sac two hours after injection**.** The asterisk indicates the site of injection. **(B)** Representative image of an embryo with positive dissemination marked by arrows, 24 hours after injection**. (C)** Graphical representation of the percentage of embryos with dissemination. Error bars represent the SEM for three independent experiments, with a minimum of 12 embryos per experiment.

4.2.3 Development of fluorescent MDA-MB-231 cells for zebrafish xenograft assay

Prior to MDA-MB-231 xenograft experiments it was necessary to generate fluorescently labelled cell lines, as the cell tracker dye previously used for AsPC-1 cell experiments does not label cells for an adequate amount of time to allow detection of MDA-MB-231 cells 4dpi. Wildtype, shRNA control cells and sh2 PAK1 knockdown cells were virally infected with LifeAct-RFP which labels the actin cytoskeleton. Sh2 cells were selected over sh1 cells as they express a lower level of PAK1 **(Figure 3.2)**. Unfortunately, as the CRISPR PAK1 knockdown cells show an increase in PAK1 expression as the cells' passage number increases **(Figure 3.8),** it would not be viable to generate these cells with LifeAct-RFP, as the PAK1 expression would no longer be significantly reduced after the viral infection protocol had been completed.

Wildtype, control and sh2 cells expressing LifeAct-RFP were successfully generated **(Figure 4.5)**.

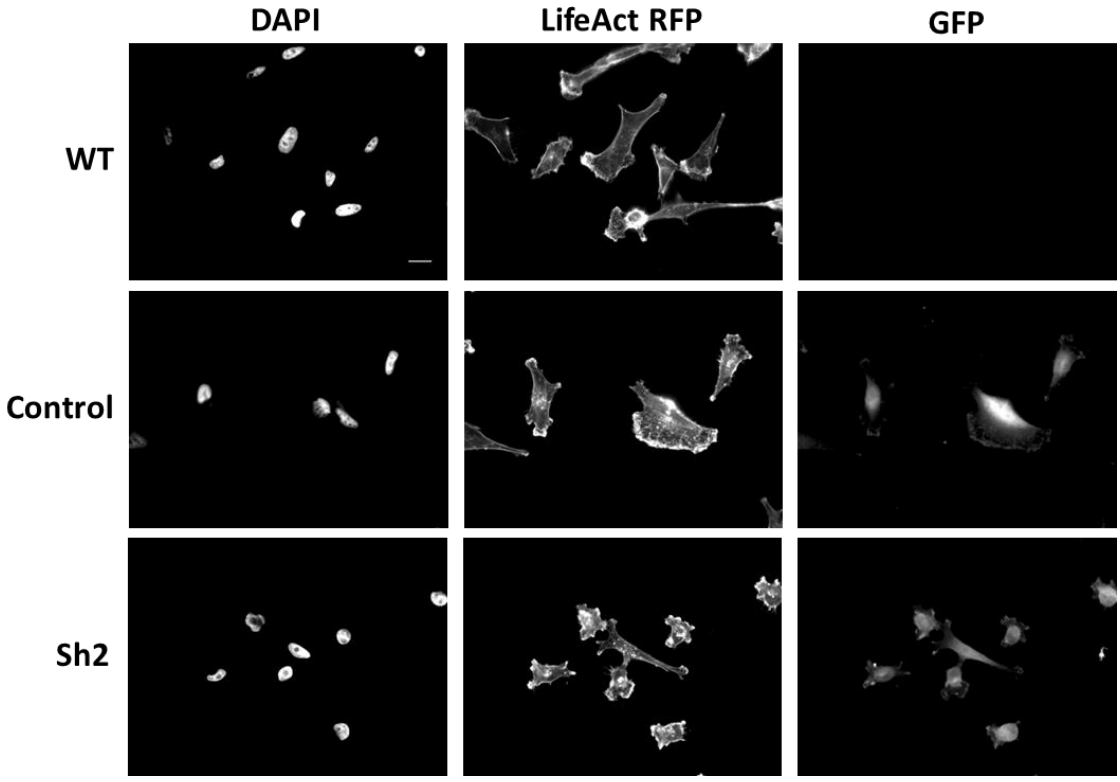

Figure 4.5 Successful generation of wildtype, control and PAK1 knockdown cells labelled with LifeAct-RFP. Representative images of wildtype, control and PAK1 knockdown cells, sh2, expressing LifeAct-RFP which labels the actin cytoskeleton, DAPI which stains the nucleus and GFP which here demonstrates the presence of either control of PAK1 shRNA constructs. Scale bar represents 10μm.

4.2.4 Optimisation of the zebrafish xenograft assay for MDA-MB-231 cells

Once the fluorescent wildtype, control and PAK1 knockdown MDA-MB-231 cells were generated a protocol previously used in the Wells' lab was employed to inject the cells into the yolk sac of the embryo, to establish a successful xenograft. Unfortunately, this protocol was not sufficient to xenograft the cells into the embryos and therefore needed to be optimised for the MDA-MB-231 cells. Three parameters of the experimental conditions were assessed on two different readouts, the percentage of embryos which died and the percentage of embryos with a successful xenograft, 24 hours after injection. All optimisation procedures were performed using wildtype MDA-MB-231 cells labelled with LifeAct-RFP **(Figure 4.5)**.

Firstly, the size of the needle was assessed as previously in the Wells' lab two different sizes had been used depending on the cells being injected. Needles with the internal diameters of 0.58mm and 0.78mm were assessed. The 0.78mm needle was selected as it resulted in a higher percentage of embryos with a successful xenograft **(Table 4.1)**.

Secondly, the density of the cells injected was optimised. MDA-MB-231 cells were prepared at 1.6×10^4, 2.1×10^4 and 3.2×10^4 cells per µl. These densities were selected from previous protocols in the Wells' lab and appropriate literature. The 2.1×10^4 cells/µl density was selected as it resulted in a higher percentage of embryos with a successful xenograft **(Table 4.2)**.

Finally, the pulse duration of injection was optimised. Three pulse durations were assessed- 200, 400 and 600ms based on previous protocols used in the Wells' lab. The 600ms duration gave a highest percentage of embryos with a successful xenograft compared to the 400ms condition, however the high percentage of embryo death in this condition meant the small increase in percentage of embryos with a successful xenograft was deemed not beneficial **(Table 4.3)**. The 400ms duration was therefore selected as it resulted in a high percentage of embryos with successful xenografts and relatively low percentage of embryo death at 24 hours **(Table 4.3)**.

For all further zebrafish xenograft experiments cells prepared at a density of .1 x 10^4cells/μl were injected using a needle with a 0.78mm internal diameter with a pulse duration of 400ms.

		Percentage of fish dead at 24 hours (%)	Percentage of fish with xenograft at 24 hours (%)
Needle size, internal diameter (mm)	0.58	20	35
	0.78	18	65

Table 4.1 Zebrafish xenograft assay needle size optimisation.
Values are averages of three independent experiments, 100 embryos injected per experiment, per condition.

		Percentage of fish dead at 24 hours (%)	Percentage of fish with xenograft at 24 hours (%)
Cell density (cells/µl)	1.6×10^4	17	12
	2.1×10^4	18	68
	3.2×10^4	20	22

Table 4.2 Zebrafish xenograft assay cell density optimisation. Values are averages of three independent experiments, 100 embryos injected per experiment, per condition.

		Percentage of fish dead at 24 hours (%)	Percentage of fish with xenograft at 24 hours (%)
Pulse duration (ms)	200	10	24
	400	21	61
	600	55	67

Table 4.3 Zebrafish xenograft assay pulse duration of injection optimisation. Values are averages of three independent experiments, 100 embryos injected per experiment, per condition.

4.2.5 PAK1 kinase activity plays a role in *in vivo* cell migration

Once the zebrafish xenograft assay had been optimised for MDA-MB-231 cells the requirement for PAK1 in *in vivo* cell migration was assessed. Wildtype, control and sh2 cells were injected into 2dpf zebrafish embryos. 24 hours after injection the embryos were screened from the presence of fluorescence in the yolk sac **(Figure 4.6A)** and 4dpi the embryos were screened for the presence of fluorescent deposits in the tail, outside of the vasculature, indicating dissemination of MDA-MB-231 cells from the yolk sac to the tail **(Figure 4.6B)**. The percentage of embryos with dissemination when injected with the sh2 PAK1 knockdown cells was significantly decreased compared to embryos injected with both wildtype and control cells **(Figure 4.6C)**.

This demonstrates PAK1 is important in *in vivo* cell migration however it remained unclear if this is due to its kinase activity. To assess this wildtype cells were injected into 2dpf embryos and after 24 hours the embryos were screened for fluorescence in the yolk sac **(Figure 4.7A)**, the embryo water was then supplemented with either DMSO or IPA-3, the inhibitor of PAK1 kinase activity. A 5µM concentration of IPA-3 was used based on previous publications (Jagadeeshan et al., 2017). A control of water that embryos are normally kept in was also present. 4dpi the embryos were screened for the presence of fluorescent deposits in the tail, outside of the vasculature, indicating dissemination of MDA-MB-231 cells from the yolk sac to the tail **(Figure 4.7B)**. The percentage of embryos with dissemination when the embryo water was supplemented with IPA-3 was significantly reduced compared to the percentage of dissemination seen from embryos in water which was not supplemented or water which was supplemented with DMSO **(Figure 4.7C)**.

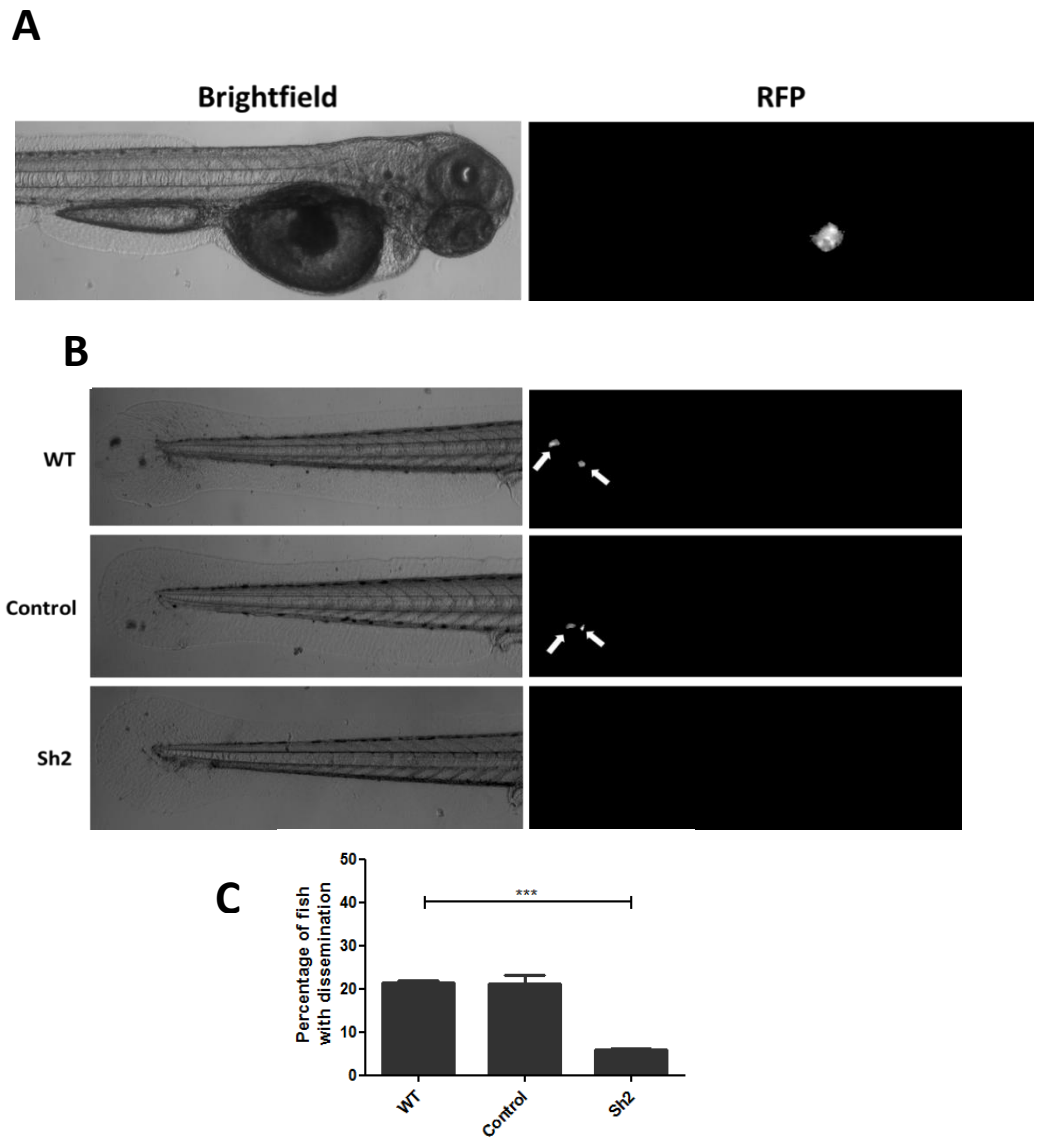

Figure 4.6 PAK1 knockdown leads to a decrease in *in vivo* cell migration. LifeAct-RFP wildtype, control and PAK1 knockdown (sh2) cells were injected into 2dpf zebrafish embryos. **(A)** Representative image of an embryo with a positive fluorescent signal in the yolk sac 24 hours after injection**. (B)** Representative images of embryos injected with wildtype, control and sh2 cells 4dpi. Arrows indicate sites of dissemination. **(C)** Graphical representation of the percentage of embryos with dissemination. Error bars represent the SEM for three independent experiments, with a minimum of 15 embryos per experiment, per condition. Statistical analysis was carried out using t-tests (*** $p<0.001$).

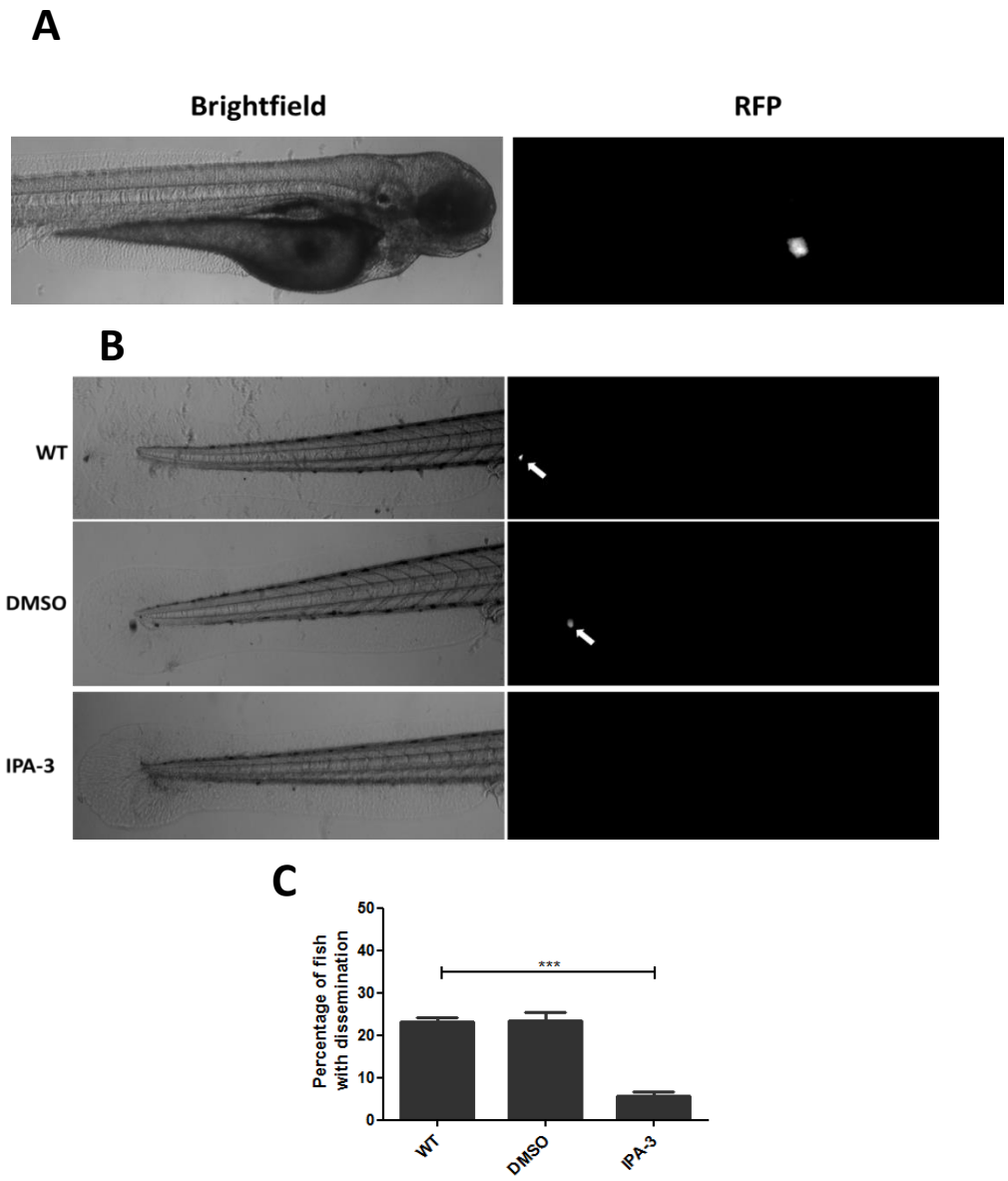

Figure 4.7 IPA-3 pharmacological inhibition of PAK1 leads to a decrease in *in vivo* cell migration. Wildtype cells were injected into 2dpf zebrafish embryos. **(A)** Representative images of embryos with a positive fluorescent signal in the yolk sac 24 hours after injection**. (B)** Representative images of embryo maintained in routine water or water supplemented with DMSO or IPA-3 4dpi. Arrows indicate sites of dissemination. **(C)** Graphical representation of the percentage of embryos with dissemination. Error bars represent the SEM for three independent experiments, with a minimum of 19 embryos per experiment, per condition. Statistical analysis was carried out using t-tests (*** $p<0.001$).

4.3 Discussion

This chapter aimed to assess the requirements of PAK1 in breast cancer cell 3D invasion and *in vivo* migration as little is known about PAK1 in this context. These two assays are useful tools to study cancer cell migration and invasion as they offer a greater physiological relevance than morphological and 2D migration studies.

Firstly, a 3D spheroid invasion assay was employed to assess if PAK1 plays a role in breast cancer cell invasion in 3D. In this assay PAK1 knockdown via both shRNA and CRISPR-cas9 technology showed a significant decrease in MDA-MB-231 cell invasion compared to wildtype and control cells **(Figure 4.1 and 4.2)**. This highlighted the importance of PAK1 in 3D cell invasion. To further explore kinase dependence IPA-3, the inhibitor of PAK1 kinase activity, was employed and demonstrated that this PAK1 function was dependent of its kinase activity, as IPA-3 treated MDA-MB-231 cells also show a significant decrease in cell invasion compared to wildtype and DMSO control cells **(Figure 4.3)**. Although the role of PAK1 in 3D invasion is not extensively reported existing studies do support a role for PAK1 in cell invasion, as demonstrated in this chapter.

PAK1 also plays a role in 3D invasion of melanoma cells (Nicholas et al., 2016). Li et al (2008) report a critical role for PAK1 in Ras-transformed MCF10A cells when assessing invasion using a 3D reconstituted basal membrane overlay culture assay. Hammer et al (2013) demonstrate a role for PAK1 in 3D invasion of TMX2–28 cells, a highly invasive ER negative clone of MCF-7 breast cancer cells, believed to be due to PAK1s ability to aid expression and secretion of MMPs which can degrade the surrounding matrix.

3D spheroid invasion assays demonstrated that PAK1 plays a role in breast cancer cell 3D invasion. To assess if PAK1 also plays a role in *in vivo* cell migration a zebrafish xenograft assay was employed.

Zebrafish xenograft assays offer many advantages to study cancer cell invasion and metastasis. Whilst at first being challenging to learn, once the expertise of transplantation is learnt the assay it relatively simple and reproducible (Stoletov and Klemke, 2008).

Zebrafish spawn in large numbers allowing access to many embryos which develop *ex-utero* (Rubinstein, 2003). These embryos are optically translucent meaning they are suitable for high resolution microscopy if desired and the zebrafish xenograft migration assay can be analysed by simple microscopy observations (Rodrigues et al., 2018). These factors ensure the assay is relatively cheap and simple way to study human cancer cell migration *in vivo* (Stoletov and Klemke, 2008). In addition to this, the zebrafish embryos used for these assays have not yet developed an adaptive immune system but do however allow human cancer cell and innate immune system interactions (Rodrigues et al., 2018).

Whilst 2D migration assays in the form of monolayer scratch and 2D random migration assays are much cheaper and offer better viability for the cancer cells being studied they are very substrate dependent and interactions between the cancer cells and extracellular environments are very limited and therefore less physiologically relevant that the zebrafish xenograft assay (Rodrigues et al., 2018). However, 2D migration assays are a very useful tool to identify proteins of interest involved in cell migration and invasion which may also play a key role in cancer cell metastasis and should therefore be studied in more detail.

3D invasion assays offer a bridge between 2D migration and *in vivo* migration assays. In comparison to 2D migration assays they offer greater interactions between the cancer cells and ECM allowing the regulation of proliferation and differentiation of the cancer cells (Rodrigues et al., 2018). 3D assays are also relatively easy to perform, and identification of invading cancer cells by immunofluorescence or immunohistochemistry is simple (Rodrigues et al., 2018). They also offer a great platform for drug screening when investigation novel targets and pathways to combat cancer cell migration (Rodrigues et al., 2018). Whilst drug screening can be performed with zebrafish there are a lot more caveats involved when considering the drug effect on the zebrafish embryos itself and whether this could potentially be detrimental to the assay itself (Rubinstein, 2003).

Drosophila also offer a valuable tool to study human cancers, particularly the initial stages of metastasis such as EMT, which is more challenging in zebrafish xenograft assays (Rodrigues et al., 2018). Whilst the genes and signalling pathways of drosophila have been

well studied and are highly conserved to humans, they lack mammalian systems and organs such as lungs, a liver and pancreas (Rodrigues et al., 2018). In this sense, zebrafish are more physiologically relevant in the study of cancer cell migration where the innate immune system is present, and angiogenesis can occur and be studied (Rodrigues et al., 2018, Stoletov and Klemke, 2008).

Mice are the one model organism routinely used which offer greater physiological relevance to humans than zebrafish (Rodrigues et al., 2018). They allow the formation of metastasis to relevant mammalian organs, e.g. the breast cancer cells metastasising to the lungs which naturally occurs in patients (Rodrigues et al., 2018, Dent et al., 2009). The study of metastasis formation in zebrafish xenograft assays is usually limited to the tail of the embryo and is therefore less physiologically relevant. However, mice need to be immunocompromised or immune-deficient meaning there is inadequate modelling of immune human responses (Rodrigues et al., 2018). Although embryos in zebrafish xenograft assays have not developed and adaptive immune system they do allow the interaction of the human cancer cells and innate immune system (Rodrigues et al., 2018). Mice studies also take a lot longer and are more costly than other methods of studying cancer cell migration and invasion (Stoletov and Klemke, 2008, Amatruda et al., 2002).

All methods offer advantages and limitations for studying cancer cell invasion and migration however all have a fundamental place in modern cell biology. Depending on what exactly is being studied and the resources available a combination of these tools can be used to shed light onto proteins and pathways involved in cancer cell biology. The zebrafish method although initially challenging to learn can cover valuable middle ground between 2D/3D and mice assays when considering physiological relevance to human cancer metastasis in patients.

In this chapter, the MDA-MB-231 cells did not initially xenograft successfully into the zebrafish using the existing injection protocol in the Wells' lab. This is most probably because this protocol was optimised for a different cell type which may have different properties that influence their ability for a successful injection and xenograft. To overcome this obstacle three different experimental parameters were optimised. Firstly, the internal

diameter of the needle was optimised. The internal diameter size of 0.78mm was selected as it results in a greater number of embryos with successful xenograft 24 hours post injection **(Table 4.1)**. This is most likely because the smaller diameter needle, 0,58mm, caused cell clumping within the tip of needle during injections, causing fewer cells to exit the needle and enter the yolk sac of the zebrafish. The second parameter to be optimised was the density of the injected cells. The 2.1 x 10^4 cells/µl was selected for further injections as this cell density resulted in the highest percentage of successful xenografts at 24 hours post injection **(Table 4.2)**. The lower density tested (1.6 x 10^4 cells/µl) was too low to ensure enough cells exited the needle and the higher density tested (3.2 x 10^4 cells/µl) resulted in clumping of cells in the needle and therefore not enough entering the fish when injected. Finally, the last parameter tested was the pulse duration during injection. The pulse duration of 400ms was selected as it resulted in a high percentage of embryos with a successful xenograft in relation to the number of embryos dead at 24 hours **(Table 4.3)**. The 200ms pulse duration was too short to allow enough cells to exit the needle and the 600ms pulse duration most likely caused too much damage to the embryo which resulted in a higher percentage in embryo death compared to the other conditions **(Table 4.3)**. MDA-MB-231 cells were successfully xenografted in a satisfactory number of zebrafish embryos when these experimental parameters were used.

Here it is found wildtype MDA-MB-231 cells cause dissemination in ~21-22% of zebrafish embryos 4dpi. This is lower than numbers reported in the literature where dissemination was described to be >40% in control shRNA MDA-MB-231 cells (Li et al., 2016) and >75% in DMSO treated MDA-MB-231 cells (Xie et al., 2016). This is most likely due to significant difference in protocol. In previous studies there is a variation in site of injection, the zebrafish incubation temperature and the dissemination period. For example, when injecting MDA-MB-231 cells, Xie et al (2016) injected into the yolk sac, maintained their embryos at 34°C and quantified the percentage of embryos with dissemination 2dpi whereas Li et al (2016) injected into the Duct of Cuvier, maintained their embryos at 33°C and quantified the percentage of embryos with dissemination just two hours post

injection. Injection into the Duct of Cuvier is a less robust way to study cell migration and dissemination than yolk sac injections, as the cells are injected directly into the embryos circulation. This accounts for why shorter time frames are used. The yolk sac is the only site of injection in the embryo which ensures migration can only be achieved through active cell motility (Veinotte et al., 2014), making injection into this site the most reliable way to assess a cell types ability to migrate. For the experiments reported in this chapter the cells are injected into the yolk sac, embryos are then maintained at 33°C and are analysed for percentage of embryos with dissemination 4dpi. An injection of 2dpf embryos into the yolk sac is the most commonly practiced variation and is adopted here. This is because it is an acellular environment which provides nutrients to the injected cells which allow for cell growth (Veinotte et al., 2014). 35^{o}C has been suggested as the optimum temperature for the cancer cell survival and embryo development (Veinotte et al., 2014) however in the Wells' lab a high rate of embryo cell death is observed at this temperature and therefore 33^{o}C is used as it appears more suitable for this assay as there is less embryo death but MDA-MB-231 cells still survive and migrate.

Interestingly, PAK1 has only once been previously published in any zebrafish xenograft migration studies however this was in melanoma cells (Nicholas et al., 2016). Here it is shown PAK1 plays a critical role for *in vivo* cell migration as injection of PAK1 knockdown cells causes a significant reduction in the percentage of embryos with dissemination compared to wildtype and control cells **(Figure 4.6)**. IPA-3 studies show this role of PAK1 is dependent on its kinase domain as when this inhibitor is used to supplement the zebrafish water, a significant decrease in the percentage of embryos with dissemination compared to water not supplemented or supplemented with DMSO as a control is observed **(Figure 4.7)**. It is important to note, the concentration of the IPA-3 inhibitor used to supplement the zebrafish water, 5µM, does not cause any damage to the embryos themselves (Jagadeeshan et al., 2017) and therefore the results observed are due to the inhibitor of PAK1's kinase activity and not due to any effect the drug could have on the zebrafish embryos development.

Taken together, this chapter highlights the importance of PAK kinase activity in 3D cell invasion and *in vivo* cell migration.

4.4 Future work

Confirming the requirement for PAK1 in 3D spheroid and zebrafish xenograft migration assays in other breast cancer cell line would further highlight the importance that PAK1 plays in both 3D invasion and *in vivo* cell migration. For example, from chapter 3 and related literature it is apparent that the TNBC cell line BT-549 express PAK1, which has been shown to play a role in cell migration in this cell line (Zhan et al., 2017). It would be noteworthy to examine if PAK1 knockdown and pharmacological inhibition also caused a decrease in 3D cell invasion and *in vivo* cell migration. It would also be interesting to note if the zebrafish xenograft assay would perform more optimally if another cell type was used, for example the BT-549 cell line which has not been previously published in the zebrafish xenograft assay.

Ideally, both the 3D invasion spheroid assay and zebrafish xenograft assay would be repeated using MDA-MB-231 cells which were complete knockout for PAK1 at the genomic level. The requirement of PAK1 and its kinase activity could then be assessed further by knocking in constitutively active or kinase dead mutants by utilising CRISPR-cas9 technology, to a cell line with no PAK1 expression. The role of PAK1 kinase activity could then be assessed when expression is at endogenous levels rather than depletion or pharmacological inhibition of the protein.

Confirming the findings here in other cancer cell lines in 3D cell invasion and *in vivo* cell migration could further support the concept that PAK1 could be an effective therapeutic target to help reduce metastasis in a clinical setting.

Chapter 5

Utilise an inducible PAK1 model system to monitor PAK1 specific cellular responses

Chapter 5 Utilise an inducible PAK1 model system to monitor PAK1 specific cellular responses

5.1 Introduction

In chapter 3, PAK1 knockdown and pharmacological inhibition morphological studies implicated PAK1 in regulating cell spread area, a role dependent on PAK1 kinase activity **(Figure 3.3, 3.9 and 3.11)**. Although many signalling pathways downstream of PAK1 in regards to cell migration are known, PAK1's role in spreading is not well studied. Therefore little is known about the role of PAK1 in cell spreading and the downstream signalling effectors involved.

Like in cell migration, cell spreading also requires rearrangement of the actin cytoskeleton. It is therefore not surprising that many of the key proteins involved in cell migration also have significant importance in cell spreading. For example, the Rho GTPases play essential roles in both cell spreading and migration (Lawson and Burridge, 2014). Rac1 is important for lamellipodia formation and cell spreading due it its ability to stimulate Arp2/3 via the WAVE complex (Miki et al., 1998, Machesky and Insall, 1998, Chen et al., 2017). Rac1 also plays a role in focal complex formation as it is activated downstream of both integrin engagement and the FAK-Src complex, and is then recruited to membrane ruffles and adhesion sites via its binding to β-Pix (ten Klooster et al., 2006). Interestingly, PAK1 has been shown to regulate the Rac1 and β-Pix interaction to controls cell spreading (ten Klooster et al., 2006). Like Rac1, PAK1 is activated downstream of integrin-dependent adhesion, and is implicated in focal adhesion regulation (Radu et al., 2014). Taken together, these studies indicate a role for PAK1 in cell spreading; however, this has not been widely researched especially in the context of breast cancer.

Whilst studies have highlighted the importance of PAK1 and its kinase activity in cell spreading and migration, current methods employed to measure PAK1 activity have limitations. Phospho-PAK1 antibodies are employed to study PAK1 activity (Sells et al.,

2000); however, this provides little insight into the role of PAK1 kinase activity in living cells, only highlights where active PAK1 is localised.

Inducible systems offer an alternative approach to study kinase activity. Being able to activate a protein on demand allows the study of kinase activity in a temporal manner. Thus, kinase activity can be directly correlated with any observed cell behaviour changes. Therefore, to dissect a specific role in cell spreading, a PAK1 inducible system has been employed in this chapter.

The inducible PAK1 construct is a single chain construct which combines iFKBP and FRB domains (together termed uniRapR) inserted into the 288-293 loop in the PAK1 kinase domain, an allosteric site which is not evolutionary conserved (Dagliyan et al., 2017). This site does not interact with any structural elements in the protein, including the regulatory domain and dimerisation interface (Dagliyan et al., 2017). This non-evolutionarily conserved loop allosterically coupled and moves in concert with the ATP-binding loop in PAK1's kinase domain (Dagliyan et al., 2017). In the absence of rapamycin, the uniRapR domain renders the 288-293 loop and therefore the ATP binding-loop unstable however on addition of rapamycin binding of the iFKBP and FRB domains occur thus stabilising both loops, allowing for activation of PAK1 (Dagliyan et al., 2017).

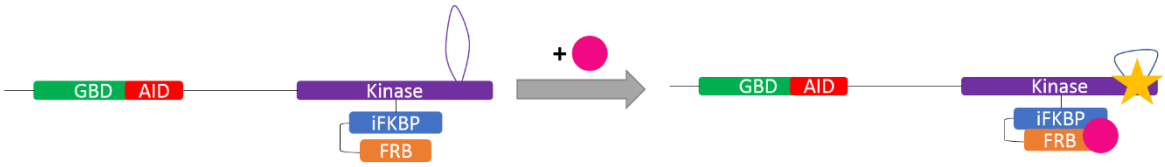

Figure 5.1 A schematic diagram of rapamycin induces PAK1-rap stability and activity. A uniRapR domain, which consists of an iFKBP and FRB domains, is inserted into the 288-293 loop of PAK1's kinase domain. In the absence of rapamycin this causes instability of PAK1 due to the destabilisation of the ATP binding-loop in the kinase domain, indicated by a purple loop. On addition of rapamycin, indicated by the pink circle, the iFKBP and FRB domains of the uniRapR domain bind causing the kinase domain of PAK1 to become active, indicated by a yellow star, as the ATP binding-loop is stabilised.

Little is known about the specific role PAK1 plays in breast cancer cell dynamics and the downstream effectors involved in such events. This chapter therefore aims to access the specific role of PAK1 in MDA-MB-231 morphological responses and identify putative downstream targets of PAK1 utilising an inducible PAK1 system.

5.2 Results

5.2.1 UniRapR-PAK1 is stably expressed in MDA-MB-231 cells

Wild-type MDA-MB-231 cells and MDA-MB-231 cells stably expressing an inducible PAK1 construct **(Figure 5.1)** were received from Dr Klaus Hahn, University of North Carolina (Dagliyan et al., 2017).

To confirm protein expression of the PAK1-rap construct in the MDA-MB-231 cells which are stably expressing the PAK1-rap construct (in this chapter termed S44 cells) and the absence of this expression in the wild-type cells that the S44 cells were derived from (in this chapter termed UNC-WT) cell lysates were probed for PAK1. Both the S44 and UNC-WT cells show endogenous PAK1 expression at 68kDa, however only the S44 cells show expression of the PAK1-rap protein at 112kDa **(Figure 5.2)**.

For all subsequent experiments the UNC-WT cells are used as a control to eliminate any morphological or biochemical responses induced by rapamycin, given its inhibitory effects on mammalian target of rapamycin (mTOR) (Ballou and Lin, 2008).

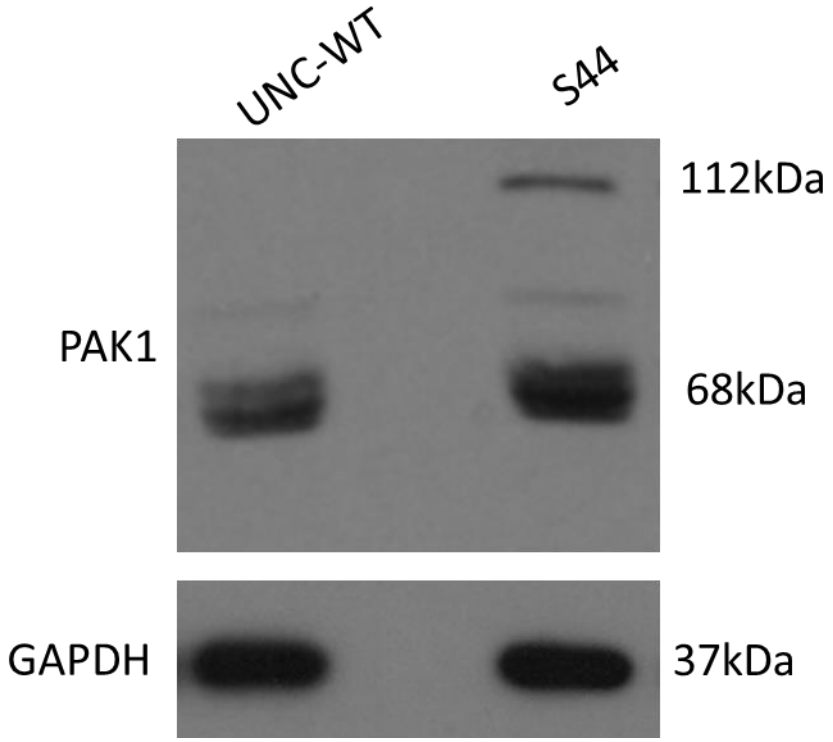

Figure 5.2 Expression of PAK1-rap in S44 cells. Representative western blot from whole cell lysates were prepared from S44 and UNC-WT cells probed for PAK1. GAPDH was used as a loading control. Blot representative of three independent experiments.

5.2.2 Significant differences in cell morphology identified between MDA-MB-231 wild-type populations

During initial culturing for generation of lysates **(Figure 5.2)** it was observed that the UNC-WT cells exhibited an increased spread area compared to wildtype MDA-MB-231 from King's (K-WT) utilised in chapters 3 and 4. Subsequent cell spread area analysis revealed a significant difference between the two wildtype populations **(Figure 5.3)**. Therefore, the UNC-WT cells were used as the wild-type control cells for the remainder of this chapter as these are the wild-type cells the S44 cells were generated from.

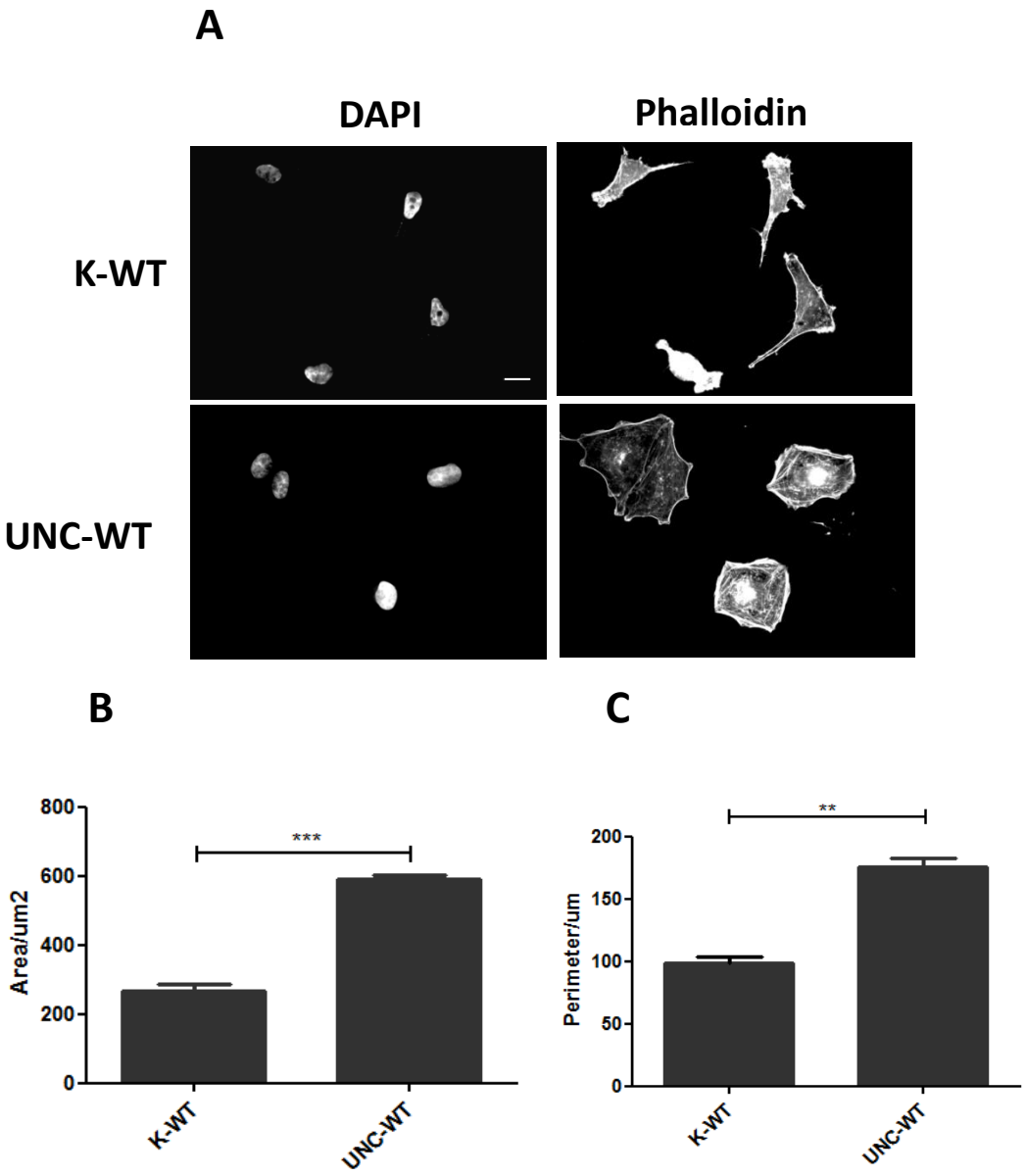

Figure 5.3 Morphology of K-WT and UNC-WT cells. (A) K-WT and UNC-WT cells were seeded onto coverslips, fixed and stained for DAPI and phalloidin. Cells were then subject to morphological analysis using ImageJ. The scale bar represents 10µm. **(B and C)** Graphical representation of cell area (B) and perimeter (C) for K-WT and UNC-WT cells. Error bars represent SEM for three independent experiments, 30 cells per experiment. Statistical analysis was carried out using t-tests (** $p<0.01$, *** $p<0.001$).

5.2.3 Phosphorylation levels of PAK1-rap increase on rapamycin stimulation

To confirm the activation of the PAK1-rap construct on addition of rapamycin, S44 and UNC-WT were stimulated with rapamycin for five, 20 and 60 minutes. The cells were lysed and probed for pPAK1 threonine 423, as a marker of activation and kinase activity (Zenke et al., 1999). The samples were also probed for total PAK1 to ensure levels of total protein remained stable, and GAPDH as a loading control. An increase of pPAK1 thr423 of the PAK1-rap is observed at the five-minute time point for S44 cells however the phosphorylation level is beginning to decay within 20 minutes **(Figure 5.4)**. This increase is not observed in the UNC-WT cells as they do not express the PAK1-rap construct **(Figure 5.5)**. No increase in the phosphorylation of threonine 423 of endogenous PAK1 was observed in either S44 or UNC-WT cells **(Figure 5.5 and 5.6)**.

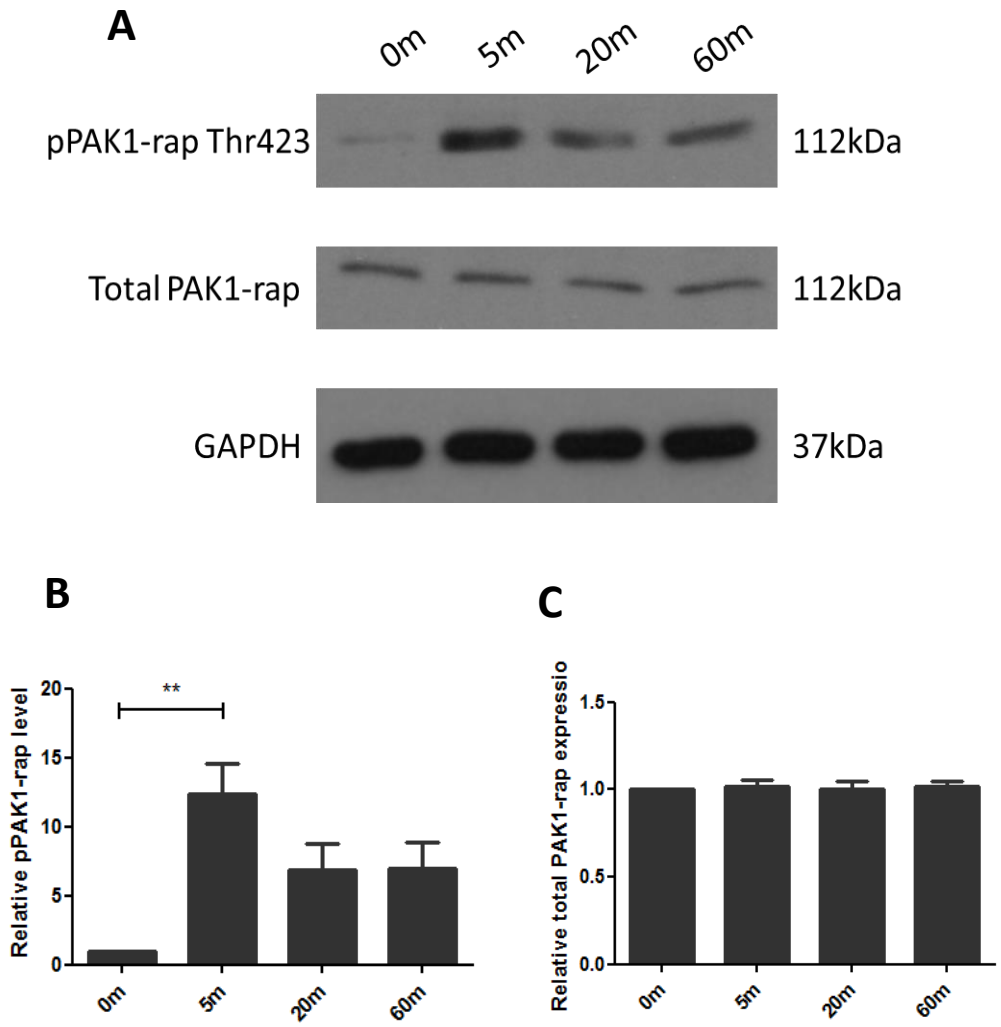

Figure 5.4 Phosphorylation levels of PAK1-rap at threonine 423 increase on stimulation of rapamycin in S44 cells. Whole cell lysates prepared from S44 cells stimulated with rapamycin for five, 20 and 60 minutes. **(A)** Representative western blot indicating the level of pPAK1 thr423 for the PAK1-rap protein and the level of total PAK1-rap protein. GAPDH was used as a loading control. **(B)** Densitometric analysis on ImageJ was used to compare the levels of pPAK1 thr423, normalised to the loading control and background noise. **(C)** Densitometric analysis on ImageJ was used to compare the levels of total PAK1, normalised to the loading control and background noise. Error bars represent SEM for three independent experiments. Statistical analysis was carried out using t-tests (** $p<0.01$).

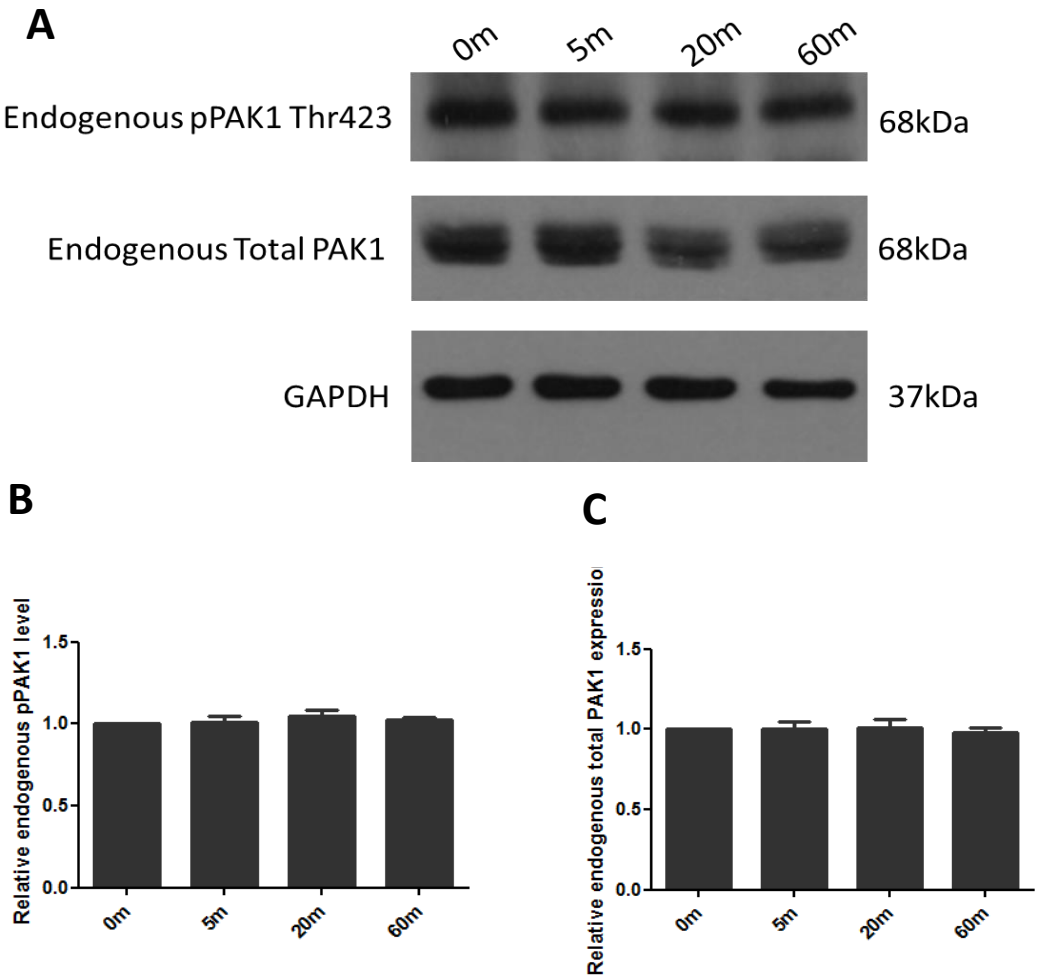

Figure 5.5 No change in endogenous PAK1 threonine 423 phosphorylation levels on stimulation of rapamycin in S44 cells. Whole cell lysates prepared from S44 cells stimulated with rapamycin for five, 20 and 60 minutes. **(A)** Representative western blot indicating the level of PAK1 thr423 for the endogenous PAK1 and the level of total endogenous PAK1. GAPDH was used as a loading control. **(B)** Densitometric analysis on ImageJ was used to compare the levels of pPAK1 thr423, normalised to the loading control and background noise. **(C)** Densitometric analysis on ImageJ was used to compare the levels of total PAK1, normalised to the loading control and background noise. Error bars represent SEM for three independent experiments.

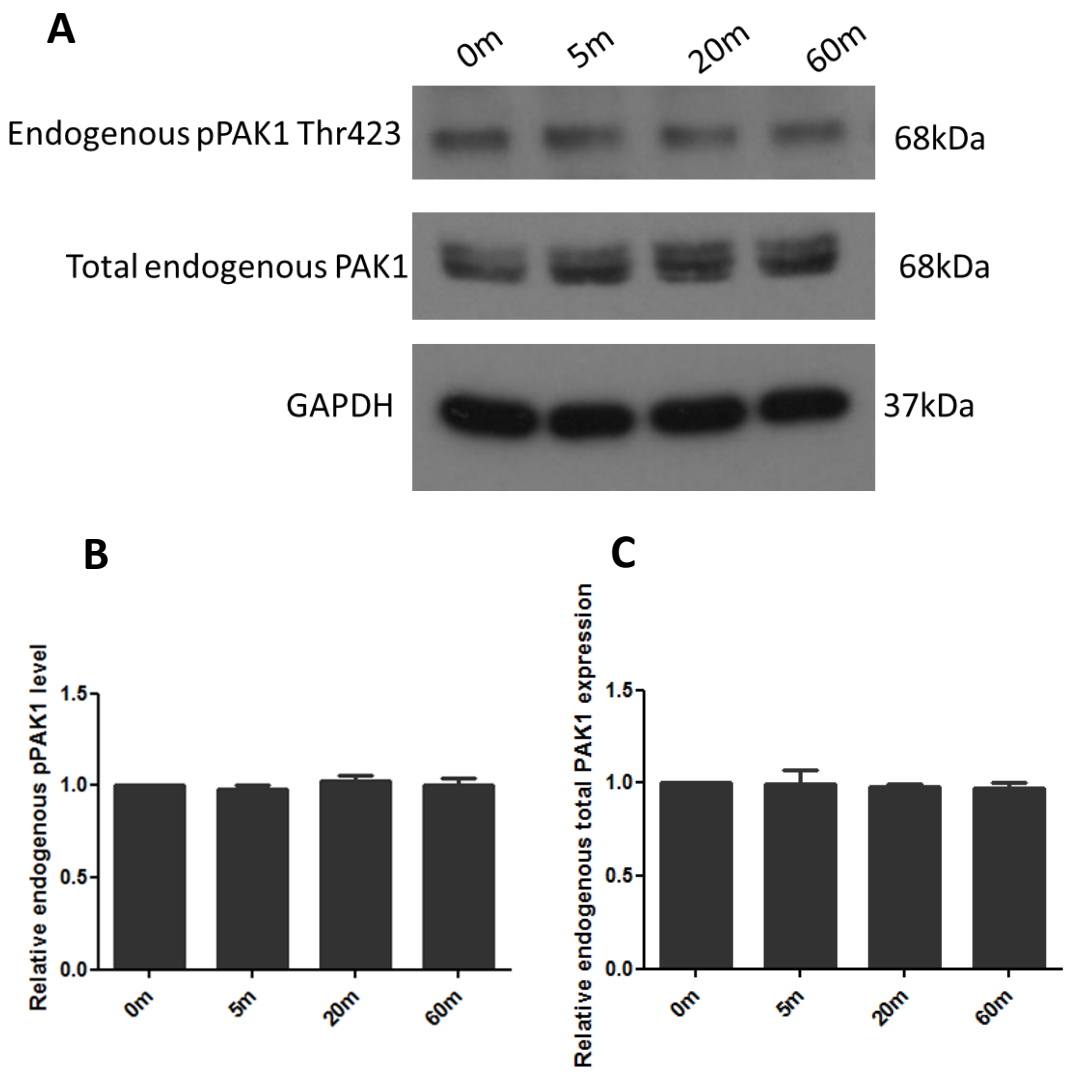

Figure 5.6 No change in endogenous PAK1 threonine 423 phosphorylation levels on stimulation of rapamycin in WT-UNC cells. Whole cell lysates prepared from WT-UNC cells stimulated with rapamycin for five, 20 and 60 minutes. **(A)** Representative western blot indicating the level of PAK1 thr423 for the endogenous PAK1 and the level of total endogenous PAK1. GAPDH was used as a loading control. **(B)** Densitometric analysis on ImageJ was used to compare the levels of pPAK1 thr423, normalised to the loading control and background noise. **(C)** Densitometric analysis on ImageJ was used to compare the levels of total PAK1, normalised to the loading control and background noise. Error bars represent SEM for three independent experiments.

5.2.4 Specific activation of PAK1 induces MDA-MB-231 cell spreading

Having confirmed an increase in the phospho-thr423 levels of PAK1-rap, S44 cells were incubated with rapamycin for five, 20 and 60 minutes on coverslips, then fixed, stained and subjected to morphological analysis.

On all the tested matrices (collagen, fibronectin and glass) activation of PAK1-rap induces a rapid cell spreading response; within five minutes. The increase in cell spread area is short lived with the stimulated cells returning to basal levels within 20 minutes **(Figure 5.7 and 5.8).** No increase in cell area or perimeter was observed for the UNC-WT cells **(Figure 5.9 and 5.10)**.

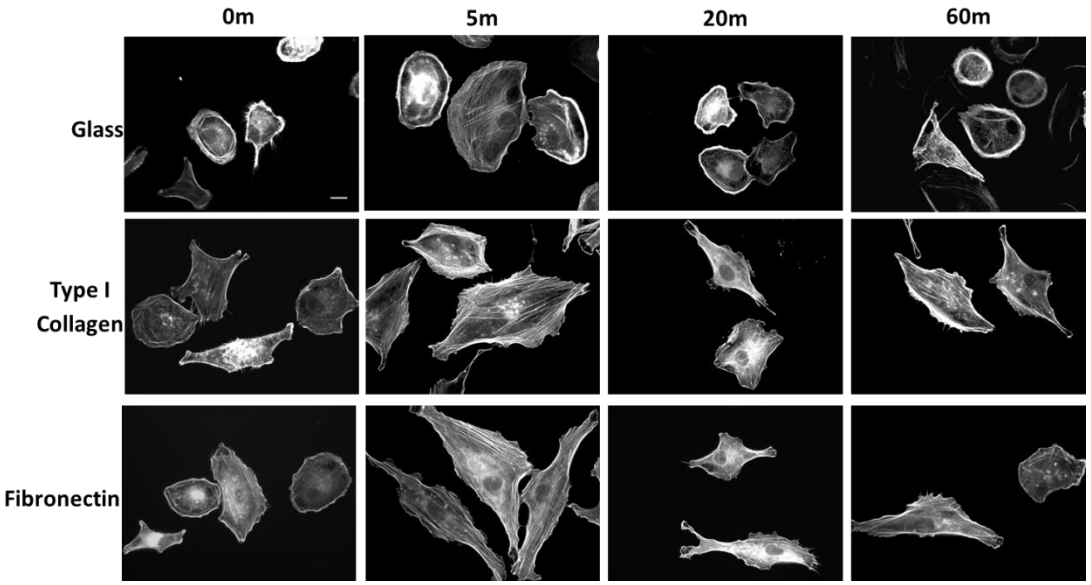

Figure 5.7 Rapamycin activation of PAK1-rap induces S44 cell spreading. Representative images of S44 cells seeded on either glass, type I collagen or fibronectin and stimulated with rapamycin for five, 20 or 60 minutes. The cells were fixed and stained with phalloidin. The scale bar represents 10μm.

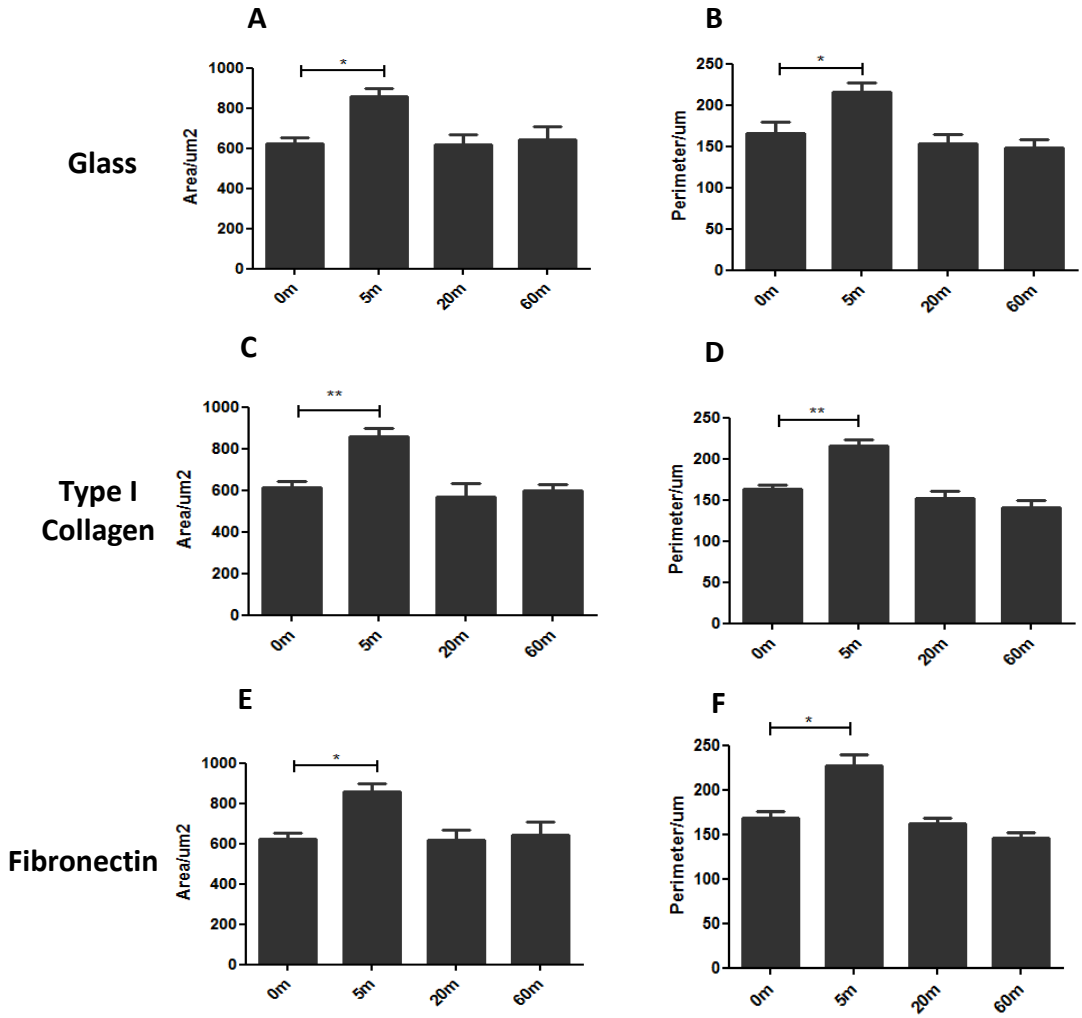

Figure 5.8 Statistical analysis of S44 cell spreading on rapamycin induced PAK1-rap activation. S44 cells seeded on either glass, type I collagen or fibronectin and stimulated with rapamycin for five, 20 or 60 minutes. The cells were fixed and stained with phalloidin and subject to morphological analysis using ImageJ. **(A, C and E)** Graphical representation of cell area on glass, type I collagen and fibronectin respectively. **(B, D and F)** Graphical representation of cell perimeter on glass, type I collagen and fibronectin respectively. Error bars represent SEM for three independent experiments, 30 cells per experiment. Statistical analysis was carried out using t-tests (* $p<0.05$, ** $p<0.01$).

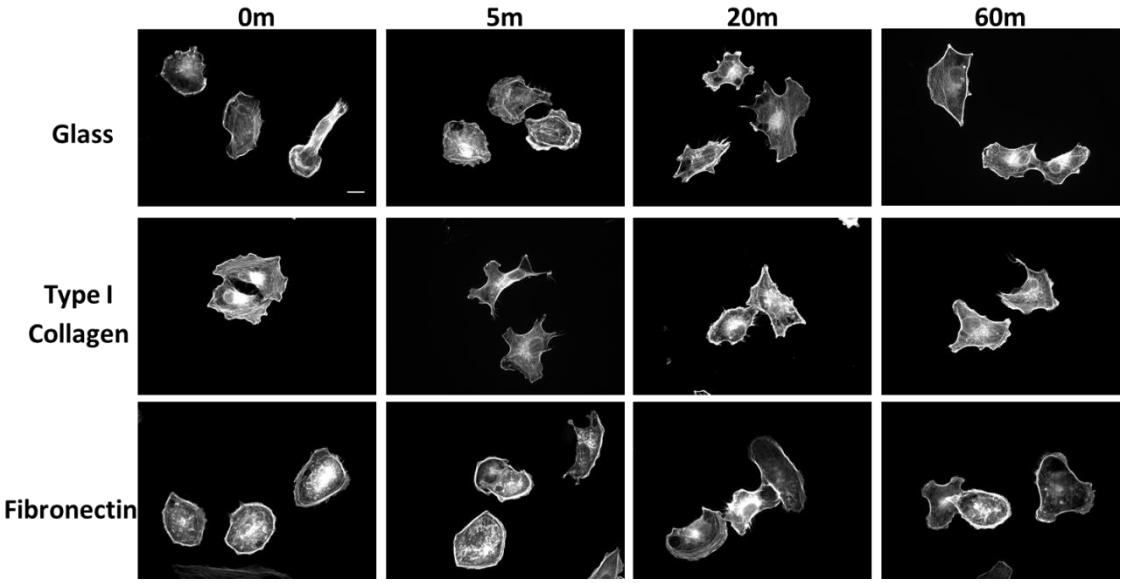

Figure 5.9 No change in UNC-WT cell area or perimeter on rapamycin stimulation in UNC-WT cells. Representative images of UNC-WT cells seeded on either glass, type I collagen or fibronectin and stimulated with rapamycin for five, 20 or 60 minutes. The cells were fixed and stained with phalloidin. The scale bar represents 10μm.

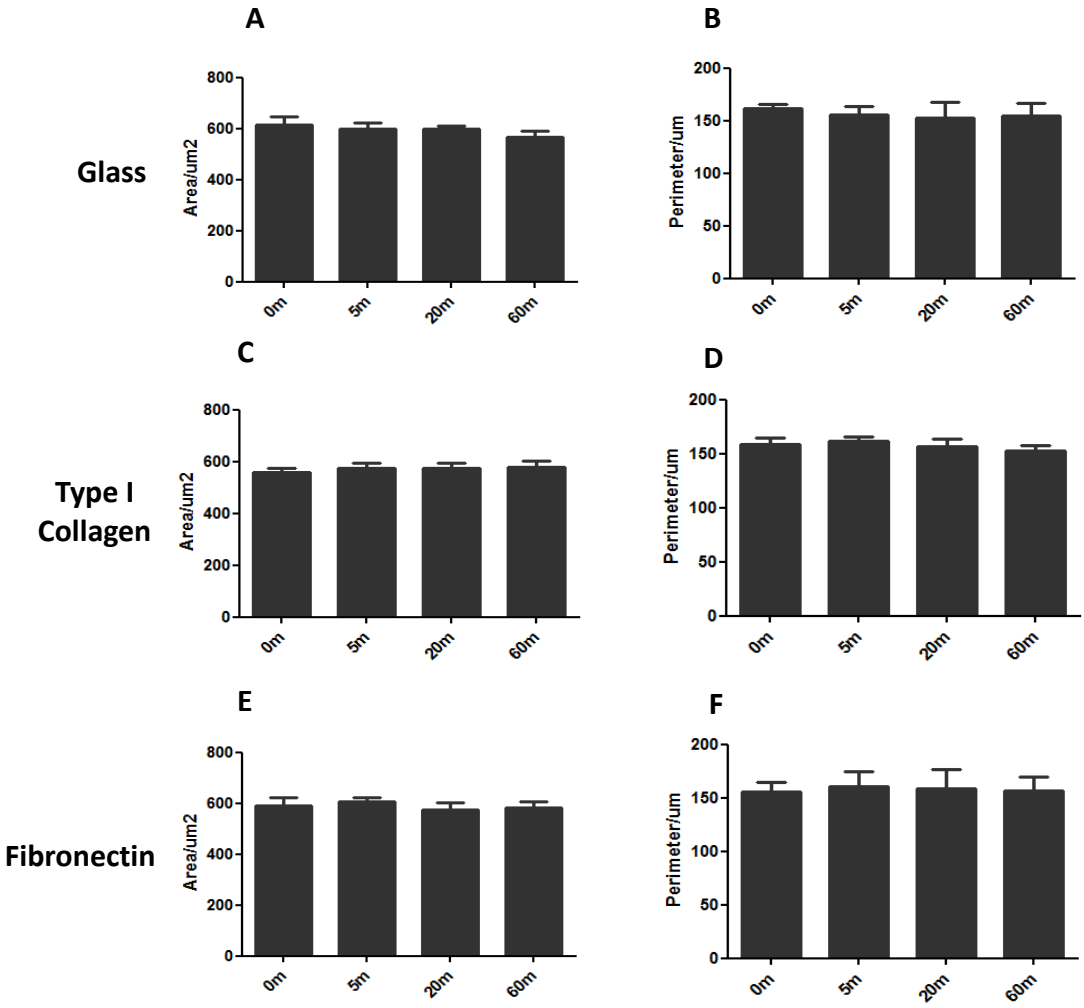

Figure 5.10 Rapamycin stimulation of UNC-WT induced no significant changes to cell area or perimeter. UNC-WT cells seeded on either glass, type I collagen or fibronectin and stimulated with rapamycin for five, 20 or 60 minutes. The cells were fixed and stained with phalloidin and subject to morphological analysis using ImageJ. **(A, C and E)** Graphical representation of cell area on glass, type I collagen and fibronectin respectively. **(B, D and F)** Graphical representation of cell perimeter on glass, type I collagen and fibronectin respectively. Error bars represent SEM for three independent experiments, 30 cells per experiment.

5.2.5 Cytoskeletal phospho-array reveals changes in protein phosphorylation levels on PAK1 activation

The identification of an acute cellular response (within five minutes) to PAK1 activation provided an opportunity to identify downstream targets most likely to drive this cell behaviour. Thus, a commercial cytoskeletal phospho-array which enables qualitative protein phosphorylation profiling analysis was employed.

S44 cells stimulated with rapamycin for five minutes and S44 cells with no rapamycin stimulation (used as a baseline control) were lysed, biotinylated, incubated with the ELISA based antibody array and detected by dye conjugated streptavidin. The array slides were scanned **(Figure 5.13)** and changes in protein phosphorylation sites that occurred on PAK1 activation were quantified **(Table 5.1)**, as described in 2.2.24.

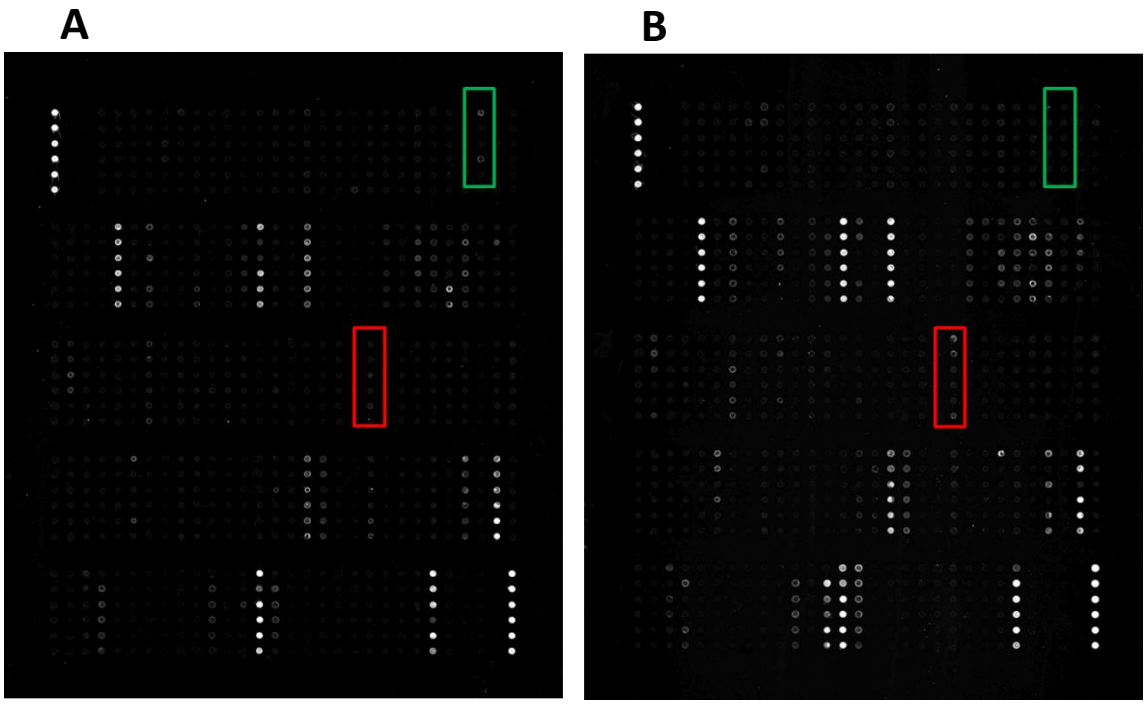

Figure 5.11 Cytoskeletal phospho-array slide images. Unstimulated and rapamycin stimulated S44 cells were lysed and analysed using a cytoskeletal phospho-array. Each vertical line containing six dots is representative of a different antibody. The green and red boxes demonstrate proteins where the phosphorylation of a specific site has decreased or increased respectively on rapamycin induced PAK1 activation. **(A)** Unstimulated S44 cell. **(B)** S44 cells stimulated with rapamycin for five minutes to induce PAK1 activation.

Protein	Fold increase	Fold decrease
pCrkII Tyr221	-	2.2
pVASP Ser238	-	1.7
pCAMK2 Thr305	-	1.1
pSrc Tyr418	-	1.1
pEzrin Thr567	1.8	-
pFAK Ser910	1.6	-
pFAK Tyr925	1.6	-
pPKC α/β II Thr638	1.4	-
pC-Raf Ser296	1.3	-
pMKK6 Ser207	1.3	-
pCortactin Tyr421	1.2	-
pLIMK1 Thr508	1.2	-
pMyosin light chain 2 Ser19	1.2	-
pERK3 Ser189	1.1	-

Table 5.1 Proteins with altered phosphorylation levels on PAK1 activation

5.2.6 Phosphorylation levels of LIMK1 threonine 508 and LIMK2 threonine 505 increase on PAK1 activation

An increase in cell area and perimeter on the rapamycin induced activation of PAK1 was observed **(Figure 5.7 and 5.8)** and an increase in the phosphorylation of LIMK1 threonine 508 was observed on PAK1 activation in the cytoskeletal phospho-array **(Table 5.1)**.

LIMK is a known downstream target of PAK1 and has previously been implicated in PAK1 dependent cytoskeletal changes (Edwards et al., 1999). Interestingly, it has previously been reported that expression of dominant negative LIMK inhibits Rac induced cytoskeletal reorganisations, membrane ruffling and lamellipodia formation (Edwards et al., 1999, Yang et al., 1998), indicating LIMK could play a role in cell spreading. It was therefore decided to examine whether the increase in LIMK phosphorylation on the array could be validated.

S44 and UNC-WT cells were stimulated with rapamycin for five, 20 and 60 minutes. The cells were lysed and probed for phosphorylation levels of threonine 508 on LIMK1 and threonine 508 on LIMK2. Cells were also probed for total LIMK1 and total LIMK2 to ensure levels of total protein were not changing, and for GAPDH which was used as a loading control. An increase in pLIMK1/2 Thr508/Thr505 was observed at the five-minute time point but is beginning to decay within 20 minutes in the S44 cells **(Figure 5.11)**. No increase was observed in the UNC-WT cells **(Figure 5.12)**.

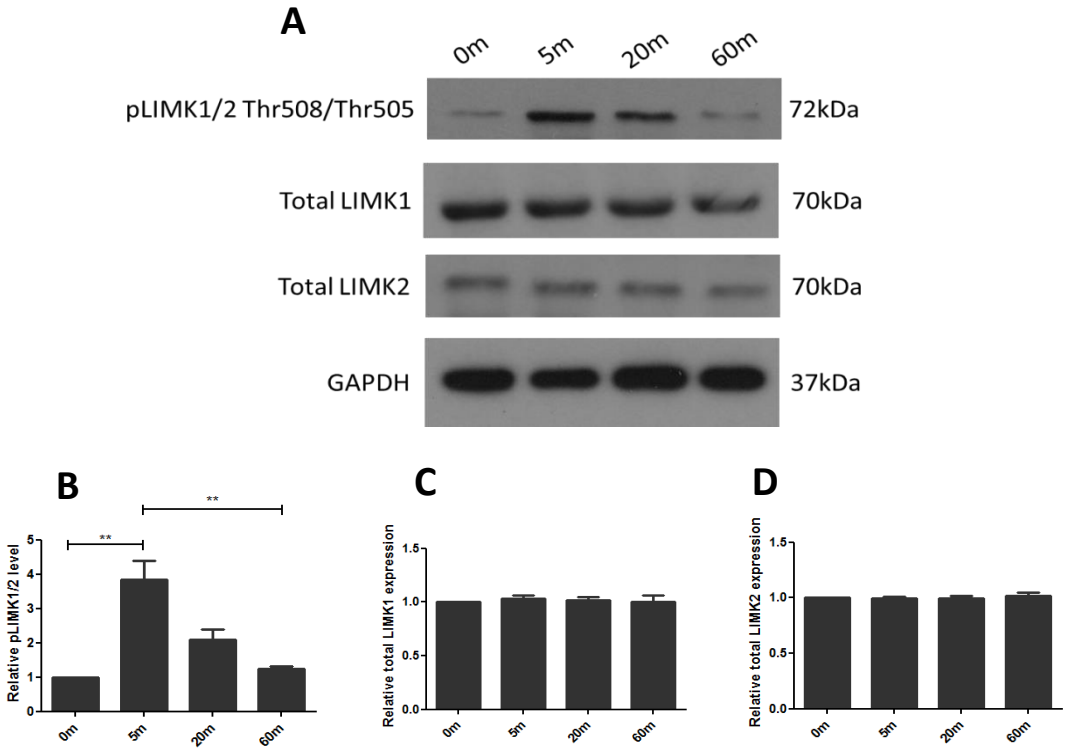

Figure 5.12 Phosphorylation levels of LIMK1 threonine 508 and LIMK2 threonine 505 increase on PAK1 activation in S44 cells. Whole cell lysates prepared from S44 cells stimulated with rapamycin for five, 20 and 60 minutes. **(A)** Representative western blot indicating the level of pLIMK1/2 thr508/thr505 and the level of total LIMK1 and total LIMK2. GAPDH was used as a loading control. **(B)** Densitometric analysis on ImageJ was used to compare the levels of pLIMK1/2 thr508/thr505, normalised to the loading control and background noise. **(C and D)** Densitometric analysis on ImageJ was used to compare the levels of total LMK1 and LIMK2 respectively, normalised to the loading control and background noise. Error bars represent SEM for three independent experiments. Statistical analysis was carried out using t-tests (** $p<0.01$).

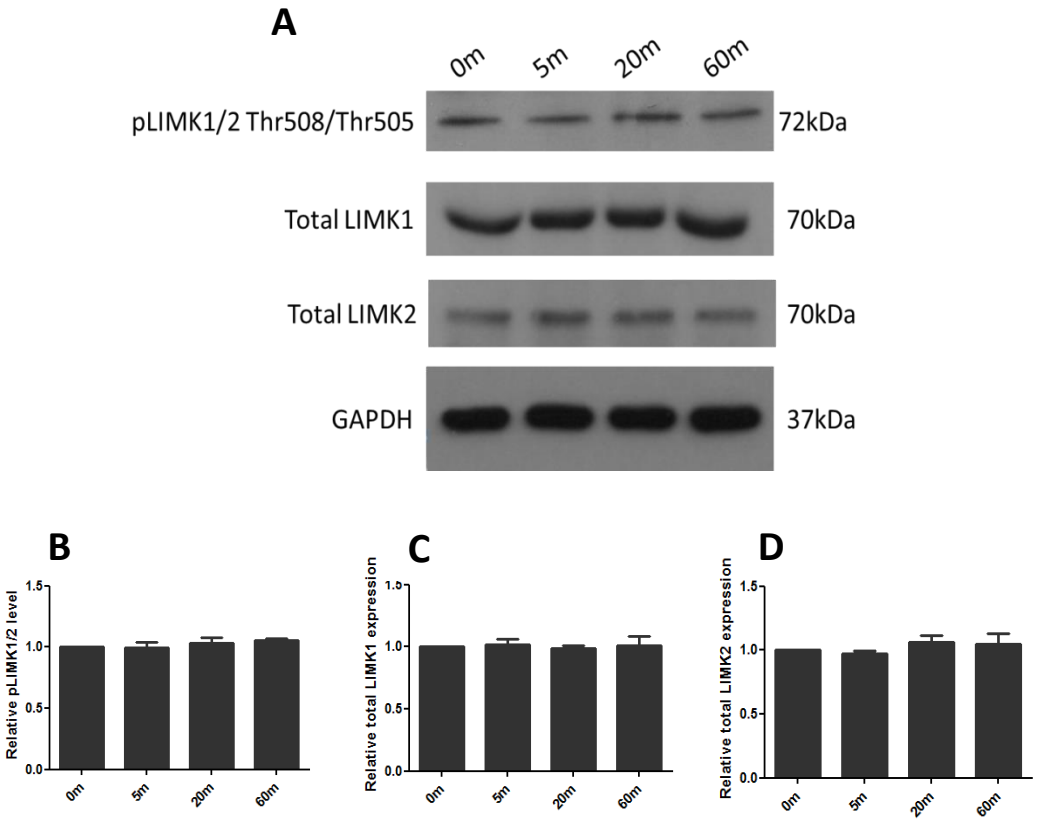

Figure 5.13 No change in the phosphorylation levels of LIMK1 threonine 508 and LIMK2 threonine 505 on PAK1 activation in UNC-WT cells. Whole cell lysates prepared from UNC-WT cells stimulated with rapamycin for five, 20 and 60 minutes. **(A)** Representative western blot indicating the level of pLIMK1/2 thr508/thr505 and the level of total LIMK1 and total LIMK2. GAPDH was used as a loading control. **(B)** Densitometric analysis on ImageJ was used to compare the levels of pLIMK1/2 thr508/thr505, normalised to the loading control and background noise. **(C and D)** Densitometric analysis on ImageJ was used to compare the levels of total LMK1 and LIMK2 respectively, normalised to the loading control and background noise. Error bars represent SEM for three independent experiments.

5.2.7 Phosphorylation levels of CRKII tyrosine 221 decrease on PAK1 activation

To further validate the array, complementary to validation of an increase in phospho-LIMK, the decrease in CRKII at tyrosine 221 was investigated **(Table 5.1)**. S44 and UNC-WT cells were stimulated with rapamycin for five, 20 and 60 minutes, lysed and probed for phosphorylation levels of tyrosine 221 on CRKII using a phospho-specific antibody. A decrease in phospho-CRKII tyrosine 221 levels was observed at the five-minute time point in S44 cells which begins to recover at 20 minutes post treatment **(Figure 5.14)**. No change in the level of pCRKII tyrosine 221 was observed in the treated UNC-WT cells **(Figure 5.15)**.

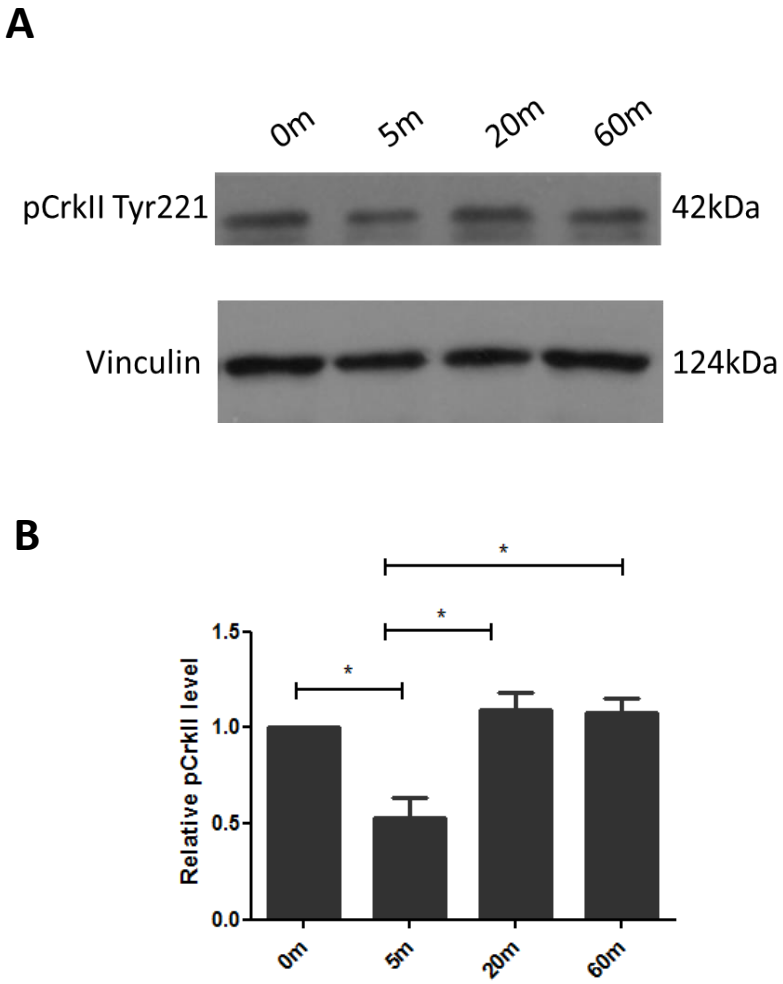

Figure 5.14 Phosphorylation levels of CRKII tyrosine 221 decrease on PAK1 activation in S44 cells. Whole cell lysates prepared from S44 cells stimulated with rapamycin for five, 20 and 60 minutes. **(A)** Representative western blot indicating the level of pCRKII tyr221. Vinculin was used as a loading control. **(B)** Densitometric analysis on ImageJ was used to compare the level of pCRKII tyr221, normalised to the loading control and background noise. Error bars represent SEM for three independent experiments. Statistical analysis was carried out using t-tests (* $p<0.05$).

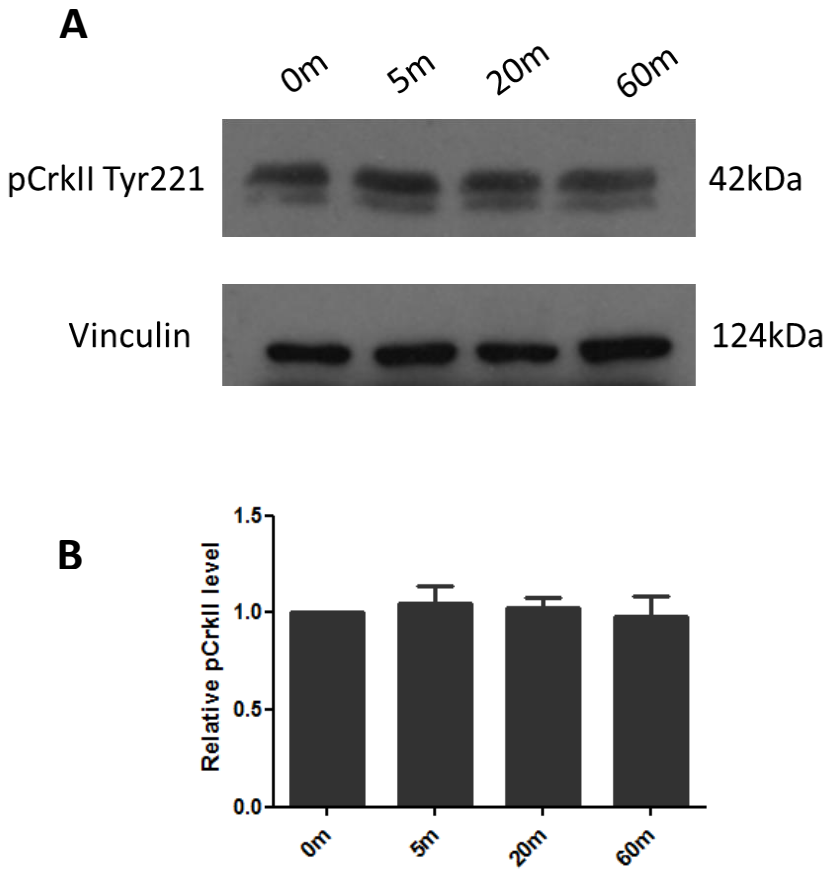

Figure 5.15 No change in the phosphorylation levels of CRKII tyrosine 221 on PAK1 activation in UNC-WT cells. Whole cell lysates prepared from UNC-WT cells stimulated with rapamycin for five, 20 and 60 minutes. **(A)** Representative western blot indicating the level of pCRKII tyr221. Vinculin was used as a loading control. **(B)** Densitometric analysis on ImageJ was used to compare the level of pCRKII tyr221, normalised to the loading control and background noise. Error bars represent SEM for three independent experiments.

5.2.8 Phosphorylation levels of FAK serine 910 increase on PAK1 activation

LIMK and CRKII's respective increase and decrease in phosphorylation successfully validated the cytoskeletal phospho-array. However, LIMK being a downstream target of PAK1 is not novel (Edwards et al., 1999), and the decrease in phosphorylation to a tyrosine residue of CRKII cannot be a direct target of PAK1, a threonine/serine kinase. Other findings from the cytoskeletal phospho-array were therefore investigated.

FAK has been implicated in cell spreading and migration (Owen et al., 1999) and two of its phosphorylation sites were shown to increase on PAK1 activation in the phospho-array **(Table 5.1)**. Indeed the phosphorylation of FAK serine 910 was very intriguing, especially as this finding has only been previously reported once, which was not in breast cancer cells (Li et al., 2010).

S44 and UNC-WT cells were stimulated with rapamycin for five, 20 and 60 minutes, lysed and probed for phosphorylation levels of serine 910 on FAK. GAPDH was also probed for as this was used as the loading control. In S44 cells an increase in the phosphorylation of FAK at serine 910 was observed at the five-minute time point which then begins to decay within 20 minutes **(Figure 5.16)**. No change in the level the phosphorylation of FAK at serine 910 was observed for the UNC-WT cells **(Figure 5.17)**.

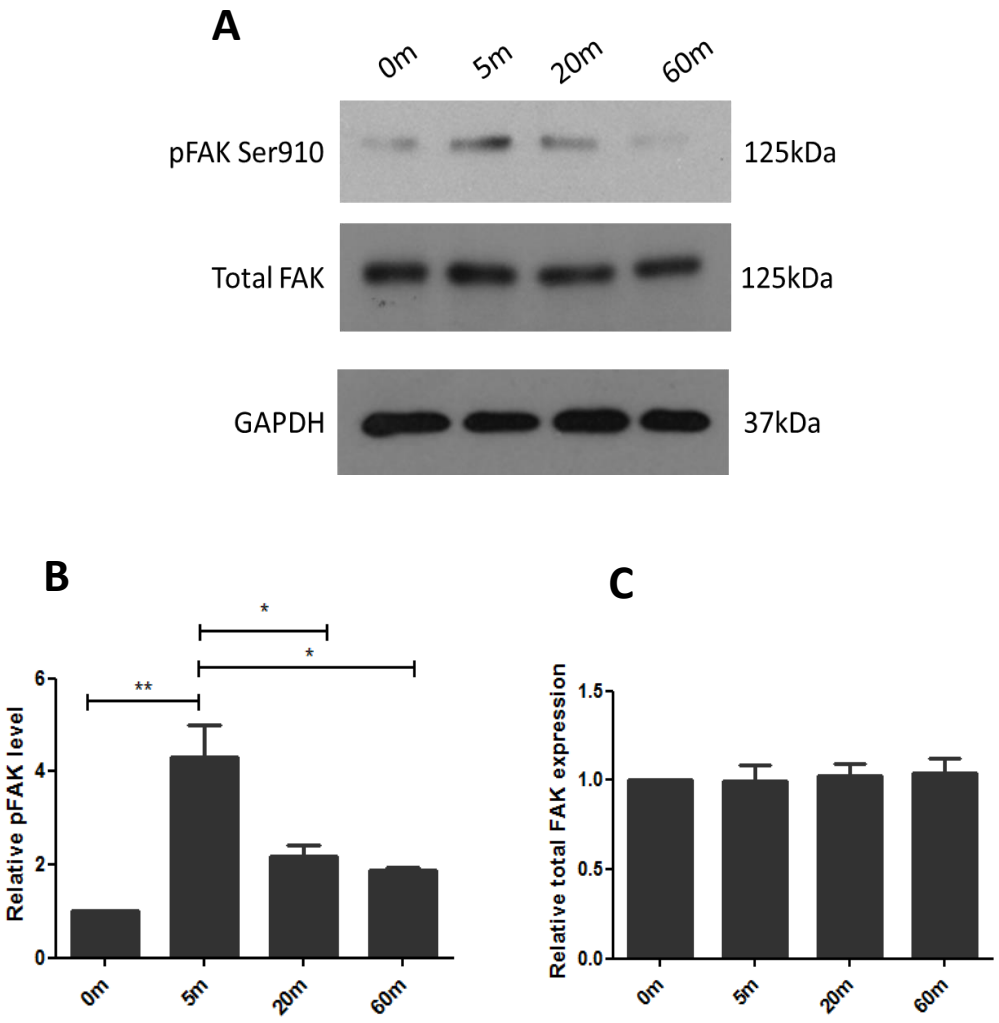

Figure 5.16 Phosphorylation levels of FAK serine 910 increase on PAK1 activation in S44 cells. Whole cell lysates prepared from S44 cells stimulated with rapamycin for five, 20 and 60 minutes. **(A)** Representative western blot indicating the level of FAK serine 910 and total FAK. GAPDH was used as a loading control. **(B)** Densitometric analysis on ImageJ was used to compare the level of pFAK ser910, normalised to the loading control and background noise. **(C)** Densitometric analysis on ImageJ was used to compare the level of total FAK, normalised to the loading control and background noise. Error bars represent SEM for three independent experiments. Statistical analysis was carried out using t-tests (* $p<0.05$, ** $p<0.01$).

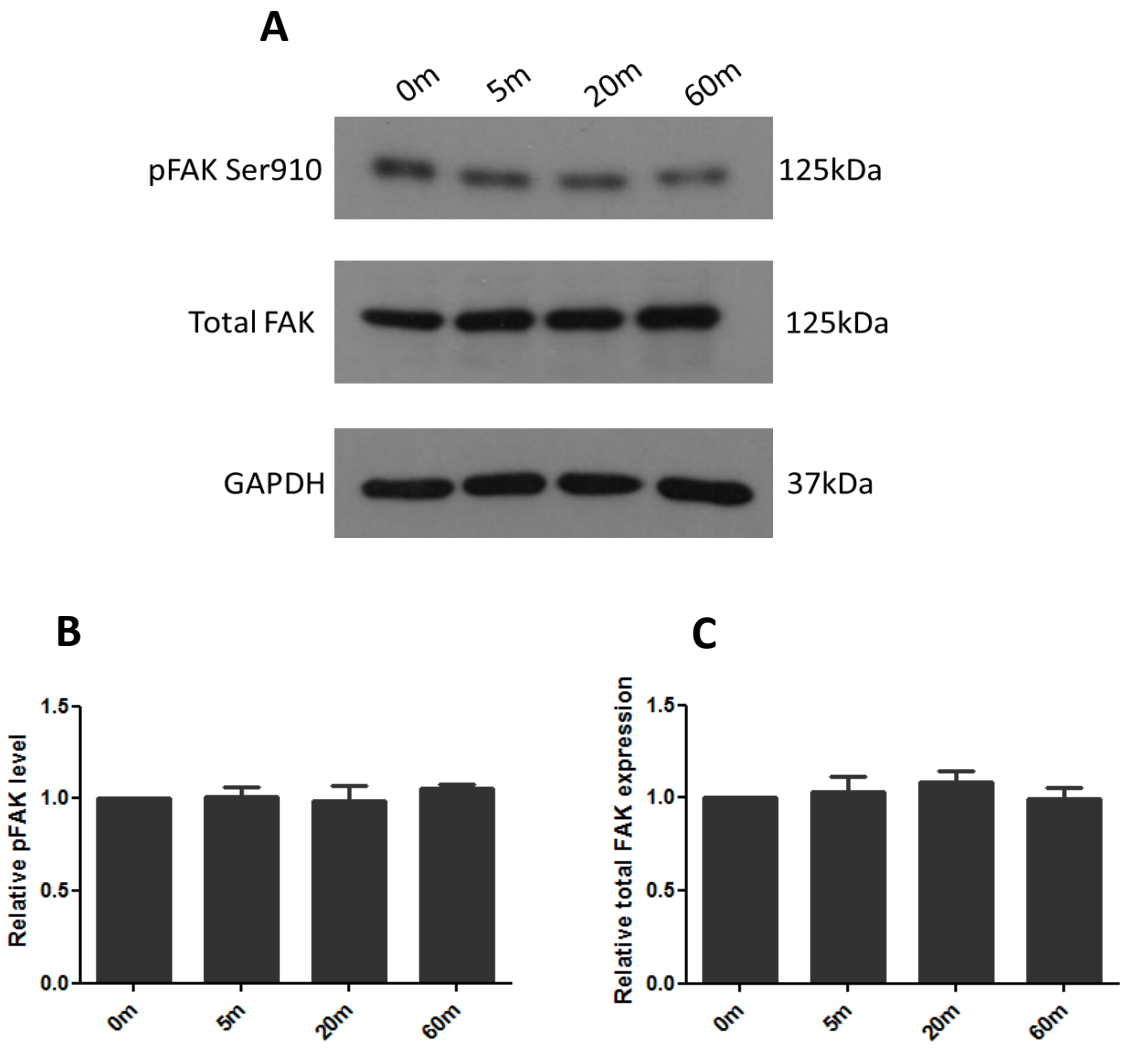

Figure 5.17 No change in the phosphorylation levels of FAK serine 910 on PAK1 activation in UNC-WT cells. Whole cell lysates prepared from UNC-WT cells stimulated with rapamycin for five, 20 and 60 minutes. **(A)** Representative western blot indicating the level of FAK serine 910 and total FAK. GAPDH was used as a loading control. **(B)** Densitometric analysis on ImageJ was used to compare the level of pFAK ser910, normalised to the loading control and background noise. **(C)** Densitometric analysis on ImageJ was used to compare the level of total FAK, normalised to the loading control and background noise. Error bars represent SEM for three independent experiments.

5.2.9 Phosphorylation levels of ERK1 threonine 202 and ERK2 tyrosine 204 remain constant on PAK1 activation

The previous report identifying a PAK1 phosphorylation of FAK serine 910 established a dependence on ERK1/2 in colorectal cancer cells. Incubating PAK1 overexpressing cells with the ERK inhibitor U0126, caused a decrease in FAK serine 910 phosphorylation in a dose-dependent manner (Li et al., 2010). To test this hypothesis rapamycin treated S44 cells were probed for ERK1/2 activation.

S44 cells were therefore stimulated with rapamycin for five, 20 and 60 minutes. The cells were lysed and probed for phosphorylation levels of threonine 202 on ERK1 and tyrosine 204 on ERK2. Vinculin was used as a loading control. No changes in pERK1/2 thr202/tyr204 levels in S44 cells were detected at any of the time points **(Figure 5.18)**.

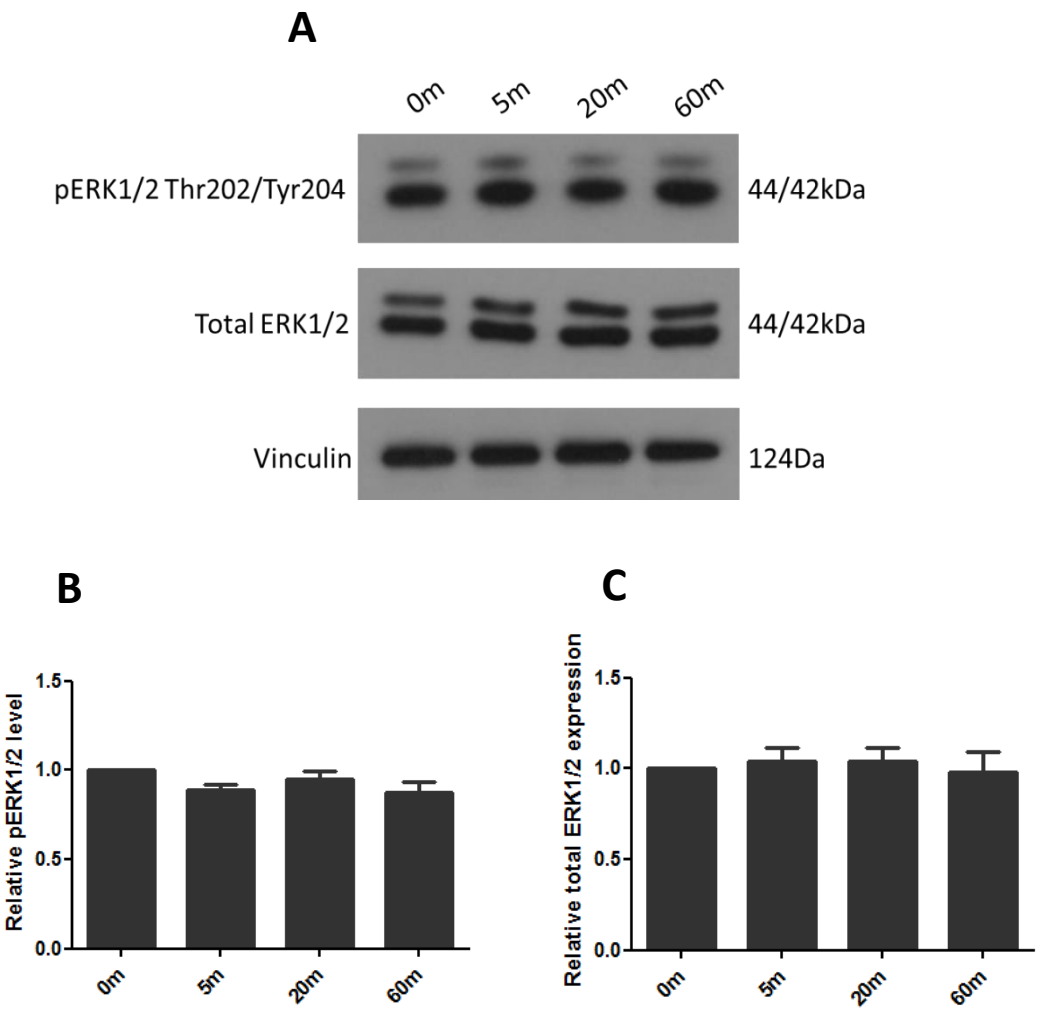

Figure 5.18 No change in the phosphorylation levels of ERK1 threonine 202 and ERK2 tyrosine 204 on PAK1 activation in S44 cells. Whole cell lysates prepared from S44 cells stimulated with rapamycin for five, 20 and 60 minutes. (A) A representative western blot indicating the phosphorylation level of ERK1 threonine 202/ERK2 tyrosine 204 and total ERK1/2. Vinculin was used as a loading control. (B) Densitometric analysis on ImageJ was used to compare the level of pERK1/2 thr202/tyr204, normalised to the loading control and background noise. (C) Densitometric analysis on ImageJ was used to compare the level of total ERK1/2, normalised to the loading control and background noise. Error bars represent SEM for three independent experiments.

5.2.10 Phosphorylation levels of ERK3 serine 189 increase on PAK1 activation

Data here suggests the phosphorylation of FAK serine 910 upon PAK1 activation is not dependent on the activation of ERK1/2, therefore other kinases were considered. The serine 189 site on ERK3 has previously been identified as a substrate of PAK1 (De la Mota-Peynado et al., 2011, Deleris et al., 2011), and was detected here in the cytoskeletal phospho-array **(Table 5.1).** ERK3 phosphorylation at serine 189 has previously been linked to changes in cell spread area in MDA-MB-231 cells (Al-Mahdi et al., 2015). To determine if the FAK ser910 phosphorylation was via ERK3 was phosphorylated following acute PAK1 activation, S44 and UNC-WT cells were stimulated with rapamycin for five, 20 and 60 minutes. The cells were lysed and probed for phosphorylation levels of serine 189 on ERK3. GAPDH was used as a loading control. An increase in pERK3 serine 189 levels were observed at the five-minute time point for S44 cells but this signal begins to decay within 20 minutes **(Figure 5.19)**. No change in pERK3 serine 189 levels was observed in UNC-WT cells **(Figure 5.20)**.

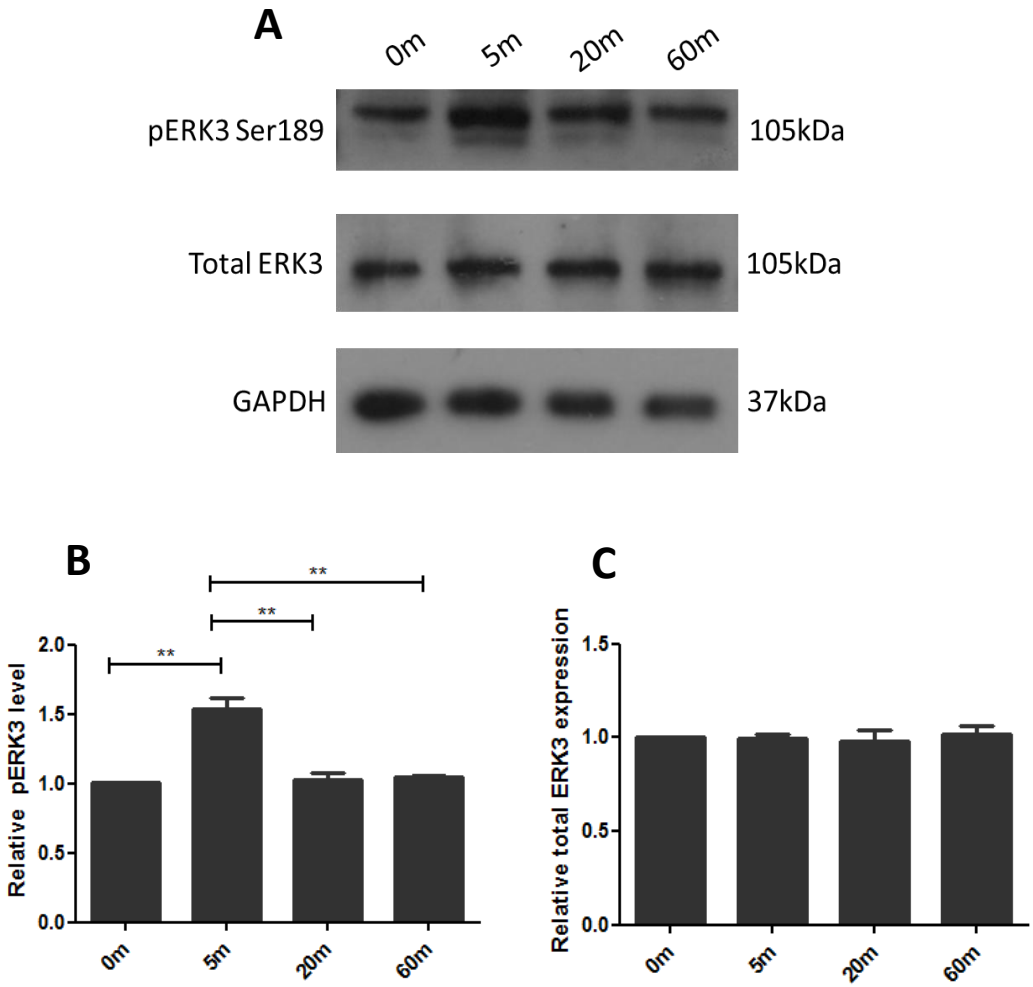

Figure 5.19 Phosphorylation levels of ERK3 serine 189 increase on PAK1 activation in S44 cells. Whole cell lysates prepared from S44 cells stimulated with rapamycin for five, 20 and 60 minutes. **(A)** Representative western blot indicating the level of ERK3 serine 189 and total ERK. GAPDH was used as a loading control. **(B)** Densitometric analysis on ImageJ was used to compare the level of pERK3 ser189, normalised to the loading control and background noise. **(C)** Densitometric analysis on ImageJ was used to compare the level of total ERK3, normalised to the loading control and background noise. Error bars represent SEM for three independent experiments. Statistical analysis was carried out using t-tests (** $p<0.01$).

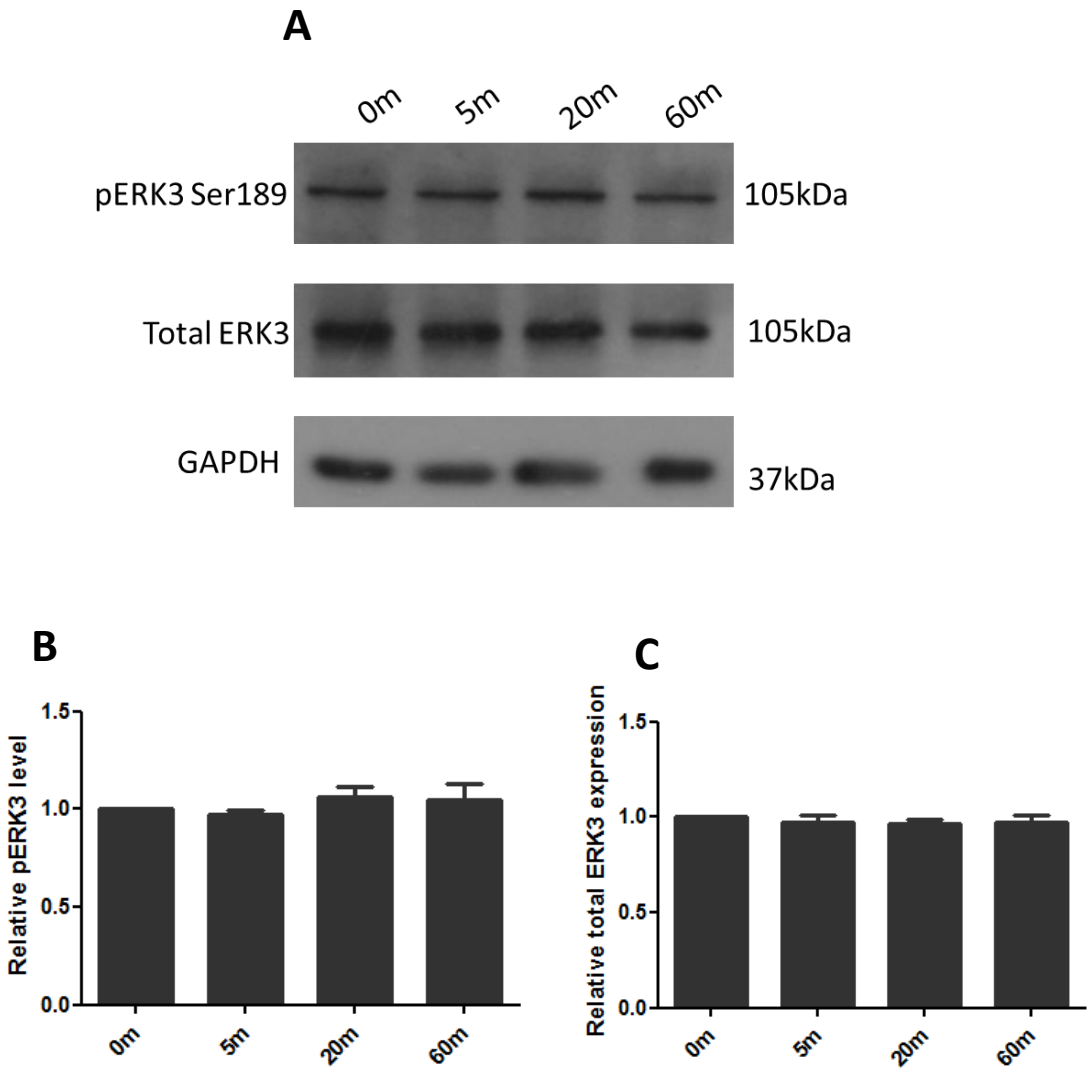

Figure 5.20 No change in the phosphorylation levels of ERK3 serine 189 on PAK1 activation in UNC-WT cells. Whole cell lysates prepared from UNC-WT cells stimulated with rapamycin for five, 20 and 60 minutes. **(A)** A representative western blot indicating the phosphorylation level of ERK3 serine 189 and total ERK3. GAPDH was used as a loading control. **(B)** Densitometric analysis on ImageJ was used to compare the level of pERK3 ser189, normalised to the loading control and background noise. **(C)** Densitometric analysis on ImageJ was used to compare the level of total ERK3, normalised to the loading control and background noise. Error bars represent SEM for three independent experiments.

5.3 Discussion

Whilst PAK1 has been implicated in cell spreading, due to its ability to regulate the actin cytoskeleton and focal adhesions (Radu et al., 2014), its role in breast cancer cell spreading has not been well established. This chapter therefore investigates downstream signalling implicated in PAK1 activated cell spreading by utilising an inducible PAK1 system.

First, the MDA-MB-231 wildtype and S44 cell received from Dr Klaus Hahn, University of North Carolina, were examined for their expression of the PAK1-rap construct. Successful expression of the PAK1-rap construct was identified in the S44 cells but not the wildtype MDA-MB-231 cells **(Figure 5.2)**. This ensures appropriate expression of the PAK1-rap construct enabling further experiments to be performed using these cells.

An increase in phosphorylation at threonine 423 on the PAK1-rap construct is observed when rapamycin is added to the S44 cells for five minutes, this signal decreases within 20 minutes **(Figure 5.4)**. The increase in PAK1 phosphorylation indicates the PAK1 kinase domain is active, confirming the addition of rapamycin causes the kinase domain of PAK1 to stabilise and activate, therefore showing the PAK1-rap construct is functioning correctly. No increase in the levels of threonine 423 on endogenous PAK1 were observed in S44 cells or wildtype cells **(Figure 5.5 and 5.6)**, ensuring the rapamycin was specifically activating the PAK1-rap only.

Initially morphological experiments following addition of rapamycin were performed using wildtype cells from the Well's lab (K-WT cells), wildtype cells from the Hahn lab (UNC-WT cells) and the S44 cells which are the UNC-WT cells engineered to express the PAK1-rap construct. A significant difference in cell area and perimeter was observed between K-WT cells and UNC-WT cells **(Figure 5.3)**. This is most likely due to the heterogeneity of MDA-MB-231 cells population. If these cells have been cultured using different approaches or reagents, over time selection of cells with specific properties may be favoured resulting in morphological drift. Therefore, the UNC-WT cells were used as a control for the following experiments.

The PAK1 inducible system allowed a direct correlation between spread area and biochemistry and therefore morphological changes associated with this increase in PAK1 activity were investigated. An increase in cell spread area is observed in the S44 cells at the five-minute time point on glass, collagen type I and fibronectin **(Figure 5.7 and 5.8)**. This is compelling evidence for a direct role of PAK1's role in regulating cell morphology and supports the findings of knockdown and pharmacological inhibition of PAK1 on cell morphology in chapter 3.

Garcia Arguinzonis et al. (2002) highlight a role for PAK1 kinase activity in cell spreading of mouse cardiac fibroblasts. VASP negative cells have a significant increase in cell spread area, which is linked to elevated PAK1 activation (Garcia Arguinzonis et al., 2002). However, some studies report that PAK1 inhibits cell spreading. Constitutively active PAK1 expression causes inhibition of cell spreading in baby hamster kidney-21 and HeLa cells due to its ability to regulate myosin light chain kinase phosphorylation of the regulatory myosin light chain (Sanders et al., 1999). This study conflicts with data presented in this chapter, however this could be due to the nature of the experiment performed. In this chapter, based on the phosphorylation of PAK1 at threonine 423, there appears to be only an acute temporal activation of PAK1 compared to a continuous overexpression of constitutively active PAK1 in the Sanders et al studies. This is likely to be a contributing factor to the opposing results observed from these studies.

Adam et al. (2000) demonstrate that a lack of PAK1 kinase activity causes cell spreading. An overexpression of a kinase dead PAK1 mutant causes enhanced cell spreading in the MDA-MB-435 breast cancer cell line and conditional expression of a kinase dead PAK1 mutant causes cell spreading and a decrease in cell invasiveness in MDA-MB-231 cells (Adam et al., 2000). This study appears to conflict with data reported in this chapter however this is potentially due to different interpretations of cell spreading. In this chapter, the cell spreading observed is not persistent as an increase in cell spread area is only observed at the five-minute time point and has returned to basal levels within 20 minutes **(Figure 5.7 and 5.8)**. As the cell spread area phenotype couples with the

activation of the kinase activity of PAK1 **(Figure 5.4)**, and chapters 3 and 4 highlight a role in PAK1 kinase activity in breast cancer cell migration and invasion, the transient cell spreading observed in these experiments may be more accurately attributed to cell spreading during cell migration as opposed to a persistent cell spreading reported by Adam et al. (2000).

It is unclear why the signal and morphological phenotypes decrease from 20 minutes. Although possible, it is unlikely the rapamycin is dissociating from the UniRapR domain as they bind with a very high affinity. It is more possible that once the PAK1-rap is activated it is shuttled elsewhere in the cell where it is no longer in close enough proximity to phosphorylate its downstream effectors. Alternatively, a phosphatase removes the phosphate group on the threonine 423 causing a decrease in the PAK1-rap kinase activity. Both scenarios would explain the decrease in phosphorylation signals of the downstream effectors studied (LIMK1/2, CRKII, FAK and ERK3) and the decrease in the cell spread area, at the 20 and 60-minute time points compared to the five-minute time point. It is important to note the tight correlation between the cells' morphological response and the associated downstream signalling.

An increase in pLIMK1/2 Thr508/Thr505 was observed at the five-minute time point but starts to decay within 20 minutes in the S44 cells **(Figure 5.12)**. No increase was observed in the UNC-WT cells **(Figure 5.13)**. The increase in LIMK phosphorylation levels mirrors the increase in PAK1 kinase activity which heavily supports data that illustrates LIMK as a downstream target of PAK1 (Edwards et al., 1999). Prunier et al. (2016) highlight the importance of LIMK in breast cancer cell invasion and cell morphology using the LIMK inhibitor, Pyr1. Pry1 treated cells have a higher percentage of rounded cells compared to wildtype and control MDA-MB-231 cells (Prunier et al., 2016). This indicates a role for LIMK in cell morphology, as reported in this chapter. Li et al. (2013) demonstrate a role for LIMK in breast cancer cell invasion *in vitro*, as expression of a dominant negative mutant, RNA interference and pharmacological inhibition of LIMK all caused a decrease in breast cancer cell invasion. Interestingly, it has also been reported that expression of LIMK1 in MDA-MB-

435 breast cancer cell line increased cell invasiveness *in vitro* and increase metastasis to the liver and lungs *in vivo* (Bagheri-Yarmand et al., 2006). Taken together it is clear LIMK plays a role in breast cancer cell morphology, migration and invasion which support the idea that the transient cell spreading on PAK1 activation observed in this chapter is potentially due to an increase in cell dynamics associated with cell migration.

A decrease in CRKII phosphorylation at tyrosine 221 levels after five minutes of rapamycin induced PAK1-rap activation was observed **(Table 5.1 and Figure 5.14)**. Many studies demonstrate a role for CRKII in cell migration and invasion in multiple cancer types (Rodrigues et al., 2005) which has been linked to PAK1 kinase activity (Rettig et al., 2012). Rettig et al. (2012) report PAK1 can phosphorylate CRKII at the serine 41 site which causes an increase in the cell motility and invasiveness of non-small cell lung carcinomas, due to the downstream down regulation of p120-catenin. This however is not a phosphorylation site present in the cytoskeletal phospho-array. Tyrosine 221 phosphorylation is shown to decrease on PAK1 activation, as PAK1 is a serine/threonine kinase this is not likely due to a direct interaction with PAK1. Phosphorylation of CRKII at tyrosine 221 has been reported to enhance CRKII interactions with SH3 domain proteins such as AbI (Anafi et al., 1996). Other studies suggest that phosphorylation of tyrosine 221 causes a decrease in cell migration (Takino et al., 2003) which is surprising as the findings in this chapter suggest PAK1 kinase activity, which is widely associated with an increase in cell migration, causes a decrease in the phosphorylation of tyrosine 221 on CRKII. The difference in cell type and expression levels PAK1 may explain the discrepancies observed between the findings in this chapter and Takino et al. (2003) as the experiments published in this paper were performed on non-cancerous human embryonic kidney or fibrosarcoma cell line where PAK1 has not been overexpressed.

A CRKII Y221F mutant, which cannot be phosphorylated at tyrosine 221, fails to induce membrane ruffling and cell motility, which is most likely caused by the inability of CRKII to activate Rac signalling (Abassi and Vuori, 2002). This study conflicts with results displayed in this chapter, a decrease in CRKII tyrosine 221 phosphorylation caused by PAK1 kinase

activity does not support the role for PAK1 in cell spreading and migration. However, these experiments were conducted in COS-7 cells, a fibroblast like cell line derived from monkey kidney tissue, which were not overexpressing PAK1 and this could account for the different results obtained in this chapter.

It remains unclear why an increase in PAK1 kinase activity would cause a decrease in CRKII 221 tyrosine levels as this has not been previously reported in the literature. One hypothesis could be that this occurs as a feedback mechanism of PAK1 activation. When PAK1 is activated it could increase the activity of a phosphatase for the CRKII tyrosine site, this would then result in a decrease in cell ruffling and migration as described by both Takino et al. (2003) and Abassi and Vuori (2002). This hypothesis is supported by the increase in CRKII tyrosine 221 levels and decrease in cell spread area from the five-minute time point and 20 and 60-minute time points **(Figure 5.14)**. An alternative hypothesis relates to other functions of the PAK1 kinase domain. On activation of PAK1-rap, it is possible multiple signalling pathways downstream are activated. The decrease in CRKII phosphorylation may be cause by PAK1 kinase activity but is not directly linked to the cell spreading phenotype.

Further validation of the cytoskeletal phospho-array came from investigating the increase in FAK serine 910 levels observed on PAK1 activation **(Table 5.1 and Figure 5.16)**. The FAK gene is amplified and overexpressed in breast cancers and expression often correlates with poor prognosis and incidence of metastatic disease (Luo and Guan, 2010), it is therefore not surprising the phospho-array and western blotting experiments indicate it in having a role in breast cancer cell spreading in this chapter. FAK has been implicated in cell spreading and migration in numerous studies (Luo and Guan, 2010).

The effect of serine 910 phosphorylation on FAK is not well studied compared to other phosphorylation sites on the protein. However, a few studies have implicated phosphorylation of serine 910 to cell spreading and migration. Phosphorylation at the serine 910 site has been shown to play a role in regulating cell spreading and sarcomere reorganisation in cardiac myocytes (Chu et al., 2011). It has also been reported

phosphorylation at serine 910 recruits its downstream effectors PIN1 and PTP-PEST which colocalise with FAK to the lamellipodia of migration cells (Zheng et al., 2009). These effectors also cause dephosphorylation of FAK at tyrosine 397, via a pathway involving PAK1, and this causes an increase in cell migration and invasion (Zheng et al., 2009). This demonstrates a potential mechanism for how an increase in FAK serine 910 phosphorylation could be linked to an increase in cell spreading and migration.

An increase in FAK serine 910 phosphorylation has also linked to increased cell motility in colorectal cancer cell lines (Li et al., 2010). Interestingly signalling of Rac1, an upstream regulator of PAK1 kinase activity, increases serine 910 phosphorylation which plays a role in focal adhesion regulation during cell spreading (Flinder et al., 2011). However, very little is known about the mechanistic or structural consequences of FAK phosphorylation at serine 910 causes to the FAK protein. The serine 910 residue sits in the N-terminal focal adhesion targeting (FAT) sequence which is responsible for the proteins localisation to focal adhesions (Kadare et al., 2015). Kadare et al. (2015) suggest that phosphorylation at this site is associated with FAT opening that is linked to focal adhesion turnover which can influence cell migration. These studies support the idea that an increase in serine 910 on FAK, seen on increased PAK1 kinase activity in this chapter, promotes cell spreading associated with cell migration.

Previous reports of the relationship between PAK1 and FAK serine 910 suggested it was via ERK1/2 (Li et al., 2010, Hunger-Glaser et al., 2004, Jiang et al., 2007) although none of these reporting studies are performed using breast cancer cells. No increase in ERK1/2 activity is observed on the rapamycin induced activation of PAK1 **(Figure 5.18)**, therefore the FAK serine 910 phosphorylation on PAK1 activation is not likely due to ERK1/2 activity as previously demonstrated in the literature. Interestingly, Villa-Moruzzi (2007) reports ERK1/2 does not phosphorylate FAK at the serine 910 site in MDA-MB-231 cells, thus supporting the hypothesis that the kinase responsible for FAK serine 910 phosphorylation differs between cell lines. In this study, ERK5 is implicated as the kinase responsible for FAK serine 910 phosphorylation (Villa-Moruzzi, 2007).

As phosphorylation of FAK serine 910 does not appear to be dependent on ERK1/2 activity, other proteins that could mediate this phosphorylation event were studied. ERK3 serine 189 phosphorylation increased with PAK1 activity in the cytoskeletal phospho-array and western blots **(Table 5.1 and Figure 5.19)** although interestingly, there have been no previous publication linking ERK3 and FAK. However, it could be hypothesised that PAK1 induces phosphorylation of FAK at serine 910 via ERK3, this hasn't previously been reported although is plausible. ERK3 is a known downstream effector of PAK1 (De la Mota-Peynado et al., 2011, Deleris et al., 2011) and it is able to phosphorylate serine residues (Boulton et al., 1991).

ERK3 is a member of the atypical MAP kinase family however its physiological role is not well known (Al-Mahdi et al., 2015). Whilst no mutations are reported in the gene coding for ERK3 in breast cancer (Kostenko et al., 2012) it is reported to be overexpressed in the transcriptome of breast cancers associated with metastasis (Evtimova et al., 2001). It is not surprising ERK3 was identified as a downstream effector of PAK1 in the cytoskeletal phospho-array as it has previously been implicated in cancer cell migration and cytoskeletal regulation. ERK3 been shown to promote head and neck cancer cell migration (Elkhadragy et al., 2017) and the invasiveness of lung cancer *in vitro* and *in vivo* (Long et al., 2012). However, the role ERK3 in breast cancer has not been widely studied. In MDA-MB-231 cells, overexpression of ERK3 causes an increase in cell migration (Al-Mahdi et al., 2015). This study also implicated ERK3 expression with a reduction in cell spread area, however this is in a longitudinal study, not comparable to the assays performed in this chapter (Al-Mahdi et al., 2015). Although not the main focus of the paper, Al-Mahdi et al. (2015) did report a decrease in cell spread area of ERK3 knockdown cells at an early time point when MDA-MB-231 cells are seeded onto collagen coated coverslips a much more closely related observation to studies performed here. This implicates ERK3 in cell spreading which is also observed in this chapter, due to the tight correlation of MDA-MB-231 cell spreading **(Figure 5.7 and 5.8)** and an increase in ERK3 activity **(Figure 5.19)**.

Thus, in this study, findings demonstrated PAK1 kinase activity induces cells spreading and have highlighted the immediate downstream effectors that could play a role in breast cancer cell spreading.

5.4 Future work

5.4.1 Further exploration of FAK and ERK3

Having identified PAK1 and its downstream effectors, ERK3 and FAK, have a potential role in spreading in this inducible system, it would be important to validate this in wildtype MDA-MB-231 cells. To do so nascent cell spreading would need to be stimulated. This could be done using a drop assay where cells are detached from a flask with cell dissociation buffer and dropped onto a new plate. After a specified amount of time the dropped cells could be lysed, and westerns would indicate if the PAK1 threonine 423, the FAK serine 910 and the ERK3 serine 189 levels had increased. Wildtype cells which were lysed when pelleted before being dropped onto a different plate would be used as a control in this experiment. This would give further confirmation that these proteins and phosphorylation sites are important in cell spreading.

Another way to confirm the importance of ERK3 and FAK in this spreading cascade would be to knockdown each protein individually in S44 cells, repeat the rapamycin induced PAK1 activation spreading experiment and observe if there were any significant differences in cell spread area compared to wildtype and control cells. This would also help confirm if PAK1 phosphorylated FAK serine 910 directly or if this is caused indirectly via ERK3 serine 189 activation. Interaction studies between the three proteins could also aid understanding of this signalling cascade.

Creating stable MDA-MB-231 ERK3 and FAK knockdown cells and subjecting these to morphological, 2D migration, 3D invasion and *in vivo* zebrafish xenograft assay, as performed in chapters 3 and 4, would also confirm the importance of these proteins in cell migration and invasion.

5.4.2 Further exploration into the reduction in cell spreading and downstream signalling

Research into why the PAK1 induced spreading and downstream signalling only occurs between 0 and five minutes would be useful. There are multiple theories to explain why this occurs. For example, the PAK1-rap construct could be shuttled by another protein inside the cell, away from its downstream effectors. Continuous phosphorylation of PAK1 to its downstream effectors would therefore not be possible and signalling would stop, causing the decrease in cell spread area and phosphorylation of downstream proteins. As the PAK1-rap construct is mCherry tagged this could be used to determine the localisation of the construct at different time points when the cells are stimulated with rapamycin using high resolution confocal microscopy.

Alternatively, screening for a phosphatase which removes the phosphate group from the threonine 423 site of PAK1 could also explain why the spreading phenotype and downstream signalling decays. This could provide novel understanding of PAK1 regulation in MDA-MB-231 cells. A phosphatase which causes a decrease in PAK1 signalling would also be a potential therapeutic target; however, where specific activation of this enzyme rather than inhibition could help reduce breast cancer cell migration, and therefore the occurrence of metastatic disease in breast cancer patients.

Chapter 6

Concluding remarks

Chapter 6 Concluding remarks

Triple negative breast cancer is heavily associated with poor prognosis, short progression free survival and low overall survival (Costa and Gradishar, 2017). This disease is often lethal due to its highly aggressive and metastatic behaviour (Dent et al., 2007). Treatment of TNBC relies on standard chemotherapy regimens and cannot benefit from targeted therapies used for ER and HER2 positive tumours which have significantly improved clinical outcomes (Reis-Filho and Tutt, 2008). There is a distinct lack of therapeutic targets for TNBC (Hudis and Gianni, 2011). This study therefore focused on the role that PAK1 plays in triple negative breast cancer cell spreading and migration and investigated whether it could be a potential therapeutic target to inhibit metastatic spread. Notably a key question posed was how important the kinase activity of PAK1 is in these cellular processes as this would lend PAK1 to pharmacological inhibition.

First, PAK1 expression was noted in pancreatic, prostate and TNBC cell lines **(Figure 3.1)** indicating a role for the protein in cancer progression as previously published (King et al., 2014). This also allowed selection of the TNBC cell line with the highest PAK1 expression, MDA-MB-231. Establishing PAK1 knock down MDA-MB-231 cell lines via shRNA and CRISPR-Cas9 technologies allowed phenotypes resulting from PAK1 depletion to be studied. Both methods of PAK1 knockdown demonstrated an importance for PAK1 in MDA-MB-231 cell morphology as a decrease in cell spread area and perimeter was observed **(Figure 3.3 and 3.9)**. The phenotypic morphology of cancer cells has been widely linked to their ability to migrate (Clark and Vignjevic, 2015). The shRNA and CRISPR PAK1 knockdown cell lines also showed a reduction in 2D cell migration compared to WT and control cells **(Figure 3.4 and 3.10)**. The shRNA and CRIPSR PAK1 knockdown cell's morphological and 2D migration phenotypes are very comparable **(Table 3.1 and 3.2)** further demonstrating the importance of PAK1 in cell morphology and migration. Importantly the morphological and 2D migratory phenotypes were replicated on pharmacological inhibition of PAK1, by IPA-3, indicating the kinase activity of PAK1 is responsible for these phenotypes **(Figures 3.10 and 3.11)**.

Next, the importance of PAK1 and its kinase activity was demonstrated in assays which offer greater physiological relevance. Depletion and pharmacological inhibition of PAK1 resulted in a decrease in 3D cell invasion **(Figures 4.1, 4.2 and 4.3)** and *in vivo* cell migration **(Figure 4.6 and 4.7)**.

Employing an inducible PAK1 system to activate its kinase activity provided further evidence of the importance of PAK1 kinase activity in cell spreading, as PAK1 kinase activation caused an increase in cell spread area and perimeter **(Figure 5.7 and 5.8)**. This change in cell size was associated with an increase in LIMK1/2 phosphorylation at threonine 508/505 **(Figure 5.11)**. It is well established that LIMK activation at this site causes phosphorylation of cofilin to inhibit its actin severing activities allowing actin stabilisation and growth (Edwards et al., 1999, Arber et al., 1998, Yang et al., 1998). It is therefore thought that PAK1 induction of LIMK activity allows actin polymerisation causing lamellipodia formation and cell spreading/migration **(Figure 6.1)**.

A decrease in phosphorylation of CRKII at tyrosine 221 was observed on PAK1 activation **(Figure 5.14)**. As PAK1 is a serine/threonine kinase this is not a direct event however PAK1 could activate a phosphatase responsible for the decrease in phosphorylation levels at this site. As an increase in phosphorylation levels at this CRKII site is associated with membrane ruffling and cell migration (Takino et al., 2003, Abassi and Vuori, 2002) it is unlikely that PAK1 modulation of CRKII plays a specific role in the cell spreading phenotype observed. Multiple downstream pathways could be activated on PAK1 activation. CRKII could be part of alternative pathways which result in phenotypes other than cell spreading, which have not been studied here **(Figure 6.1)**.

PAK1 activation also induced an increase in the phosphorylation of FAK at serine 910 **(Figure 5.16)**. The phosphorylation of FAK serine 910 is potentially via the phosphorylation and activation of ERK3 at serine 189. This is hypothesised as ERK3 serine 189 phosphorylation levels also increase on PAK1 activation **(Figure 5.19)**. This serine site on ERK3 is a known downstream target of PAK1 (De la Mota-Peynado et al., 2011, Deleris et al., 2011), previous studies have demonstrated the ability of ERK proteins to

phosphorylate FAK at serine 910 (Li et al., 2010, Hunger-Glaser et al., 2004, Jiang et al., 2007) and ERK3 is able to phosphorylate serine residues (Boulton et al., 1991). However, the serine/threonine kinase PAK1 could also phosphorylate the serine 910 site on FAK directly. Whilst it is not clear how this pathway could be directly coordinated to cell migration it is possible this is due to the continuous antagonistic relationship and cross talk between RhoA and Rac1/Cdc42 (Byrne et al., 2016). The tight spatial and temporal regulation between these Rho GTPases could also regulate this pathway by causing the activation of PAK1, as PAK1 is downstream major downstream effector of both Rac1 and Cdc42 (King et al., 2014).

Interestingly, FAK serine 910 phosphorylation has previously been linked to cell spreading and migration. Zheng et al. (2009) have previously demonstrated that FAK serine 910 phosphorylation recruits PIN1 and PTP-PEST which colocalise to the lamellipodia of migrating cells with FAK. PAK1 is involved in this pathway which causes the serine 910 phosphorylation, resulting in the dephosphorylation of FAK at tyrosine 397 and an increase in cell migration (Zheng et al., 2009). A Rac1 induced signalling pathway has also been demonstrated to cause phosphorylation of FAK at serine 910, resulting in focal adhesion turnover during cell spreading (Flinder et al., 2011). This is another pathway that PAK1 could be implicated in as PAK1 is a direct downstream effector of Rac1 (Manser et al., 1994).

Other studies have indicated a role for serine 910 phosphorylation of FAK and focal adhesion turnover. The FAT domain of FAK ensures its recruitment to focal adhesions via paxillin binding (Kadare et al., 2015). FAT domain opening is essential for focal adhesion turnover, and FAK mutants which facilitate FAT opening are capable of restoring focal adhesion turnover in FAK deficient cells (Kadare et al., 2015). These FAT domain opening mutants are associated with an increase in serine 910 phosphorylation therefore indicating this phosphorylation may play a role in focal adhesion turnover (Kadare et al., 2015). It has previously been speculated that phosphorylation of FAK at serine 910 results in reduced binding between FAK and paxillin leading to adhesion turnover (Hunger-Glaser

et al., 2004). It is therefore hypothesised PAK1 induced phosphorylation of FAK at serine 910 causes focal adhesion turnover and allows cell spreading associated with cell migration **(Figure 6.1)**. The cell spreading observed on PAK1 activation in the inducible system would require rapid adhesion turnover. Similarly, adhesions turnover is also required during cell migration and therefore could explain why perturbation of PAK1 by knockdown and pharmacological inhibition causes a decrease 2D migration, 3D invasion and *in vivo* cell migration.

In conclusion, this thesis demonstrated the importance of PAK1 in TNBC cell morphology which impacts migratory phenotypes. 2D migration, 3D invasion and *in vivo* cell migration were all impaired on the depletion of PAK1, highlighting its importance in TNBC cell migration. The role of PAK1 in cell spreading and migration was attributed to its kinase activity as pharmacological inhibition of the protein also resulted in the same morphological and migratory phenotypes. Finally, potential PAK1 downstream signalling pathways were identified which are shown in the proposed model **(Figure 6.1)**.

Future validation of this pathway is needed. Creating a cell line with depleted or complete knockout levels of ERK3 and FAK expression would serve as an invaluable tool to study this pathway further. 2D migration, 3D invasion and zebrafish xenograft assays could then be performed to identify the role of these proteins in breast cancer cell migration and invasion. Phenocopy of the results observed for PAK1 depleted studies in this thesis would be strongly indicate these proteins were part of the same pathway. Furthermore, further validation of the nature of the phosphorylation of FAK at serine 910 by PAK1, whether it be direct or indirect, would be beneficial to identify potentially novel therapeutic targets to combat cancer cell migration and metastasis that are in this pathway. This could be done by in vitro phosphorylation assays, interaction studies, inhibitor studies that target PAK1 and ERK3, and mutational studies which target key residues of PAK1 and ERK3 to determine the effects of FAK serine 910 phosphorylation. Once completed suitable therapeutic targets in this pathway could be identified, experiments with existing

inhibitors could be performed and novel drug design would allow further investigation into the validity of this pathway being targeted in a clinical setting.

From new proteins involved in cell migration being identified, to feedback mechanisms between different signalling pathways being uncovered, the study of cancer cell migration, invasion and metastasis is a rapidly growing field. This project helps to identify and validify important regulators of cell migration and novel potential targets to combat metastasis. A new term coined 'migrastatics' refers to drugs that interfere with all modes of cancer cell migration and invasion (Gandalovicova et al., 2017). There is a growing belief within the field of cancer research that metastasis needs to be prevented and/or treated to cure a patient of their disease. With continuous research into cancer cell migration and invasion, the identification of novel therapeutic targets and development of anti-metastatic drugs it is promising that migrastatics agents could soon enter clinical trials and enter clinical practice to improve patient prognosis and survival.

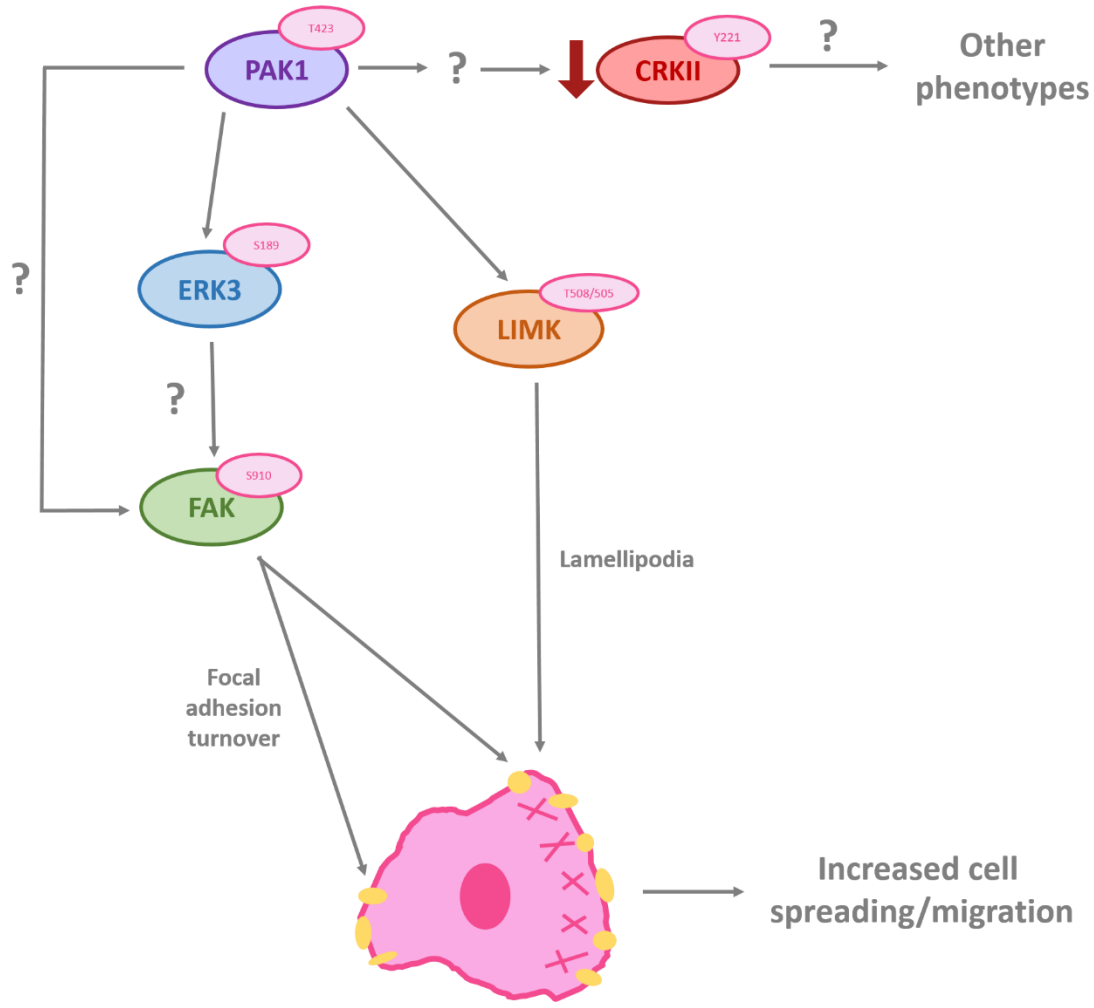

Figure 6.1 A schematic diagram of PAK1 downstream signalling to promote cell spreading and migration. PAK1 can phosphorylate LIMK1/2 at threonine 508/505 which, due to its inhibitory effects on cofilin's actin severing abilities can promote lamellipodia formation. PAK1 can also phosphorylate ERK3 at serine 189, this is thought to phosphorylate FAK at serine 910, however PAK1 could potentially phosphorylate FAK at serine 910 directly. Phosphorylation of FAK serine 910 plays a role in focal adhesion turnover. Both lamellipodia formation and focal adhesion turnover are required for efficient cell spreading and migration. PAK1 kinase activation indirectly cause a decrease in phosphorylation of CRKII at tyrosine 221, however the mechanism by which it does so is not known. The decrease in CRKII tyrosine 221 phosphorylation is which is unlikely to play a role in cell spreading or migration and therefore may play a role in other potential phenotypes.

References

ABASSI, Y. A. & VUORI, K. 2002. Tyrosine 221 in Crk regulates adhesion-dependent membrane localization of Crk and Rac and activation of Rac signaling. EMBO J, 21, 4571-82.

ADAM, L., VADLAMUDI, R., KONDAPAKA, S. B., CHERNOFF, J., MENDELSOHN, J. & KUMAR, R. 1998. Heregulin regulates cytoskeletal reorganization and cell migration through the p21-activated kinase-1 via phosphatidylinositol-3 kinase. J Biol Chem, 273, 28238-46.

ADAM, L., VADLAMUDI, R., MANDAL, M., CHERNOFF, J. & KUMAR, R. 2000. Regulation of microfilament reorganization and invasiveness of breast cancer cells by kinase dead p21-activated kinase-1. J Biol Chem, 275, 12041-50.

AKSAMITIENE, E., KIYATKIN, A. & KHOLODENKO, B. N. 2012. Cross-talk between mitogenic Ras/MAPK and survival PI3K/Akt pathways: a fine balance. *Biochem Soc Trans,* 40**,** 139-46.

AL-AZAYZIH, A., GAO, F. & SOMANATH, P. R. 2015. P21 activated kinase-1 mediates transforming growth factor beta1-induced prostate cancer cell epithelial to mesenchymal transition. Biochim Biophys Acta, 1853, 1229-39.

AL-MAHDI, R., BABTEEN, N., THILLAI, K., HOLT, M., JOHANSEN, B., WETTING, H. L., SETERNES, O. M. & WELLS, C. M. 2015. A novel role for atypical MAPK kinase ERK3 in regulating breast cancer cell morphology and migration. Cell Adh Migr, 9, 483-94.

ALTHUIS, M. D., FERGENBAUM, J. H., GARCIA-CLOSAS, M., BRINTON, L. A., MADIGAN, M. P. & SHERMAN, M. E. 2004. Etiology of hormone receptor-defined breast cancer: a systematic review of the literature. Cancer Epidemiol Biomarkers Prev, 13, 1558-68.

AMATRUDA, J. F., SHEPARD, J. L., STERN, H. M. & ZON, L. I. 2002. Zebrafish as a cancer model system. Cancer Cell, 1, 229-31.

ANAFI, M., ROSEN, M. K., GISH, G. D., KAY, L. E. & PAWSON, T. 1996. A potential SH3 domain-binding site in the Crk SH2 domain. J Biol Chem, 271, 21365-74.

AOKI, H., YOKOYAMA, T., FUJIWARA, K., TARI, A. M., SAWAYA, R., SUKI, D., HESS, K. R., ALDAPE, K. D., KONDO, S., KUMAR, R. & KONDO, Y. 2007. Phosphorylated Pak1 level in the cytoplasm correlates with shorter survival time in patients with glioblastoma. Clin Cancer Res, 13, 6603-9.

ARBER, S., BARBAYANNIS, F. A., HANSER, H., SCHNEIDER, C., STANYON, C. A., BERNARD, O. & CARONI, P. 1998. Regulation of actin dynamics through phosphorylation of cofilin by LIM-kinase. Nature, 393, 805-9.

ARIAS-ROMERO, L. E. & CHERNOFF, J. 2008. A tale of two Paks. Biol Cell, 100, 97-108.

ARIAS-ROMERO, L. E., VILLAMAR-CRUZ, O., PACHECO, A., KOSOFF, R., HUANG, M., MUTHUSWAMY, S. K. & CHERNOFF, J. 2010. A Rac-Pak signaling pathway is essential for ErbB2-mediated transformation of human breast epithelial cancer cells. *Oncogene,* 29**,** 5839-49.

AYALA, I., BALDASSARRE, M., GIACCHETTI, G., CALDIERI, G., TETE, S., LUINI, A. & BUCCIONE, R. 2008. Multiple regulatory inputs converge on cortactin to control invadopodia biogenesis and extracellular matrix degradation. J Cell Sci, 121, 369-78.

BAGHERI-YARMAND, R., MAZUMDAR, A., SAHIN, A. A. & KUMAR, R. 2006. LIM kinase 1 increases tumor metastasis of human breast cancer cells via regulation of the urokinase-type plasminogen activator system. Int J Cancer, 118, 2703-10.

BALASENTHIL, S., SAHIN, A. A., BARNES, C. J., WANG, R. A., PESTELL, R. G., VADLAMUDI, R. K. & KUMAR, R. 2004. p21-activated kinase-1 signaling mediates cyclin D1 expression in mammary epithelial and cancer cells. J Biol Chem, 279, 1422-8.

BALLESTREM, C., EREZ, N., KIRCHNER, J., KAM, Z., BERSHADSKY, A. & GEIGER, B. 2006. Molecular mapping of tyrosine-phosphorylated proteins in focal adhesions using fluorescence resonance energy transfer. J Cell Sci, 119, 866-75.

BALLOU, L. M. & LIN, R. Z. 2008. Rapamycin and mTOR kinase inhibitors. J Chem Biol, 1, 27-36.

BANIN HIRATA, B. K., ODA, J. M., LOSI GUEMBAROVSKI, R., ARIZA, C. B., DE OLIVEIRA, C. E. & WATANABE, M. A. 2014. Molecular markers for breast cancer: prediction on tumor behavior. Dis Markers, 2014, 513158.

BASKARAN, Y., NG, Y. W., SELAMAT, W., LING, F. T. & MANSER, E. 2012. Group I and II mammalian PAKs have different modes of activation by Cdc42. EMBO Rep, 13, 653-9.

BEKRI, S., ADELAIDE, J., MERSCHER, S., GROSGEORGE, J., CAROLI-BOSC, F., PERUCCA-LOSTANLEN, D., KELLEY, P. M., PEBUSQUE, M. J., THEILLET, C., BIRNBAUM, D. & GAUDRAY, P. 1997. Detailed map of a region commonly amplified at 11q13-->q14 in human breast carcinoma. Cytogenet Cell Genet, 79, 125-31.

BIANCHINI, G., BALKO, J. M., MAYER, I. A., SANDERS, M. E. & GIANNI, L. 2016. Triple-negative breast cancer: challenges and opportunities of a heterogeneous disease. Nat Rev Clin Oncol, 13, 674-690.

BISHOP, A. L. & HALL, A. 2000. Rho GTPases and their effector proteins. Biochem J, 348 Pt 2, 241-55.

BLANCHOIN, L., BOUJEMAA-PATERSKI, R., SYKES, C. & PLASTINO, J. 2014. Actin dynamics, architecture, and mechanics in cell motility. Physiol Rev, 94, 235-63.

BOKOCH, G. M. 2003. Biology of the p21-activated kinases. Annu Rev Biochem, 72, 743-81.

BOS, J. L., REHMANN, H. & WITTINGHOFER, A. 2007. GEFs and GAPs: critical elements in the control of small G proteins. Cell, 129, 865-77.

BOSTNER, J., AHNSTROM WALTERSSON, M., FORNANDER, T., SKOOG, L., NORDENSKJOLD, B. & STAL, O. 2007. Amplification of CCND1 and PAK1 as predictors of recurrence and tamoxifen resistance in postmenopausal breast cancer. Oncogene, 26, 6997-7005.

BOULTON, T. G., NYE, S. H., ROBBINS, D. J., IP, N. Y., RADZIEJEWSKA, E., MORGENBESSER, S. D., DEPINHO, R. A., PANAYOTATOS, N., COBB, M. H. & YANCOPOULOS, G. D. 1991. ERKs: a family of protein-serine/threonine kinases that are activated and tyrosine phosphorylated in response to insulin and NGF. Cell, 65, 663-75.

BRIGHT, M. D., GARNER, A. P. & RIDLEY, A. J. 2009. PAK1 and PAK2 have different roles in HGF-induced morphological responses. Cell Signal, 21, 1738-47.

BROWN, L. A., KALLOGER, S. E., MILLER, M. A., SHIH IE, M., MCKINNEY, S. E., SANTOS, J. L., SWENERTON, K., SPELLMAN, P. T., GRAY, J., GILKS, C. B. & HUNTSMAN, D. G. 2008. Amplification of 11q13 in ovarian carcinoma. Genes Chromosomes Cancer, 47, 481-9.

BROWN, M. C., CARY, L. A., JAMIESON, J. S., COOPER, J. A. & TURNER, C. E. 2005. Src and FAK kinases cooperate to phosphorylate paxillin kinase linker, stimulate its focal adhesion localization, and regulate cell spreading and protrusiveness. Mol Biol Cell, 16, 4316-28.

BROWN, M. C., WEST, K. A. & TURNER, C. E. 2002. Paxillin-dependent paxillin kinase linker and p21-activated kinase localization to focal adhesions involves a multistep activation pathway. Mol Biol Cell, 13, 1550-65.

BYRNE, K. M., MONSEFI, N., DAWSON, J. C., DEGASPERI, A., BUKOWSKI-WILLS, J. C., VOLINSKY, N., DOBRZYNSKI, M., BIRTWISTLE, M. R., TSYGANOV, M. A., KIYATKIN, A., KIDA, K., FINCH, A. J., CARRAGHER, N. O., KOLCH, W., NGUYEN, L. K., VON KRIEGSHEIM, A. & KHOLODENKO, B. N. 2016. Bistability in the Rac1, PAK, and RhoA Signaling Network Drives Actin Cytoskeleton Dynamics and Cell Motility Switches. Cell Syst, 2, 38-48.

CAILLEAU, R., YOUNG, R., OLIVE, M. & REEVES, W. J., JR. 1974. Breast tumor cell lines from pleural effusions. J Natl Cancer Inst, 53, 661-74.

CARRAGHER, N. O., WESTHOFF, M. A., FINCHAM, V. J., SCHALLER, M. D. & FRAME, M. C. 2003. A novel role for FAK as a protease-targeting adaptor protein: regulation by p42 ERK and Src. Curr Biol, 13, 1442-50.

CARTER, J. H., DOUGLASS, L. E., DEDDENS, J. A., COLLIGAN, B. M., BHATT, T. R., PEMBERTON, J. O., KONICEK, S., HOM, J., MARSHALL, M. & GRAFF, J. R. 2004. Pak-1 expression increases with progression of colorectal carcinomas to metastasis. Clin Cancer Res, 10, 3448-56.

CAU, J. & HALL, A. 2005. Cdc42 controls the polarity of the actin and microtubule cytoskeletons through two distinct signal transduction pathways. J Cell Sci, 118, 2579-87.

CHAN, K. T., CORTESIO, C. L. & HUTTENLOCHER, A. 2009. FAK alters invadopodia and focal adhesion composition and dynamics to regulate breast cancer invasion. J Cell Biol, 185, 357-70.

CHEN, B., CHOU, H. T., BRAUTIGAM, C. A., XING, W., YANG, S., HENRY, L., DOOLITTLE, L. K., WALZ, T. & ROSEN, M. K. 2017. Rac1 GTPase activates the WAVE regulatory complex through two distinct binding sites. Elife, 6.

CHOW, H. Y., JUBB, A. M., KOCH, J. N., JAFFER, Z. M., STEPANOVA, D., CAMPBELL, D. A., DURON, S. G., O'FARRELL, M., CAI, K. Q., KLEIN-SZANTO, A. J., GUTKIND, J. S., HOEFLICH, K. P. & CHERNOFF, J. 2012. p21-Activated kinase 1 is required for efficient tumor formation and progression in a Ras-mediated skin cancer model. Cancer Res, 72, 5966-75.

CHU, M., IYENGAR, R., KOSHMAN, Y. E., KIM, T., RUSSELL, B., MARTIN, J. L., HEROUX, A. L., ROBIA, S. L. & SAMAREL, A. M. 2011. Serine-910 phosphorylation of focal adhesion kinase is critical for sarcomere reorganization in cardiomyocyte hypertrophy. Cardiovasc Res, 92, 409-19.

CLARK, A. G. & VIGNJEVIC, D. M. 2015. Modes of cancer cell invasion and the role of the microenvironment. Curr Opin Cell Biol, 36, 13-22.

COMBEAU, G., KREIS, P., DOMENICHINI, F., AMAR, M., FOSSIER, P., ROUSSEAU, V. & BARNIER, J. V. 2012. The p21-activated kinase PAK3 forms heterodimers with PAK1 in brain implementing trans-regulation of PAK3 activity. J Biol Chem, 287, 30084-96.

COOPER, J. A. & SEPT, D. 2008. New insights into mechanism and regulation of actin capping protein. Int Rev Cell Mol Biol, 267, 183-206.

COSTA, R. L. B. & GRADISHAR, W. J. 2017. Triple-Negative Breast Cancer: Current Practice and Future Directions. J Oncol Pract, 13, 301-303.

DAGLIYAN, O., KARGINOV, A. V., YAGISHITA, S., GALE, M. E., WANG, H., DERMARDIROSSIAN, C., WELLS, C. M., DOKHOLYAN, N. V., KASAI, H. & HAHN, K. M. 2017. Engineering Pak1 Allosteric Switches. ACS Synth Biol, 6, 1257-1262.

DART, A. E., BOX, G. M., COURT, W., GALE, M. E., BROWN, J. P., PINDER, S. E., ECCLES, S. A. & WELLS, C. M. 2015. PAK4 promotes kinase-independent stabilization of RhoU to modulate cell adhesion. J Cell Biol, 211, 863-79.

DAVIDSON, B., SHIH IE, M. & WANG, T. L. 2008. Different clinical roles for p21-activated kinase-1 in primary and recurrent ovarian carcinoma. Hum Pathol, 39, 1630-6.

DE LA MOTA-PEYNADO, A., CHERNOFF, J. & BEESER, A. 2011. Identification of the atypical MAPK Erk3 as a novel substrate for p21-activated kinase (Pak) activity. J Biol Chem, 286, 13603-11.

DEACON, S. W., BEESER, A., FUKUI, J. A., RENNEFAHRT, U. E., MYERS, C., CHERNOFF, J. & PETERSON, J. R. 2008. An isoform-selective, small-molecule inhibitor targets the autoregulatory mechanism of p21-activated kinase. Chem Biol, 15, 322-31.

DELERIS, P., TROST, M., TOPISIROVIC, I., TANGUAY, P. L., BORDEN, K. L., THIBAULT, P. & MELOCHE, S. 2011. Activation loop phosphorylation of ERK3/ERK4 by group I p21-activated kinases (PAKs) defines a novel PAK-ERK3/4-MAPK-activated protein kinase 5 signaling pathway. J Biol Chem, 286, 6470-8.

DELORME-WALKER, V. D., PETERSON, J. R., CHERNOFF, J., WATERMAN, C. M., DANUSER, G., DERMARDIROSSIAN, C. & BOKOCH, G. M. 2011. Pak1 regulates focal adhesion strength, myosin IIA distribution, and actin dynamics to optimize cell migration. J Cell Biol, 193, 1289-303.

DENT, R., HANNA, W. M., TRUDEAU, M., RAWLINSON, E., SUN, P. & NAROD, S. A. 2009. Pattern of metastatic spread in triple-negative breast cancer. Breast Cancer Res Treat, 115, 423-8.

DENT, R., TRUDEAU, M., PRITCHARD, K. I., HANNA, W. M., KAHN, H. K., SAWKA, C. A., LICKLEY, L. A., RAWLINSON, E., SUN, P. & NAROD, S. A. 2007. Triple-negative breast cancer: clinical features and patterns of recurrence. Clin Cancer Res, 13, 4429-34.

DHARMACON. A CRISPR-Cas9 gene engineering workflow: generating functional knockouts using Dharmacon™ Edit-R™ Cas9 and synthetic crRNA and tracrRNA [Online]. Available: http://dharmacon.horizondiscovery.com/uploadedFiles/Resources/edit-r-experimental-workflow-appnote.pdf.

DHARMAWARDHANE, S., BROWNSON, D., LENNARTZ, M. & BOKOCH, G. M. 1999. Localization of p21-activated kinase 1 (PAK1) to pseudopodia, membrane ruffles, and phagocytic cups in activated human neutrophils. J Leukoc Biol, 66, 521-7.

DHARMAWARDHANE, S., SANDERS, L. C., MARTIN, S. S., DANIELS, R. H. & BOKOCH, G. M. 1997. Localization of p21-activated kinase 1 (PAK1) to pinocytic vesicles and cortical actin structures in stimulated cells. J Cell Biol, 138, 1265-78.

DOBEREINER, H. G., DUBIN-THALER, B., GIANNONE, G., XENIAS, H. S. & SHEETZ, M. P. 2004. Dynamic phase transitions in cell spreading. Phys Rev Lett, 93, 108105.

DONNELLY, S. K., BRAVO-CORDERO, J. J. & HODGSON, L. 2014. Rho GTPase isoforms in cell motility: Don't fret, we have FRET. Cell Adh Migr, 8, 526-34.

DU, J., SUN, C., HU, Z., YANG, Y., ZHU, Y., ZHENG, D., GU, L. & LU, X. 2010. Lysophosphatidic acid induces MDA-MB-231 breast cancer cells migration through activation of PI3K/PAK1/ERK signaling. PLoS One, 5, e15940.

DUBIN-THALER, B. J., GIANNONE, G., DOBEREINER, H. G. & SHEETZ, M. P. 2004. Nanometer analysis of cell spreading on matrix-coated surfaces reveals two distinct cell states and STEPs. Biophys J, 86, 1794-806.

EDWARDS, D. C., SANDERS, L. C., BOKOCH, G. M. & GILL, G. N. 1999. Activation of LIM-kinase by Pak1 couples Rac/Cdc42 GTPase signalling to actin cytoskeletal dynamics. Nat Cell Biol, 1, 253-9.

ELKHADRAGY, L., CHEN, M., MILLER, K., YANG, M. H. & LONG, W. 2017. A regulatory BMI1/let-7i/ERK3 pathway controls the motility of head and neck cancer cells. Mol Oncol, 11, 194-207.

ELLOUL, S., VAKSMAN, O., STAVNES, H. T., TROPE, C. G., DAVIDSON, B. & REICH, R. 2010. Mesenchymal-to-epithelial transition determinants as characteristics of ovarian carcinoma effusions. Clin Exp Metastasis, 27, 161-72.

ELSASSER, H. P., LEHR, U., AGRICOLA, B. & KERN, H. F. 1992. Establishment and characterisation of two cell lines with different grade of differentiation derived from one primary human pancreatic adenocarcinoma. Virchows Arch B Cell Pathol Incl Mol Pathol, 61, 295-306.

ELSASSER, H. P., LEHR, U., AGRICOLA, B. & KERN, H. F. 1993. Structural analysis of a new highly metastatic cell line PaTu 8902 from a primary human pancreatic adenocarcinoma. Virchows Arch B Cell Pathol Incl Mol Pathol, 64, 201-7.

ERGUN, S., TAYEB, T. S., ARSLAN, A., TEMIZ, E., ARMAN, K., SAFDAR, M., DAGLI, H., KORKMAZ, M., NACARKAHYA, G., KIRKBES, S. & OZTUZCU, S. 2015. The investigation of miR-221-3p and PAK1 gene expressions in breast cancer cell lines. Gene, 555, 377-81.

EVTIMOVA, V., SCHWIRZKE, M., TARBE, N., BURTSCHER, H., JARSCH, M., KAUL, S. & WEIDLE, U. H. 2001. Identification of breast cancer metastasis-associated genes by chip technology. Anticancer Res, 21, 3799-806.

FALENTA, K., RODAWAY, A., JONES, G. E. & WELLS, C. M. 2013. Imaging haematopoietic cells recruitment to an acute wound in vivo identifies a role for c-Met signalling. J Microsc, 250, 200-9.

FLINDER, L. I., TIMOFEEVA, O. A., ROSSELAND, C. M., WIEROD, L., HUITFELDT, H. S. & SKARPEN, E. 2011. EGF-induced ERK-activation downstream of FAK requires rac1-NADPH oxidase. J Cell Physiol, 226, 2267-78.

FOULKES, W. D., SMITH, I. E. & REIS-FILHO, J. S. 2010. Triple-negative breast cancer. N Engl J Med, 363, 1938-48.

FRIEDL, P. 2004. Prespecification and plasticity: shifting mechanisms of cell migration. Curr Opin Cell Biol, 16, 14-23.

FRIEDL, P. & ALEXANDER, S. 2011. Cancer invasion and the microenvironment: plasticity and reciprocity. Cell, 147, 992-1009.

FRIEDL, P. & WOLF, K. 2003. Tumour-cell invasion and migration: diversity and escape mechanisms. Nat Rev Cancer, 3, 362-74.

FRIEDL, P. & WOLF, K. 2010. Plasticity of cell migration: a multiscale tuning model. J Cell Biol, 188, 11-9.

FUKATA, Y., AMANO, M. & KAIBUCHI, K. 2001. Rho-Rho-kinase pathway in smooth muscle contraction and cytoskeletal reorganization of non-muscle cells. Trends Pharmacol Sci, 22, 32-9.

FUKUMOTO, Y., KAIBUCHI, K., HORI, Y., FUJIOKA, H., ARAKI, S., UEDA, T., KIKUCHI, A. & TAKAI, Y. 1990. Molecular cloning and characterization of a novel type of regulatory protein (GDI) for the rho proteins, ras p21-like small GTP-binding proteins. Oncogene, 5, 1321-8.

GANDALOVICOVA, A., ROSEL, D., FERNANDES, M., VESELY, P., HENEBERG, P., CERMAK, V., PETRUZELKA, L., KUMAR, S., SANZ-MORENO, V. & BRABEK, J. 2017. Migrastatics-Anti-metastatic and Anti-invasion Drugs: Promises and Challenges. Trends Cancer, 3, 391-406.

GARCIA ARGUINZONIS, M. I., GALLER, A. B., WALTER, U., REINHARD, M. & SIMM, A. 2002. Increased spreading, Rac/p21-activated kinase (PAK) activity, and compromised cell motility in cells deficient in vasodilator-stimulated phosphoprotein (VASP). J Biol Chem, 277, 45604-10.

GOC, A., AL-AZAYZIH, A., ABDALLA, M., AL-HUSEIN, B., KAVURI, S., LEE, J., MOSES, K. & SOMANATH, P. R. 2013. P21 activated kinase-1 (Pak1) promotes prostate tumor growth and microinvasion via inhibition of transforming growth factor beta expression and enhanced matrix metalloproteinase 9 secretion. J Biol Chem, 288, 3025-35.

HA, B. H., DAVIS, M. J., CHEN, C., LOU, H. J., GAO, J., ZHANG, R., KRAUTHAMMER, M., HALABAN, R., SCHLESSINGER, J., TURK, B. E. & BOGGON, T. J. 2012. Type II p21-activated kinases (PAKs) are regulated by an autoinhibitory pseudosubstrate. Proc Natl Acad Sci U S A, 109, 16107-12.

HALL, A. 1998. Rho GTPases and the actin cytoskeleton. Science, 279, 509-14.

HAMMER, A., RIDER, L., OLADIMEJI, P., COOK, L., LI, Q., MATTINGLY, R. R. & DIAKONOVA, M. 2013. Tyrosyl phosphorylated PAK1 regulates breast cancer cell motility in response to prolactin through filamin A. Mol Endocrinol, 27, 455-65.

HAYAT, M. J., HOWLADER, N., REICHMAN, M. E. & EDWARDS, B. K. 2007. Cancer statistics, trends, and multiple primary cancer analyses from the Surveillance, Epidemiology, and End Results (SEER) Program. Oncologist, 12, 20-37.

HIGUCHI, M., ONISHI, K., KIKUCHI, C. & GOTOH, Y. 2008. Scaffolding function of PAK in the PDK1-Akt pathway. Nat Cell Biol, 10, 1356-64.

HOLM, C., RAYALA, S., JIRSTROM, K., STAL, O., KUMAR, R. & LANDBERG, G. 2006. Association between Pak1 expression and subcellular localization and tamoxifen resistance in breast cancer patients. J Natl Cancer Inst, 98, 671-80.

HOWE, A. K. & JULIANO, R. L. 2000. Regulation of anchorage-dependent signal transduction by protein kinase A and p21-activated kinase. Nat Cell Biol, 2, 593-600.

HSIA, D. A., MITRA, S. K., HAUCK, C. R., STREBLOW, D. N., NELSON, J. A., ILIC, D., HUANG, S., LI, E., NEMEROW, G. R., LENG, J., SPENCER, K. S., CHERESH, D. A. & SCHLAEPFER, D. D. 2003. Differential regulation of cell motility and invasion by FAK. J Cell Biol, 160, 753-67.

HSU, P. D., LANDER, E. S. & ZHANG, F. 2014. Development and applications of CRISPR-Cas9 for genome engineering. Cell, 157, 1262-78.

HUDIS, C. A. & GIANNI, L. 2011. Triple-negative breast cancer: an unmet medical need. Oncologist, 16 Suppl 1, 1-11.

HUNGER-GLASER, I., FAN, R. S., PEREZ-SALAZAR, E. & ROZENGURT, E. 2004. PDGF and FGF induce focal adhesion kinase (FAK) phosphorylation at Ser-910: dissociation from Tyr-397 phosphorylation and requirement for ERK activation. J Cell Physiol, 200, 213-22.

HUTTENLOCHER, A. & HORWITZ, A. R. 2011. Integrins in cell migration. Cold Spring Harb Perspect Biol, 3, a005074.

HUYNH, N., LIU, K. H., BALDWIN, G. S. & HE, H. 2010. P21-activated kinase 1 stimulates colon cancer cell growth and migration/invasion via ERK- and AKT-dependent pathways. Biochim Biophys Acta, 1803, 1106-13.

ILIC, D., FURUTA, Y., KANAZAWA, S., TAKEDA, N., SOBUE, K., NAKATSUJI, N., NOMURA, S., FUJIMOTO, J., OKADA, M. & YAMAMOTO, T. 1995. Reduced cell motility and enhanced focal adhesion contact formation in cells from FAK-deficient mice. Nature, 377, 539-44.

ITO, M., NISHIYAMA, H., KAWANISHI, H., MATSUI, S., GUILFORD, P., REEVE, A. & OGAWA, O. 2007. P21-activated kinase 1: a new molecular marker for intravesical recurrence after transurethral resection of bladder cancer. J Urol, 178, 1073-9.

JAFFE, A. B. & HALL, A. 2005. Rho GTPases: biochemistry and biology. Annu Rev Cell Dev Biol, 21, 247-69.

JAGADEESHAN, S., KRISHNAMOORTHY, Y. R., SINGHAL, M., SUBRAMANIAN, A., MAVULURI, J., LAKSHMI, A., ROSHINI, A., BASKAR, G., RAVI, M., JOSEPH, L. D., SADASIVAN, K., KRISHNAN, A., NAIR, A. S., VENKATRAMAN, G. & RAYALA, S. K. 2015. Transcriptional regulation of fibronectin by p21-activated kinase-1 modulates pancreatic tumorigenesis. Oncogene, 34, 455-64.

JAGADEESHAN, S., SAGAYARAJ, R. V., PANEERSELVAN, N., GHOUSE, S. S. & MALATHI, R. 2017. Toxicity and anti-angiogenicity evaluation of Pak1 inhibitor IPA-3 using zebrafish embryo model. Cell Biol Toxicol, 33, 41-56.

JEMAL, A., SIEGEL, R., XU, J. & WARD, E. 2010. Cancer statistics, 2010. CA Cancer J Clin, 60, 277-300.

JIANG, P., ENOMOTO, A. & TAKAHASHI, M. 2009. Cell biology of the movement of breast cancer cells: intracellular signalling and the actin cytoskeleton. Cancer Lett, 284, 122-30.

JIANG, X., SINNETT-SMITH, J. & ROZENGURT, E. 2007. Differential FAK phosphorylation at Ser-910, Ser-843 and Tyr-397 induced by angiotensin II, LPA and EGF in intestinal epithelial cells. Cell Signal, 19, 1000-10.

KADARE, G., GERVASI, N., BRAMI-CHERRIER, K., BLOCKUS, H., EL MESSARI, S., AROLD, S. T. & GIRAULT, J. A. 2015. Conformational dynamics of the focal adhesion targeting domain control specific functions of focal adhesion kinase in cells. J Biol Chem, 290, 478-91.

KAIGHN, M. E., NARAYAN, K. S., OHNUKI, Y., LECHNER, J. F. & JONES, L. W. 1979. Establishment and characterization of a human prostatic carcinoma cell line (PC-3). Invest Urol, 17, 16-23.

KELLY, M. L. & CHERNOFF, J. 2012. Mouse models of PAK function. Cell Logist, 2, 84-88.

KESSENBROCK, K., PLAKS, V. & WERB, Z. 2010. Matrix metalloproteinases: regulators of the tumor microenvironment. Cell, 141, 52-67.

KHALILI, A. A. & AHMAD, M. R. 2015. A Review of Cell Adhesion Studies for Biomedical and Biological Applications. Int J Mol Sci, 16, 18149-84.

KICHINA, J. V., GOC, A., AL-HUSEIN, B., SOMANATH, P. R. & KANDEL, E. S. 2010. PAK1 as a therapeutic target. Expert Opin Ther Targets, 14, 703-25.

KING, C. C., GARDINER, E. M., ZENKE, F. T., BOHL, B. P., NEWTON, A. C., HEMMINGS, B. A. & BOKOCH, G. M. 2000. p21-activated kinase (PAK1) is phosphorylated and activated by 3-phosphoinositide-dependent kinase-1 (PDK1). J Biol Chem, 275, 41201-9.

KING, H., NICHOLAS, N. S. & WELLS, C. M. 2014. Role of p-21-activated kinases in cancer progression. Int Rev Cell Mol Biol, 309, 347-87.

KING, H., THILLAI, K., WHALE, A., ARUMUGAM, P., ELDALY, H., KOCHER, H. M. & WELLS, C. M. 2017. PAK4 interacts with p85 alpha: implications for pancreatic cancer cell migration. Sci Rep, 7, 42575.

KISSIL, J. L., WILKER, E. W., JOHNSON, K. C., ECKMAN, M. S., YAFFE, M. B. & JACKS, T. 2003. Merlin, the product of the Nf2 tumor suppressor gene, is an inhibitor of the p21-activated kinase, Pak1. Mol Cell, 12, 841-9.

KOH, C. G., TAN, E. J., MANSER, E. & LIM, L. 2002. The p21-activated kinase PAK is negatively regulated by POPX1 and POPX2, a pair of serine/threonine phosphatases of the PP2C family. Curr Biol, 12, 317-21.

KOSTENKO, S., DUMITRIU, G. & MOENS, U. 2012. Tumour promoting and suppressing roles of the atypical MAP kinase signalling pathway ERK3/4-MK5. J Mol Signal, 7, 9.

KRAKHMAL, N. V., ZAVYALOVA, M. V., DENISOV, E. V., VTORUSHIN, S. V. & PERELMUTER, V. M. 2015. Cancer Invasion: Patterns and Mechanisms. Acta Naturae, 7, 17-28.

KREIS, P., ROUSSEAU, V., THEVENOT, E., COMBEAU, G. & BARNIER, J. V. 2008. The four mammalian splice variants encoded by the p21-activated kinase 3 gene have different biological properties. J Neurochem, 106, 1184-97.

KUTYS, M. L. & YAMADA, K. M. 2014. An extracellular-matrix-specific GEF-GAP interaction regulates Rho GTPase crosstalk for 3D collagen migration. Nat Cell Biol, 16, 909-17.

LAMOUILLE, S., XU, J. & DERYNCK, R. 2014. Molecular mechanisms of epithelial-mesenchymal transition. Nat Rev Mol Cell Biol, 15, 178-96.

LAWSON, C. D. & BURRIDGE, K. 2014. The on-off relationship of Rho and Rac during integrin-mediated adhesion and cell migration. Small GTPases, 5, e27958.

LE CLAINCHE, C. & CARLIER, M. F. 2008. Regulation of actin assembly associated with protrusion and adhesion in cell migration. Physiol Rev, 88, 489-513.

LEBERT, J. M., LESTER, R., POWELL, E., SEAL, M. & MCCARTHY, J. 2018. Advances in the systemic treatment of triple-negative breast cancer. Curr Oncol, 25, S142-S150.

LEE, L. M., SEFTOR, E. A., BONDE, G., CORNELL, R. A. & HENDRIX, M. J. 2005. The fate of human malignant melanoma cells transplanted into zebrafish embryos: assessment of migration and cell division in the absence of tumor formation. Dev Dyn, 233, 1560-70.

LEI, M., LU, W., MENG, W., PARRINI, M. C., ECK, M. J., MAYER, B. J. & HARRISON, S. C. 2000. Structure of PAK1 in an autoinhibited conformation reveals a multistage activation switch. Cell, 102, 387-97.

LEONARD, D., HART, M. J., PLATKO, J. V., EVA, A., HENZEL, W., EVANS, T. & CERIONE, R. A. 1992. The identification and characterization of a GDP-dissociation inhibitor (GDI) for the CDC42Hs protein. J Biol Chem, 267, 22860-8.

LI, L. H., ZHENG, M. H., LUO, Q., YE, Q., FENG, B., LU, A. G., WANG, M. L., CHEN, X. H., SU, L. P. & LIU, B. Y. 2010. P21-activated protein kinase 1 induces colorectal cancer metastasis involving ERK activation and phosphorylation of FAK at Ser-910. Int J Oncol, 37, 951-62.

LI, Q., MULLINS, S. R., SLOANE, B. F. & MATTINGLY, R. R. 2008. p21-Activated kinase 1 coordinates aberrant cell survival and pericellular proteolysis in a three-dimensional culture model for premalignant progression of human breast cancer. Neoplasia, 10, 314-29.

LI, R., DOHERTY, J., ANTONIPILLAI, J., CHEN, S., DEVLIN, M., VISSER, K., BAELL, J., STREET, I., ANDERSON, R. L. & BERNARD, O. 2013. LIM kinase inhibition reduces breast cancer growth and invasiveness but systemic inhibition does not reduce metastasis in mice. Clin Exp Metastasis, 30, 483-95.

LI, Y., JIN, K., VAN PELT, G. W., VAN DAM, H., YU, X., MESKER, W. E., TEN DIJKE, P., ZHOU, F. & ZHANG, L. 2016. c-Myb Enhances Breast Cancer Invasion and Metastasis through the Wnt/beta-Catenin/Axin2 Pathway. Cancer Res, 76, 3364-75.

LITTLEWOOD-EVANS, A. J., BILBE, G., BOWLER, W. B., FARLEY, D., WLODARSKI, B., KOKUBO, T., INAOKA, T., SLOANE, J., EVANS, D. B. & GALLAGHER, J. A. 1997. The osteoclast-associated protease cathepsin K is expressed in human breast carcinoma. Cancer Res, 57, 5386-90.

LIU, S. & LEACH, S. D. 2011. Zebrafish models for cancer. Annu Rev Pathol, 6, 71-93.

LONG, W., FOULDS, C. E., QIN, J., LIU, J., DING, C., LONARD, D. M., SOLIS, L. M., WISTUBA, II, QIN, J., TSAI, S. Y., TSAI, M. J. & O'MALLEY, B. W. 2012. ERK3 signals through SRC-3 coactivator to promote human lung cancer cell invasion. J Clin Invest, 122, 1869-80.

LORUSSO, G. & RUEGG, C. 2012. New insights into the mechanisms of organ-specific breast cancer metastasis. Semin Cancer Biol, 22, 226-33.

LOZANO, E., FRASA, M. A., SMOLARCZYK, K., KNAUS, U. G. & BRAGA, V. M. 2008. PAK is required for the disruption of E-cadherin adhesion by the small GTPase Rac. J Cell Sci, 121, 933-8.

LU, W. & MAYER, B. J. 1999. Mechanism of activation of Pak1 kinase by membrane localization. Oncogene, 18, 797-806.

LU, W., QU, J. J., LI, B. L., LU, C., YAN, Q., WU, X. M., CHEN, X. Y. & WAN, X. P. 2013. Overexpression of p21-activated kinase 1 promotes endometrial cancer progression. Oncol Rep, 29, 1547-55.

LUO, M. & GUAN, J. L. 2010. Focal adhesion kinase: a prominent determinant in breast cancer initiation, progression and metastasis. Cancer Lett, 289, 127-39.

MACHESKY, L. M. & INSALL, R. H. 1998. Scar1 and the related Wiskott-Aldrich syndrome protein, WASP, regulate the actin cytoskeleton through the Arp2/3 complex. Curr Biol, 8, 1347-56.

MAMMOTO, T., PARIKH, S. M., MAMMOTO, A., GALLAGHER, D., CHAN, B., MOSTOSLAVSKY, G., INGBER, D. E. & SUKHATME, V. P. 2007. Angiopoietin-1 requires p190 RhoGAP to protect against vascular leakage in vivo. J Biol Chem, 282, 23910-8.

MANSER, E., HUANG, H. Y., LOO, T. H., CHEN, X. Q., DONG, J. M., LEUNG, T. & LIM, L. 1997. Expression of constitutively active alpha-PAK reveals effects of the kinase on actin and focal complexes. Mol Cell Biol, 17, 1129-43.

MANSER, E., LEUNG, T., SALIHUDDIN, H., ZHAO, Z. S. & LIM, L. 1994. A brain serine/threonine protein kinase activated by Cdc42 and Rac1. Nature, 367, 40-6.

MANSER, E., LOO, T. H., KOH, C. G., ZHAO, Z. S., CHEN, X. Q., TAN, L., TAN, I., LEUNG, T. & LIM, L. 1998. PAK kinases are directly coupled to the PIX family of nucleotide exchange factors. Mol Cell, 1, 183-92.

MAO, X., ORCHARD, G., LILLINGTON, D. M., RUSSELL-JONES, R., YOUNG, B. D. & WHITTAKER, S. J. 2003. Amplification and overexpression of JUNB is associated with primary cutaneous T-cell lymphomas. Blood, 101, 1513-9.

MARQUES, I. J., WEISS, F. U., VLECKEN, D. H., NITSCHE, C., BAKKERS, J., LAGENDIJK, A. K., PARTECKE, L. I., HEIDECKE, C. D., LERCH, M. M. & BAGOWSKI, C. P. 2009. Metastatic behaviour of primary human tumours in a zebrafish xenotransplantation model. BMC Cancer, 9, 128.

MCGRATH, J. L. 2007. Cell spreading: the power to simplify. Curr Biol, 17, R357-8.

MIKI, H., SUETSUGU, S. & TAKENAWA, T. 1998. WAVE, a novel WASP-family protein involved in actin reorganization induced by Rac. EMBO J, 17, 6932-41.

MORIMURA, S. & TAKAHASHI, K. 2011. Rac1 and Stathmin but Not EB1 Are Required for Invasion of Breast Cancer Cells in Response to IGF-I. Int J Cell Biol, 2011, 615912.

MURPHY, D. A. & COURTNEIDGE, S. A. 2011. The 'ins' and 'outs' of podosomes and invadopodia: characteristics, formation and function. Nat Rev Mol Cell Biol, 12, 413-26.

NAGANO, M., HOSHINO, D., KOSHIKAWA, N., AKIZAWA, T. & SEIKI, M. 2012. Turnover of focal adhesions and cancer cell migration. Int J Cell Biol, 2012, 310616.

NAYAL, A., WEBB, D. J., BROWN, C. M., SCHAEFER, E. M., VICENTE-MANZANARES, M. & HORWITZ, A. R. 2006. Paxillin phosphorylation at Ser273 localizes a GIT1-PIX-PAK complex and regulates adhesion and protrusion dynamics. J Cell Biol, 173, 587-9.

NICHOLAS, N. S., PIPILI, A., LESJAK, M. S., AMEER-BEG, S. M., GEH, J. L., HEALY, C., MACKENZIE ROSS, A. D., PARSONS, M., NESTLE, F. O., LACY, K. E. & WELLS, C. M. 2016. PAK4 suppresses PDZ-RhoGEF activity to drive invadopodia maturation in melanoma cells. Oncotarget, 7, 70881-70897.

NOBES, C. D. & HALL, A. 1995. Rho, rac, and cdc42 GTPases regulate the assembly of multimolecular focal complexes associated with actin stress fibers, lamellipodia, and filopodia. Cell, 81, 53-62.

O'SHAUGHNESSY, J. 2005. Extending survival with chemotherapy in metastatic breast cancer. Oncologist, 10 Suppl 3, 20-9.

O'SULLIVAN, G. C., TANGNEY, M., CASEY, G., AMBROSE, M., HOUSTON, A. & BARRY, O. P. 2007. Modulation of p21-activated kinase 1 alters the behavior of renal cell carcinoma. Int J Cancer, 121, 1930-40.

OHASHI, K., NAGATA, K., MAEKAWA, M., ISHIZAKI, T., NARUMIYA, S. & MIZUNO, K. 2000. Rho-associated kinase ROCK activates LIM-kinase 1 by phosphorylation at threonine 508 within the activation loop. J Biol Chem, 275, 3577-82.

ONG, C. C., JUBB, A. M., HAVERTY, P. M., ZHOU, W., TRAN, V., TRUONG, T., TURLEY, H., O'BRIEN, T., VUCIC, D., HARRIS, A. L., BELVIN, M., FRIEDMAN, L. S., BLACKWOOD, E. M., KOEPPEN, H. & HOEFLICH, K. P. 2011. Targeting p21-activated kinase 1 (PAK1) to induce apoptosis of tumor cells. Proc Natl Acad Sci U S A, 108, 7177-82.

ONG, C. C., JUBB, A. M., JAKUBIAK, D., ZHOU, W., RUDOLPH, J., HAVERTY, P. M., KOWANETZ, M., YAN, Y., TREMAYNE, J., LISLE, R., HARRIS, A. L., FRIEDMAN, L. S., BELVIN, M., MIDDLETON, M. R., BLACKWOOD, E. M., KOEPPEN, H. & HOEFLICH, K. P. 2013. P21-activated kinase 1 (PAK1) as a therapeutic target in BRAF wild-type melanoma. J Natl Cancer Inst, 105, 606-7.

OWEN, J. D., RUEST, P. J., FRY, D. W. & HANKS, S. K. 1999. Induced focal adhesion kinase (FAK) expression in FAK-null cells enhances cell spreading and migration requiring both auto- and activation loop phosphorylation sites and inhibits adhesion-dependent tyrosine phosphorylation of Pyk2. Mol Cell Biol, 19, 4806-18.

PALMER, T. D., ASHBY, W. J., LEWIS, J. D. & ZIJLSTRA, A. 2011. Targeting tumor cell motility to prevent metastasis. Adv Drug Deliv Rev, 63, 568-81.

PARRI, M. & CHIARUGI, P. 2010. Rac and Rho GTPases in cancer cell motility control. Cell Commun Signal, 8, 23.

PARRINI, M. C., CAMONIS, J., MATSUDA, M. & DE GUNZBURG, J. 2009. Dissecting activation of the PAK1 kinase at protrusions in living cells. J Biol Chem, 284, 24133-43.

PARRINI, M. C., LEI, M., HARRISON, S. C. & MAYER, B. J. 2002. Pak1 kinase homodimers are autoinhibited in trans and dissociated upon activation by Cdc42 and Rac1. Mol Cell, 9, 73-83.

PARSONS, J. T., HORWITZ, A. R. & SCHWARTZ, M. A. 2010. Cell adhesion: integrating cytoskeletal dynamics and cellular tension. Nat Rev Mol Cell Biol, 11, 633-43.

PAVEY, S., ZUIDERVAART, W., VAN NIEUWPOORT, F., PACKER, L., JAGER, M., GRUIS, N. & HAYWARD, N. 2006. Increased p21-activated kinase-1 expression is associated with invasive potential in uveal melanoma. Melanoma Res, 16, 285-96.

PRICE, L. S., LENG, J., SCHWARTZ, M. A. & BOKOCH, G. M. 1998. Activation of Rac and Cdc42 by integrins mediates cell spreading. Mol Biol Cell, 9, 1863-71.

PRUNIER, C., JOSSERAND, V., VOLLAIRE, J., BEERLING, E., PETROPOULOS, C., DESTAING, O., MONTEMAGNO, C., HURBIN, A., PRUDENT, R., DE KONING, L., KAPUR, R., COHEN, P. A., ALBIGES-RIZO, C., COLL, J. L., VAN RHEENEN, J., BILLAUD, M. & LAFANECHERE, L. 2016. LIM Kinase Inhibitor Pyr1 Reduces the Growth and Metastatic Load of Breast Cancers. Cancer Res, 76, 3541-52.

PRUVOT, B., JACQUEL, A., DROIN, N., AUBERGER, P., BOUSCARY, D., TAMBURINI, J., MULLER, M., FONTENAY, M., CHLUBA, J. & SOLARY, E. 2011. Leukemic cell xenograft in zebrafish embryo for investigating drug efficacy. Haematologica, 96, 612-6.

PUTO, L. A., PESTONJAMASP, K., KING, C. C. & BOKOCH, G. M. 2003. p21-activated kinase 1 (PAK1) interacts with the Grb2 adapter protein to couple to growth factor signaling. J Biol Chem, 278, 9388-93.

QU, J., LI, X., NOVITCH, B. G., ZHENG, Y., KOHN, M., XIE, J. M., KOZINN, S., BRONSON, R., BEG, A. A. & MINDEN, A. 2003. PAK4 kinase is essential for embryonic viability and for proper neuronal development. Mol Cell Biol, 23, 7122-33.

RADU, M., SEMENOVA, G., KOSOFF, R. & CHERNOFF, J. 2014. PAK signalling during the development and progression of cancer. Nat Rev Cancer, 14, 13-25.

RAYALA, S. K. & KUMAR, R. 2007. Sliding p21-activated kinase 1 to nucleus impacts tamoxifen sensitivity. Biomed Pharmacother, 61, 408-11.

REDDY, S. D., OHSHIRO, K., RAYALA, S. K. & KUMAR, R. 2008. MicroRNA-7, a homeobox D10 target, inhibits p21-activated kinase 1 and regulates its functions. Cancer Res, 68, 8195-200.

REIS-FILHO, J. S. & TUTT, A. N. 2008. Triple negative tumours: a critical review. Histopathology, 52, 108-18.

RETTIG, M., TRINIDAD, K., PEZESHKPOUR, G., FROST, P., SHARMA, S., MOATAMED, F., TAMANOI, F. & MORTAZAVI, F. 2012. PAK1 kinase promotes cell motility and invasiveness through CRK-II serine phosphorylation in non-small cell lung cancer cells. PLoS One, 7, e42012.

RIDER, L., OLADIMEJI, P. & DIAKONOVA, M. 2013. PAK1 regulates breast cancer cell invasion through secretion of matrix metalloproteinases in response to prolactin and three-dimensional collagen IV. Mol Endocrinol, 27, 1048-64.

RIDLEY, A. J. 2001. Rho GTPases and cell migration. J Cell Sci, 114, 2713-22.

RIDLEY, A. J. 2011. Life at the leading edge. Cell, 145, 1012-22.

RIDLEY, A. J. & HALL, A. 1992. The small GTP-binding protein rho regulates the assembly of focal adhesions and actin stress fibers in response to growth factors. Cell, 70, 389-99.

RIDLEY, A. J., SCHWARTZ, M. A., BURRIDGE, K., FIRTEL, R. A., GINSBERG, M. H., BORISY, G., PARSONS, J. T. & HORWITZ, A. R. 2003. Cell migration: integrating signals from front to back. Science, 302, 1704-9.

RIPPERGER, T., GADZICKI, D., MEINDL, A. & SCHLEGELBERGER, B. 2009. Breast cancer susceptibility: current knowledge and implications for genetic counselling. Eur J Hum Genet, 17, 722-31.

RODRIGUES, S. P., FATHERS, K. E., CHAN, G., ZUO, D., HALWANI, F., METERISSIAN, S. & PARK, M. 2005. CrkI and CrkII function as key signaling integrators for migration and invasion of cancer cells. Mol Cancer Res, 3, 183-94.

RODRIGUES, T., KUNDU, B., SILVA-CORREIA, J., KUNDU, S. C., OLIVEIRA, J. M., REIS, R. L. & CORRELO, V. M. 2018. Emerging tumor spheroids technologies for 3D in vitro cancer modeling. Pharmacol Ther, 184, 201-211.

ROJAS, K. & STUCKEY, A. 2016. Breast Cancer Epidemiology and Risk Factors. Clin Obstet Gynecol, 59, 651-672.

ROTTNER, K., HALL, A. & SMALL, J. V. 1999. Interplay between Rac and Rho in the control of substrate contact dynamics. Curr Biol, 9, 640-8.

RUBINSTEIN, A. L. 2003. Zebrafish: from disease modeling to drug discovery. Curr Opin Drug Discov Devel, 6, 218-23.

SAHAI, E. 2005. Mechanisms of cancer cell invasion. Curr Opin Genet Dev, 15, 87-96.

SANDERS, L. C., MATSUMURA, F., BOKOCH, G. M. & DE LANEROLLE, P. 1999. Inhibition of myosin light chain kinase by p21-activated kinase. Science, 283, 2083-5.

SANZ-MORENO, V. & MARSHALL, C. J. 2010. The plasticity of cytoskeletal dynamics underlying neoplastic cell migration. Curr Opin Cell Biol, 22, 690-6.

SCHOBER, M., RAGHAVAN, S., NIKOLOVA, M., POLAK, L., PASOLLI, H. A., BEGGS, H. E., REICHARDT, L. F. & FUCHS, E. 2007. Focal adhesion kinase modulates tension signaling to control actin and focal adhesion dynamics. J Cell Biol, 176, 667-80.

SCHRAML, P., SCHWERDTFEGER, G., BURKHALTER, F., RAGGI, A., SCHMIDT, D., RUFFALO, T., KING, W., WILBER, K., MIHATSCH, M. J. & MOCH, H. 2003. Combined array comparative genomic hybridization and tissue microarray analysis suggest PAK1 at 11q13.5-q14 as a critical oncogene target in ovarian carcinoma. Am J Pathol, 163, 985-92.

SELLS, M. A., KNAUS, U. G., BAGRODIA, S., AMBROSE, D. M., BOKOCH, G. M. & CHERNOFF, J. 1997. Human p21-activated kinase (Pak1) regulates actin organization in mammalian cells. Curr Biol, 7, 202-10.

SELLS, M. A., PFAFF, A. & CHERNOFF, J. 2000. Temporal and spatial distribution of activated Pak1 in fibroblasts. J Cell Biol, 151, 1449-58.

SHADEO, A. & LAM, W. L. 2006. Comprehensive copy number profiles of breast cancer cell model genomes. Breast Cancer Res, 8, R9.

SIEG, D. J., HAUCK, C. R., ILIC, D., KLINGBEIL, C. K., SCHAEFER, E., DAMSKY, C. H. & SCHLAEPFER, D. D. 2000. FAK integrates growth-factor and integrin signals to promote cell migration. Nat Cell Biol, 2, 249-56.

SIT, S. T. & MANSER, E. 2011. Rho GTPases and their role in organizing the actin cytoskeleton. J Cell Sci, 124, 679-83.

SIU, M. K., WONG, E. S., CHAN, H. Y., KONG, D. S., WOO, N. W., TAM, K. F., NGAN, H. Y., CHAN, Q. K., CHAN, D. C., CHAN, K. Y. & CHEUNG, A. N. 2010. Differential expression and phosphorylation of Pak1 and Pak2 in ovarian cancer: effects on prognosis and cell invasion. Int J Cancer, 127, 21-31.

SMITH, S. D., JAFFER, Z. M., CHERNOFF, J. & RIDLEY, A. J. 2008. PAK1-mediated activation of ERK1/2 regulates lamellipodial dynamics. J Cell Sci, 121, 3729-36.

STOCKTON, R. A., SCHAEFER, E. & SCHWARTZ, M. A. 2004. p21-activated kinase regulates endothelial permeability through modulation of contractility. J Biol Chem, 279, 46621-30.

STOFEGA, M. R., SANDERS, L. C., GARDINER, E. M. & BOKOCH, G. M. 2004. Constitutive p21-activated kinase (PAK) activation in breast cancer cells as a result of mislocalization of PAK to focal adhesions. Mol Biol Cell, 15, 2965-77.

STOLETOV, K., KATO, H., ZARDOUZIAN, E., KELBER, J., YANG, J., SHATTIL, S. & KLEMKE, R. 2010. Visualizing extravasation dynamics of metastatic tumor cells. J Cell Sci, 123, 2332-41.

STOLETOV, K. & KLEMKE, R. 2008. Catch of the day: zebrafish as a human cancer model. Oncogene, 27, 4509-20.

TAKINO, T., TAMURA, M., MIYAMORI, H., ARAKI, M., MATSUMOTO, K., SATO, H. & YAMADA, K. M. 2003. Tyrosine phosphorylation of the CrkII adaptor protein modulates cell migration. J Cell Sci, 116, 3145-55.

TALUKDER, A. H., MENG, Q. & KUMAR, R. 2006. CRIPak, a novel endogenous Pak1 inhibitor. Oncogene, 25, 1311-9.

TEN KLOOSTER, J. P., JAFFER, Z. M., CHERNOFF, J. & HORDIJK, P. L. 2006. Targeting and activation of Rac1 are mediated by the exchange factor beta-Pix. J Cell Biol, 172, 759-69.

TENG, Y., XIE, X., WALKER, S., WHITE, D. T., MUMM, J. S. & COWELL, J. K. 2013. Evaluating human cancer cell metastasis in zebrafish. BMC Cancer, 13, 453.

THIERY, J. P., ACLOQUE, H., HUANG, R. Y. & NIETO, M. A. 2009. Epithelial-mesenchymal transitions in development and disease. Cell, 139, 871-90.

THULLBERG, M., GAD, A., BEESER, A., CHERNOFF, J. & STROMBLAD, S. 2007. The kinase-inhibitory domain of p21-activated kinase 1 (PAK1) inhibits cell cycle progression independent of PAK1 kinase activity. Oncogene, 26, 1820-8.

TOLIAS, K. F., HARTWIG, J. H., ISHIHARA, H., SHIBASAKI, Y., CANTLEY, L. C. & CARPENTER, C. L. 2000. Type Ialpha phosphatidylinositol-4-phosphate 5-kinase mediates Rac-dependent actin assembly. Curr Biol, 10, 153-6.

VADLAMUDI, R. K., ADAM, L., WANG, R. A., MANDAL, M., NGUYEN, D., SAHIN, A., CHERNOFF, J., HUNG, M. C. & KUMAR, R. 2000. Regulatable expression of p21-activated kinase-1 promotes anchorage-independent growth and abnormal organization of mitotic spindles in human epithelial breast cancer cells. J Biol Chem, 275, 36238-44.

VADLAMUDI, R. K., LI, F., ADAM, L., NGUYEN, D., OHTA, Y., STOSSEL, T. P. & KUMAR, R. 2002. Filamin is essential in actin cytoskeletal assembly mediated by p21-activated kinase 1. Nat Cell Biol, 4, 681-90.

VADLAMUDI, R. K., LI, F., BARNES, C. J., BAGHERI-YARMAND, R. & KUMAR, R. 2004. p41-Arc subunit of human Arp2/3 complex is a p21-activated kinase-1-interacting substrate. EMBO Rep, 5, 154-60.

VALASTYAN, S. & WEINBERG, R. A. 2011. Tumor metastasis: molecular insights and evolving paradigms. Cell, 147, 275-92.

VEGA, F. M. & RIDLEY, A. J. 2008. Rho GTPases in cancer cell biology. FEBS Lett, 582, 2093-101.

VEINOTTE, C. J., DELLAIRE, G. & BERMAN, J. N. 2014. Hooking the big one: the potential of zebrafish xenotransplantation to reform cancer drug screening in the genomic era. Dis Model Mech, 7, 745-54.

VIAUD, J. & PETERSON, J. R. 2009. An allosteric kinase inhibitor binds the p21-activated kinase autoregulatory domain covalently. Mol Cancer Ther, 8, 2559-65.

VILLA-MORUZZI, E. 2007. Targeting of FAK Ser910 by ERK5 and PP1delta in non-stimulated and phorbol ester-stimulated cells. Biochem J, 408, 7-18.

WANG, R. A., ZHANG, H., BALASENTHIL, S., MEDINA, D. & KUMAR, R. 2006. PAK1 hyperactivation is sufficient for mammary gland tumor formation. Oncogene, 25, 2931-6.

WANG, Y., GRATZKE, C., TAMALUNAS, A., WIEMER, N., CIOTKOWSKA, A., RUTZ, B., WAIDELICH, R., STRITTMATTER, F., LIU, C., STIEF, C. G. & HENNENBERG, M. 2016. P21-Activated Kinase Inhibitors FRAX486 and IPA3: Inhibition of Prostate Stromal Cell Growth and Effects on Smooth Muscle Contraction in the Human Prostate. PLoS One, 11, e0153312.

WANG, Z., FU, M., WANG, L., LIU, J., LI, Y., BRAKEBUSCH, C. & MEI, Q. 2013. p21-activated kinase 1 (PAK1) can promote ERK activation in a kinase-independent manner. J Biol Chem, 288, 20093-9.

WEBB, D. J., DONAIS, K., WHITMORE, L. A., THOMAS, S. M., TURNER, C. E., PARSONS, J. T. & HORWITZ, A. F. 2004. FAK-Src signalling through paxillin, ERK and MLCK regulates adhesion disassembly. Nat Cell Biol, 6, 154-61.

WEIGELT, B., PETERSE, J. L. & VAN 'T VEER, L. J. 2005. Breast cancer metastasis: markers and models. Nat Rev Cancer, 5, 591-602.

WELCH, M. D., IWAMATSU, A. & MITCHISON, T. J. 1997. Actin polymerization is induced by Arp2/3 protein complex at the surface of Listeria monocytogenes. Nature, 385, 265-9.

WHALE, A., HASHIM, F. N., FRAM, S., JONES, G. E. & WELLS, C. M. 2011. Signalling to cancer cell invasion through PAK family kinases. Front Biosci (Landmark Ed), 16, 849-64.

WOLF, K., MAZO, I., LEUNG, H., ENGELKE, K., VON ANDRIAN, U. H., DERYUGINA, E. I., STRONGIN, A. Y., BROCKER, E. B. & FRIEDL, P. 2003. Compensation mechanism in tumor cell migration: mesenchymal-amoeboid transition after blocking of pericellular proteolysis. J Cell Biol, 160, 267-77.

WU, Y. J., TANG, Y., LI, Z. F., LI, Z., ZHAO, Y., WU, Z. J. & SU, Q. 2014. Expression and significance of Rac1, Pak1 and Rock1 in gastric carcinoma. Asia Pac J Clin Oncol, 10, e33-9.

XIA, C., MA, W., STAFFORD, L. J., MARCUS, S., XIONG, W. C. & LIU, M. 2001. Regulation of the p21-activated kinase (PAK) by a human Gbeta -like WD-repeat protein, hPIP1. Proc Natl Acad Sci U S A, 98, 6174-9.

XIE, X., TANG, S. C., CAI, Y., PI, W., DENG, L., WU, G., CHAVANIEU, A. & TENG, Y. 2016. Suppression of breast cancer metastasis through the inactivation of ADP-ribosylation factor 1. Oncotarget, 7, 58111-58120.

YAMAGUCHI, H. & CONDEELIS, J. 2007. Regulation of the actin cytoskeleton in cancer cell migration and invasion. Biochim Biophys Acta, 1773, 642-52.

YANG, N., HIGUCHI, O., OHASHI, K., NAGATA, K., WADA, A., KANGAWA, K., NISHIDA, E. & MIZUNO, K. 1998. Cofilin phosphorylation by LIM-kinase 1 and its role in Rac-mediated actin reorganization. Nature, 393, 809-12.

YANG, Y., DU, J., HU, Z., LIU, J., TIAN, Y., ZHU, Y., WANG, L. & GU, L. 2011. Activation of Rac1-PI3K/Akt is required for epidermal growth factor-induced PAK1 activation and cell migration in MDA-MB-231 breast cancer cells. J Biomed Res, 25, 237-45.

YILMAZ, M. & CHRISTOFORI, G. 2009. EMT, the cytoskeleton, and cancer cell invasion. Cancer Metastasis Rev, 28, 15-33.

YOON, D. S., WERSTO, R. P., ZHOU, W., CHREST, F. J., GARRETT, E. S., KWON, T. K. & GABRIELSON, E. 2002. Variable levels of chromosomal instability and mitotic spindle checkpoint defects in breast cancer. Am J Pathol, 161, 391-7.

YOUSEF, E. M., TAHIR, M. R., ST-PIERRE, Y. & GABOURY, L. A. 2014. MMP-9 expression varies according to molecular subtypes of breast cancer. BMC Cancer, 14, 609.

ZEGERS, M. M., FORGET, M. A., CHERNOFF, J., MOSTOV, K. E., TER BEEST, M. B. & HANSEN, S. H. 2003. Pak1 and PIX regulate contact inhibition during epithelial wound healing. EMBO J, 22, 4155-65.

ZENKE, F. T., KING, C. C., BOHL, B. P. & BOKOCH, G. M. 1999. Identification of a central phosphorylation site in p21-activated kinase regulating autoinhibition and kinase activity. J Biol Chem, 274, 32565-73.

ZHAN, M. N., YU, X. T., TANG, J., ZHOU, C. X., WANG, C. L., YIN, Q. Q., GONG, X. F., HE, M., HE, J. R., CHEN, G. Q. & ZHAO, Q. 2017. MicroRNA-494 inhibits breast cancer progression by directly targeting PAK1. Cell Death Dis, 8, e2529.

ZHAO, Z. S., MANSER, E., LOO, T. H. & LIM, L. 2000. Coupling of PAK-interacting exchange factor PIX to GIT1 promotes focal complex disassembly. Mol Cell Biol, 20, 6354-63.

ZHENG, Y., XIA, Y., HAWKE, D., HALLE, M., TREMBLAY, M. L., GAO, X., ZHOU, X. Z., ALDAPE, K., COBB, M. H., XIE, K., HE, J. & LU, Z. 2009. FAK phosphorylation by ERK primes ras-induced tyrosine dephosphorylation of FAK mediated by PIN1 and PTP-PEST. Mol Cell, 35, 11-25.

ZHOU, W., JUBB, A. M., LYLE, K., XIAO, Q., ONG, C. C., DESAI, R., FU, L., GNAD, F., SONG, Q., HAVERTY, P. M., AUST, D., GRUTZMANN, R., ROMERO, M., TOTPAL, K., NEVE, R. M., YAN, Y., FORREST, W. F., WANG, Y., RAJA, R., PILARSKY, C., DE JESUS-ACOSTA, A., BELVIN, M., FRIEDMAN, L. S., MERCHANT, M., JAFFEE, E. M., ZHENG, L., KOEPPEN, H. & HOEFLICH, K. P. 2014. PAK1 mediates pancreatic cancer cell migration and resistance to MET inhibition. J Pathol, 234, 502-13.